Joint Production and Energy Modeling for Sustainable Manufacturing Systems

BY

YONG WANG
B.S., Huazhong University of Science and Technology, 2003
M.S., Huazhong University of Science and Technology, 2006
Ph.D., Huazhong University of Science and Technology, 2010

THESIS

Submitted as partial fulfillment of the requirements
for the degree of Doctor of Philosophy
in Industrial Engineering and Operations Research
in the Graduate College of the
University of Illinois at Chicago, 2015

Chicago, Illinois

Defense Committee:

Lin Li, Chair and Advisor
David He
Prashant Banerjee
Houshang Darabi
Jie Lin, Civil and Materials Engineering

DEDICATION

In memory of my mother.

ACKNOWLEDGEMENTS

I would like to thank my advisor Professor Lin Li, Director of the Sustainable Manufacturing Systems Research Laboratory (SMSRL) in the University of Illinois at Chicago, for his persistent support during my PhD study. I am grateful for his generous help in rigorously training and preparing me for an academic career. I would also like to thank the members in my dissertation committee--Professor David He, Professor Prashant Banerjee, Professor Houshang Darabi, and Professor Jie Lin--for their guidance from different perspectives that helped me accomplish my research goals.

It was a great pleasure working with the graduate students in the SMSRL: Zeyi Sun, Xufeng Yao, Haoxiang Yang, Chongye Wang, Haotian Cai, Josh Reese, Zhichao Zhou, Fadwa Dababneh, Nedak Efretuei, Yuntian Ge, and Yiran Yang. I sure benefited a lot from these beautiful minds through the discussions in team meetings and seminars. Thanks also go to my friends and PhD classmates in the Mechanical and Industrial Engineering Department: Zoujun Dai, Xiaorui Zhao, Jia Luo, Jie Jiang, Brandon Vanhecke, and Ashkan Sharabiani. Their respective research broadened my view in the field of industrial engineering.

Scholars from several universities in China have also inspired me in my research. I would like to thank Professor Shuhong Huang and Professor Jianlan Li from Huazhong University of S&T, Prof. Kaifu Zhang and Prof. Xiangyuan Shu from Northwestern Polytechnical University, and Professor Zhaoliang Jiang from Shandong University for providing suggestions and sharing their ideas with me.

During the course of this work, I have been sponsored by the U.S. National Science Foundation and the National Natural Science Foundation of China. The financial support from these sources is gratefully acknowledged.

I would like to express my appreciation to my caring, loving, and encouraging wife, Yujia. I am deeply grateful to my father, who has been supporting me consistently. This work is in memory of my mother, who did so much for the family.

CONTRIBUTION OF AUTHORS

The first five chapters of this dissertation are each based on a published paper I co-authored with Dr. Lin Li. Dr. Lin Li was the corresponding author of these papers and provided financial support to my research.

TABLE OF CONTENTS

LIST OF TABLES

LIST OF FIGURES

LIST OF ABBREVIATIONS

C&I	commercial and industrial
FERC	Federal Energy Regulatory Commission
GHG	greenhouse gas
kW	kilowatt(s)
kWh	kilowatt-hour(s)
MINLP	mixed integer nonlinear programming
MSM	manufacturing system modeling
NERC	North American Electric Reliability Council
PSO	particle swarm optimization
PUC	public utility commission
SLEM	second largest eigenvalue modulus
TOU	time-of-use
ZONLP	zero-one nonlinear programming

SUMMARY

This dissertation proposes a framework for addressing challenges of joint production and energy modeling for manufacturing systems. The knowledge generated is used to improve the technological readiness of manufacturing enterprises for the transition towards sustainable manufacturing in the context of smart electric grids. Detailed research tasks of the framework on the modeling of production, energy efficiency, electricity demand, cost, and demand response decision making have been implemented. Specifically, the dynamics and performance measures of general manufacturing systems with multiple machines and buffers have been modeled. Expressions of electricity energy efficiency and cost have been established based on the electricity pricing profile. Production scheduling problem formulations and the solution technique are discussed. New insights are acquired based on the applications of the established model in system parameter monotonicity analysis, rate plan switching decision making, and demand response scheduling. The findings based on case studies show that with appropriate adjustment of production routines, significant improvement in energy efficiency and substantial savings in energy cost can be achieved without sacrificing production. Appropriate implementation of this research outcome may lead to energy-efficient, electricity-demand-responsive, and cost-effective operations and thus improve the sustainability of modern manufacturing systems. The new knowledge generated can be implemented to discrete manufacturing in various industries such as automotive, electronics, appliances, aerospace, etc.

CHAPTER 1

INTRODUCTION

(Parts of this chapter were previously published as: *Wang, Y., Li, L., 2014. Joint production and energy modeling of sustainable manufacturing systems: Challenges and methods. In Proceedings of 2014 ASME International Manufacturing Science and Engineering Conference, June 9-13, 2014, Detroit, Michigan, USA.*)

1.1. Challenges and Objectives

Greenhouse-gas (GHG) emissions are recognized as the leading cause of global warming and climate change. They have become a vital issue to the sustainable development of human society. Under the increasingly rising pressures from both domestic and international societies, many countries have enacted regulations to curb the emissions. For example, the U.S. government has set up a target to achieve a 17% GHG emission reduction below the 2005 level by 2020 (U.S. Department of Energy, 2009).

GHG emissions are directly related to energy use. Among the four principle energy end-use sectors (residential, commercial, transportation, and industrial), the industrial sector is the largest energy consumer and GHG emitter in the world. It accounts for 52% of the total energy consumed globally (U.S. Energy Information Administration, 2013). It is reported that 84% of energy-related industrial CO_2 emissions and 90% of industrial energy consumptions are ascribable to manufacturing activities (Schipper, 2006). For manufacturing enterprises, the share of energy costs has been on the rise among the overall production costs. This trend is expected to accelerate and be more pronounced in the future due to the expected more stringent carbon tax regulations as well as the competitively increasing energy demands from developing countries

(Fang et al., 2011; Rentizelas et al., 2012; U.S. Energy Information Administration, 2013).

In the direction towards a more carbon-constrained world, this status quo has greatly motivated the research activities on improving energy efficiency and reducing energy cost of manufacturing systems. Since profit maximization is the primary goal of manufacturing enterprises, the research outcomes with improved energy efficiency and reduced energy cost should not be at the expense of production loss (hence weakened profit). Therefore, it is crucial that such research activities are performed on the basis of a fundamental understanding of the relationship between production and energy use in modern manufacturing systems.

To build such a base, it calls for a systematic model that is able to analytically characterize this relationship. However, joint modeling of production and energy use of manufacturing systems is difficult due to the following **challenges**:

1) Typical manufacturing systems generally consist of multiple machines and buffers. Machines are subject to unexpected failures and they are not 100% reliable. Buffers are subject to spaces and they do not have infinite capacities. The use of buffers between machines is meant to mitigate the effect of machine downtime. Since all the machines and buffers in the system are tightly coupled, the system exhibits highly complex dynamics because the operation states of each machine and the occupancy states of each buffer are determined by the states of all other machines and buffers (Li et al., 2006, 2009a, 2010). When modeling the interactions within manufacturing systems, it is essential to establish the relationship between component-level parameters (such as machine reliabilities and buffer capacities) and system-level performance measures (such as production rate or throughput) (Gershwin, 1994; Li and Meerkov, 2009; Li et al., 2009b, 2009c, 2011; Liu et al., 2012). Although simulation-based methods are capable of

partially reflecting such relationship, they are not able to reveal the fundamental mathematical expressions between the parameters and performance measures, which greatly impedes their capabilities. In addition, the development and execution of simulation models to obtain statistically useful results may become prohibitively expensive and impractically slow (Li and Meerkov, 2009).

2) Recently, there has been a rising concern on transient analysis of manufacturing systems. Manufacturing system transients depict the system behavior before reaching the steady state, when the manufacturing system is expected to operate at a more synchronized pace. Transients occur under many circumstances for manufacturing systems (Meerkov and Zhang, 2008). One of the most common circumstances is after a fresh start of a production shift, i.e., when all the buffers are empty and every machine except the first one is constantly starved before its upstream buffer is filled with parts processed by upstream machines. During the transients, the mean values of the performance measures are not stable and can be quite different from those of the steady state (Shaaban and Hudson, 2012). The transient behaviors of manufacturing system are of great importance, especially when they last for a relatively long period. The transient behaviors should be carefully characterized because they are critical for the integration of both production and energy use, which are also time-dependent in nature.

3) Among the world's total energy supply, the share of electricity is increasing and it is a major form of energy use in manufacturing systems (U.S. Energy Information Administration, 2013). Electricity must be generated, distributed, and consumed at the same time because it is a form of energy that cannot be effectively stored in bulk. Electricity consumers' needs change vastly in different seasons and even at different time

of a day (ComEd, 2012). Traditionally, manufacturing enterprises pay flat rates for each kWh of electricity they consumed. A representative example is shown in Table 1.1 (Orange and Rockland Utilities, 2013a, c). However, the real cost of electricity generation varies greatly (sometimes by a factor of two to five) due to the daily demand cycle. The flat rates are not able to represent such real cost at the time of consumption. More recently, the electric power industry is undergoing a transition to a more modern and smarter grid with the help of research and technology developments (Gungor et al., 2013; Klemes et al., 2012; Lima and Navas, 2012). Newly available electric tariffs that charge both energy consumption (in kWh) and power demand (in kW) with varying time-of-use (TOU) rates have started to gain popularity. A representative example is shown in Table 1.2 (Orange and Rockland Utilities, 2013b, c). Under such rates, the demand charge can make up as high as 70% of the electric bill (National Grid USA, 2006). The TOU pricing is an electricity demand response program that gives consumers opportunities to manage their electric bill by shifting use from on-peak periods to off-peak periods. Reducing the electricity demand during the peak load times makes it possible for the power grid to meet consumers' needs without building more costly backup infrastructures and help reduce GHG emissions. With this in mind, manufacturing enterprises are facing the following two questions: Is switching from the flat rates to the TOU rates economically sound? What changes can be made on the electricity use routines to take advantage of the TOU rates? To answer these questions, the knowledge about electricity energy efficiency and cost as a function of manufacturing system parameters and the TOU rates is needed.

All of these challenges need to be addressed and the outcomes should be synthesized for the joint modeling of production and energy use of modern manufacturing systems. The main **objectives** of this dissertation are to: address these challenges; and use the new knowledge generated to improve the technological readiness of manufacturing enterprises for the transition towards sustainable manufacturing in the context of smart electric grids. In order to achieve the objectives, a new framework will be proposed and detailed research tasks on the modeling and decision making of production, energy efficiency, cost, and electricity demand response will be implemented.

Table 1.1. A representative pricing profile with flat rates

Season	Time of day	Energy rate ($/kWh)	Account and other fixed charges ($/month)
Summer (Jun-Sep)	All time	0.18015	33.15
Winter (Oct-May)	All time	0.16052	

Table 1.2. A representative pricing profile with TOU rates

Season	Time of day	Energy rate ($/kWh)	Demand rate ($/kW)	Account and other fixed charges ($/month)
Summer (Jun-Sep)	7pm-1pm (Off-peak)	0.10551	0	51.32
	1pm-7pm (On-peak)	0.18815	19.41	
Winter (Oct-May)	9pm-10am (Off-peak)	0.10551	0	
	10am-9pm (On-peak)	0.13065	8.38	

1.2. Literature Review

Research efforts that attempt to separately address these challenges are reviewed in this section.

1.2.1. Modeling of manufacturing systems with multiple machines and buffers

Manufacturing system modeling (MSM) is extremely valuable for understanding fundamental system principles, which could facilitate optimal design and operation. The models established can be used to improve system performance (such as production rate or throughput) and provide manufacturing enterprises with a strategic competitive advantage. Many manufacturing enterprises have benefited from MSM and subsequent analysis. For example, General Motors, one of the largest auto manufacturers in the world, has increased revenue and saved over $2.1 billion since 1990s in over 30 vehicle plants using manufacturing system models for activities such as estimating system performance, identifying throughput bottlenecks, optimizing buffer allocation, and utilizing maintenance opportunities (Alden et al., 2006).

In the literature, enormous effort has been devoted to the research area of MSM, in which machine reliability parameters are assumed to follow the Bernoulli, geometric, or exponential distributions (Gershwin, 1994; Jacobs and Meerkov, 1995; Li and Meerkov, 2009). Conventionally, the research of MSM has been conducted for the purpose of steady-state analysis only, which facilitates characterizing the long-term performance of manufacturing systems. Exact analytical expressions for steady-state system performance measures exist for two-machine-one-buffer systems (Dallery and Gershwin 1992; Jacobs and Meerkov, 1995; Alexandros and Chrissoleon, 2009). Longer systems are investigated by approximate methods such as aggregation (Li and Meerkov, 2009) or decomposition (Gershwin, 1994). These methods basically transform long manufacturing systems into a series of two-machine-one-buffer systems and solve them recursively. Pure simulations have been commonly utilized to verify the accuracy of these approximation methods.

Unlike the fact that rich knowledge has been acquired for steady-state analysis of manufacturing systems, MSM for transient performance analysis is much less studied and needs further development. Transients are generally undesirable because they will cause substantial production losses. For example, Meerkov and Zhang (2008) have shown that a manufacturing system may suffer a loss of approximately 12% of production due to transients during a plant shift of eight hours after a fresh start. Some transients may be greatly reduced by properly scheduling production to build up extra work-in-process (referred to as "floats") by slow machines so that the starvation and blockage of fast machines can be avoided (Meerkov and

Zhang 2011). Transient analysis results can help identify the initial level of buffer occupancy needed. The float strategy may not be applicable to other manufacturing systems where the buffers have to be depleted at the end of each shift due to technological requirements (e.g. paint shops of automotive assembly plants) (Meerkov et al., 2010) or perishable nature of products (e.g. dairy filling and packing systems) (Wang et al., 2010). Even if the transients cannot be reduced, transient analysis will still provide valuable information for designing manufacturing systems with sufficient production capacity margins to ensure customer satisfaction. Therefore, transient analysis of manufacturing system is of great importance.

Existing publications on manufacturing transient analysis can be divided into two categories: analytical and simulation-based. Examples of simulation-based transient analysis methods include (Meerkov and Zhang, 2008; Shaaban and Hudson, 2011). In the simulation methods, discrete event models are often created for a manufacturing system. Since the simulation-based methods are meant to capture the statistical properties of system transient behaviors, a large number of repetitions would be required, which renders them less efficient. Examples of analytical transient analysis methods include (Meerkov and Zhang, 2008, 2011; Meerkov et al., 2010; Sader and Sorensen, 2010; Wang et al., 2010; Gökçe et al., 2012). However, each method in this category has its own limitation. The analytical results in (Meerkov and Zhang, 2008, 2011; Meerkov et al., 2010; Wang et al., 2010) are only applicable to two-machine-one-buffer systems. The method proposed in (Sader and Sorensen, 2010) only work for a manufacturing system with a single machine or a number of machines in parallel. The method in (Gökçe et al., 2012) requires that each buffer must have a capacity of one and each machine is 100% reliable.

1.2.2. Electricity energy efficiency and cost modeling for manufacturing systems

Recent advancements in energy or electricity related research for manufacturing mainly focus on machine tool level energy consumption modeling and monitoring. For example, Balogun and Mativenga (2013) developed a mathematical model for predicting direct electrical energy requirements in machining tool paths and validated on a milling tool path. Behrendt et al. (2012) compared energy consumption characteristics of various machine tools. Hu et al. (2012) introduced an on-line approach for energy efficiency monitoring of machine tools. Santos et al. (2011) describes the relationship between machine tool structure and energy consumption in the design of a commercial press-brake.

Some system level research on energy efficiency improvement also exists. For example, Li and Sun (2013) established an energy consumption model of typical manufacturing systems with multiple machines and buffers. They used the model to make energy control decisions based on a Markov decision process. Liu et al. (2013) built a model for the bi-objectives problem that minimizes both electricity consumption and tardiness, and they solved it with a genetic algorithm to obtain the Pareto solutions in a job shop. Luo et al. (2013) proposed an ant colony optimization meta-heuristic to integrate production efficiency and electricity cost with varying electricity prices. Duflou et al. (2012) have reviewed the energy efficiency methods in discrete part manufacturing at both the machine and system levels. However, these works are either based on flat rates or ignoring the demand charge, an important component that count towards the electric bill.

Unlike the flat rates, TOU pricing is a tariff plan that is meant to increase the elasticity of electricity consumers and moderate the extreme demand variation. It utilizes time sensitive pricing structures to spread the costs of the needs for extra equipment. The mechanism encourages the electricity consumers to shift their power demand from peak periods (with high prices) to off-peak periods (with low prices). TOU pricing is widely available from utility companies around the world (Australia Ausgrid, 2012; Ipsos MORI, 2012; King, 2010; Ontario Ministry of Energy, 2013; Torriti, 2012; Zeng et al., 2008) because it is one of the easiest implementations of demand response due to less stringent technological requirements. For example, there are more than 150 entities providing different sorts of TOU pricing programs in the U.S. alone, thanks to the *Energy Policy Act of 2005* (109th U.S. Congress, 2005). These entities represent all aspects of the electricity delivery industry: demand response providers, state and federal agencies, power marketers, rural electric cooperatives, municipal utilities, and investor-owned utilities. A full list of the entities' names is available in the appendix of the survey report by the U.S. Federal Energy Regulatory Commission (U.S. FERC, 2012).

Most TOU pricing profiles, like the one provided by Orange and Rockland Utilities (2013b, c) in Table 1.2, generally divide the day into two or three periods and assign prices for each period (Nikzad et al., 2012). The electricity use is tracked by smart meters (Cook et al., 2012; Gungor et al., 2013; Lima and Navas, 2012). Both electricity energy consumption (measured by an energy meter) and power demand (measured by a demand meter) count towards industrial consumers' monthly bill. The difference between the energy meter and the demand meter is like the difference between the odometer and the speedometer (Orange and Rockland Utilities, 2013d): "*An odometer records the accumulated miles traveled, the same way the electric (energy) meter records your total energy consumption. The speedometer measures speed, the same way the demand meter registers your rate of consumption.*" The consumption rate is formulated in \$/kWh. The charge for energy consumption is determined based on the time-of-day kWh readings. The demand rate is formulated in \$/kW. The charge for demand is determined based on the highest average kW measured in any on-peak 15-minute interval during the monthly billing period. In addition, there is a separate fixed charge, which generally includes the customer account charge and metering charges during the monthly billing period. A consumer's total bill is rendered by adding up the subtotals of all the three parts.

As illustrated in Table 1.2, the energy and demand rates of during the on-peak periods are much higher than the rates during the off-peak periods. The TOU pricing encourages customers to change their regular usage patterns in response to the variation in the price of electricity over time. Consumers have the opportunity to lower their electric bill by shifting the use from on-peak periods to off-peak periods. In doing so, the reliability of the electric power grid is enhanced and the peak generating capacity is reduced. In fact, a 5% reduction of peak power demand in the U.S. would lead to eliminating the need for installing about 625 peak power plants and operating associated power delivery infrastructure, which translates into an annual saving of $3 billion (Faruqui et al., 2007). Intensive CO_2 emissions due to low-efficient back-up generators will also be curtailed, and the consumers who choose to comply are rewarded with lower electric bill.

Although TOU programs are widely available from utility companies, customer participation from the manufacturing industry in these programs is still low. Due to the differences in the modeling methods and pricing components considered (Huisman et al., 2009; Nikzad et al., 2012; Zeng et al., 2008), the designed TOU tariffs may vary greatly from company to company. There is no guarantee that the consumers will end up paying less on the TOU rates.

1.2.3. Production scheduling for electricity demand response

In the electric power grid, in order to meet the needs during peak periods, a huge array of expensive equipment including generators, transformers, wires, and substations has to be kept on constant standby, otherwise the grid will become unstable and blackouts may occur. This requires large extra investments for those backup infrastructures. By 2030, about $2 trillion investments for new generation capacities, transmission, and distribution will be required to satisfy the growing needs (Chupka et al., 2008). On average, one kWh of electricity generation causes 1.56 pounds (0.71 kg) of GHG emissions (U.S. Enviromental Protection Agency, 2012). Backup generators are often dirtier and less efficient than base load generators, and therefore create more GHG emissions for each kWh of electricity generated.

During this period of transition to the smart grid, utility companies around the world are implementing new technologies that may promisingly reduce GHG emissions and postpone or eliminate the huge extra investments. One such technology is demand response. The U.S. Federal Energy Regulatory Commission (2012) defines demand response as "*changes in electric use by demand-side resources from their normal consumption patterns in response to changes in the price of electricity, or to incentive payments designed to induce lower electricity use at times of high wholesale market prices or when system reliability is jeopardized.*" Demand response targets at reducing peak demand to control the risk of potential disturbances, avoiding extra investments in additional infrastructures, avoiding use of more expensive and less efficient generators, and thus cutting GHG emissions. It is estimated that the implementation of demand response programs together with energy efficiency improvement can reduce the needs for new generation capacities from 214 GW to 133 GW in 2030, by 38% (Chupka et al., 2008). Recent research results have also suggested that in the grid with significant penetration of variable renewable energy sources of intermittent nature, demand response can be used as a solution to mitigate supply-demand fluctuations (Finn et al., 2011; Pina et al., 2012; Quiggin et al., 2012; Walawalkar et al., 2010).

The term demand response encompasses a wide range of solutions and mechanisms.

According to the *2012 Survey on Demand Response and Advanced Metering* by U.S. Federal Energy Regulatory Commission (2012), TOU pricing is among the most popular demand response mechanisms.

Existing applications of the TOU and other demand response programs are predominantly limited to the residential and commercial building sectors (Corno and Razzak, 2012; Finn et al., 2012; Herter and Wayland, 2010; Houwing et al., 2011; Liang et al., 2012; Motegi et al., 2007; Rastegar et al., 2012; Torriti, 2012; van Ruijven et al., 2010; Venkatesan et al., 2012; Wang et al., 2012a). Many research results have provided the guidance in various aspects for the consumers so that they can manage the electricity consumed by lighting, HVAC, kitchen appliances, and laundry equipment in response to the varying prices. Both manual and automatic control strategies have been extensively studied to reduce the electricity demand of buildings during peak periods.

By contrast, the research progress of the TOU and other demand response programs for the industrial sector lags far behind. Existing efforts in this area focus only on isolated or mutually independent machines or processes (Chao and Chen, 2005; Lewis, 2007; Logenthiran et al., 2012; McKane et al., 2008). These efforts have largely ignored the following properties shared in many industrial systems of modern manufacturing (Gershwin, 1994; Li and Meerkov, 2009): 1) the system generally consists of multiple machines and buffers; 2) machines are unreliable and they are subject to unexpected failures; 3) the use of buffers between machines may mitigate the negative effects of machine downtime; and 4) the system exhibits highly complex dynamics because each machine's operation states are determined by all the machines and buffers in the system. Therefore, it is more important and meaningful to consider the interactions within the manufacturing systems for effective demand response. As reviewed in

Section 1.2.1, MSM considering the interactions is an active research area (Colledani and Gershwin, 2013; Gershwin and Werner, 2007; Li et al., 2009a; Li et al., 2010; Li, 2009; Li et al., 2009c; Meerkov et al., 2010; Meerkov and Zhang, 2008). Although a few publications (Ashok, 2006; Fang et al., 2011) related to the demand response technology are available in this area, none of them explicitly consider practical issues such as limited buffer capacities as well as machine breakdown, starvation, and blockage. Consequently, the claimed benefits of the demand response actions may be unachievable.

In some of recent work that does consider such practical issues, Bego et al. (2013) identified the reservation capacity of manufacturing systems in the critical peak pricing electricity demand response program; Fernandez et al. (2013) proposed a concept of "Just-for-Peak" buffer inventory for peak electricity demand reduction of manufacturing systems; Sun and Li (2013) estimated the potential capability for real time electricity demand response of manufacturing systems using a Markov decision process. However, all of these efforts are based on approximate methods, and none of them has thoroughly examined the optimal TOU rate plan.

1.3. Proposed Research Framework

Despite the progresses made in the literature, the challenges remain. In order to address these challenges, we propose a research framework as shown in Figure 1.1. It is further explained as follows.

Every layer of the framework is based on all the layers within.

At the core of the framework is a new comprehensive production modeling method that removes the imposed restrictions in previous literature and is ready for energy integration. It models the manufacturing system for both steady-state and transient analyses in their general form, i.e., with multiple unreliable machines and finite buffers. We focus on serial manufacturing systems because they represent the most commonly used basic structure in manufacturing systems that are more complex. The proposed MSM is a method based on probability theory. The conditional probability formula and the law of total probability have been greatly employed to enable the proposed MSM method to derive the expressions of both steady state and transient performance measures of the manufacturing systems. Furthermore, fixed-point theory is utilized as a viable tool for solving the model established. Fixed-point theory has been used across numerous fields of mathematics for proving deep results (Border, 1985; Black, 1995; Petri, 2004; Argyros, 2007; Burden and Faires, 2011). One of its most creative applications is in game theory for market economics research by Nobel Prize winners Kenneth Arrow and Gérard Debreu (1954). At the core of the fixed-point theory are hundreds of theorems, among which Brouwer fixed-point theorem is especially useful for analyzing the complex dynamics of the manufacturing systems being studied. The process of untangling the complex system dynamics in the form of nonlinear constrained state evolution equations is exactly the process of iteratively approaching the fixed point.

Based on the production modeling, we now integrate the energy part. An analytical model is established to measure electricity energy efficiency of the manufacturing system. Mathematical expressions of peak demand and related charge as well as the total electricity cost of manufacturing a product based on the TOU rates will also be established. New knowledge of energy efficiency and the electricity cost as functions of manufacturing system parameters and the TOU rates will be generated. The research outcomes will enable manufacturers to make the best use of TOU incentives offered by utility companies and achieve significant savings in electricity cost without compromising production.

Next, we propose to research on the production scheduling formulations that leads to demand response actions and help manufacturers manage electricity costs during peak periods. A time-dependent method will be developed to determine control actions for optimal demand response. The TOU pricing is especially suitable for such application in the manufacturing industry. When the pricing profile is provided, manufacturers can make decisions by jointly considering the production target together with electricity consumption and demand. This is made possible by the utilization of buffers in the system that allow for temporary stoppage of work in one area without affecting the entire system's throughput. Therefore, a schedule can be created to control the status of each machine to minimize concurrent operations of all the machines during peak hours. The appropriate implementation of this research outcome may lead to energy-efficient, demand-responsive, and cost-effective operations of modern manufacturing systems.

Details of the proposed tasks regarding the framework are implemented in Chapters 2 through 5.

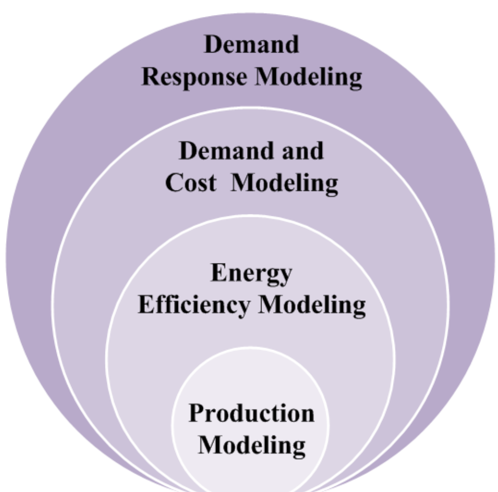

Figure 1.1. Research framework

1.4. Organization of Dissertation

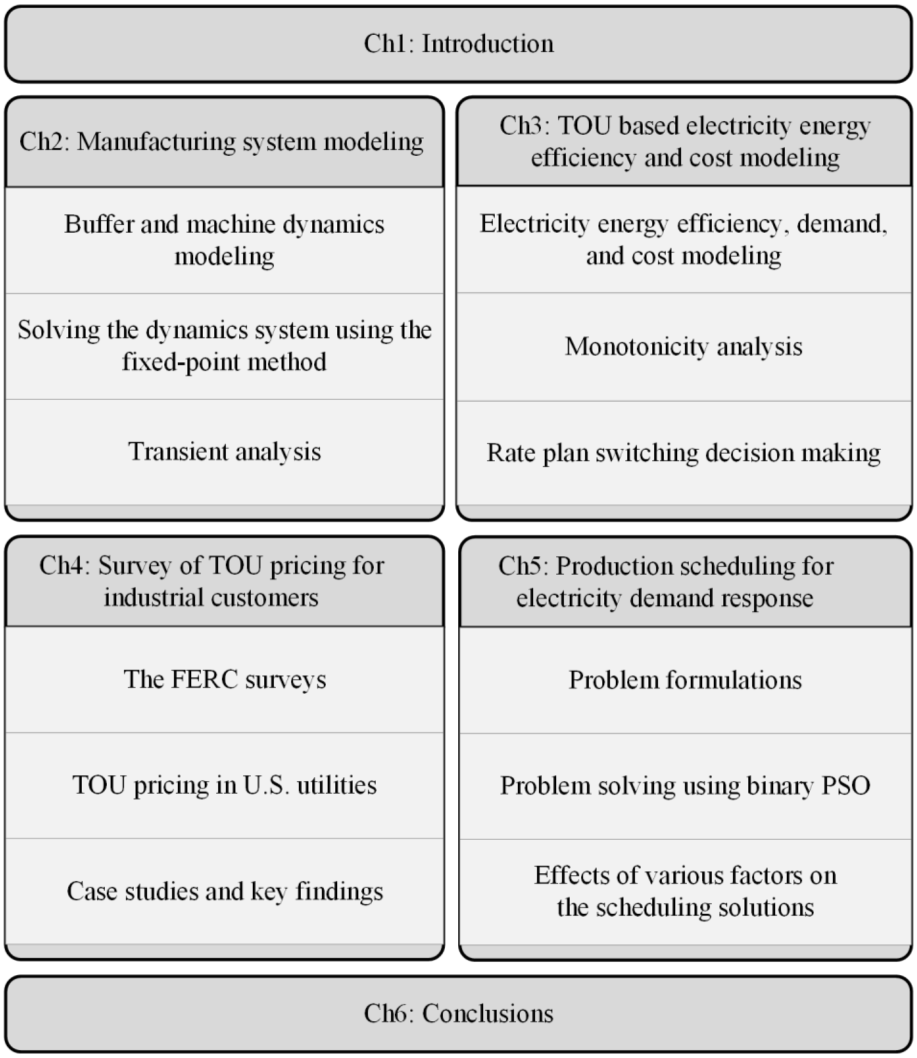

Figure 1.2. Organization of dissertation

The organization of this dissertation is shown in Figure 1.2. Chapter 1 provides a brief introduction to this doctoral research. Research motivation and objectives are presented in this chapter. Chapter 2 presents a novel production modeling method for typical manufacturing systems with multiple machines and buffers. Transient metrics are also proposed and analyzed. Chapter 3 models the TOU based electricity energy efficiency and cost of manufacturing a product. The established model is used for monotonicity analysis and rate plan switching decision making. More case studies are conducted to examine the feasibility and potential benefits of switching from flat rates to TOU rates based on a survey of utilities in 43 states in Chapter 4. Chapter 5 extends the work in Chapters 2 and 3 to formulate and solve the production scheduling problems for effective electricity demand response. New insights on the effects of various parameters on the solutions of the problem formulations are discussed. Chapter 6 draws the conclusions of this research and lists original contributions as well as potential future work.

CHAPTER 2

NOVEL PRODUCTION MODELING OF TYPICAL MANUFACTURING SYSTEMS FOR ENERGY INTEGRATION

(Parts of this chapter were previously published as: *Wang, Y., Li, L., 2014. A novel modeling method for both steady-state and transient analyses of serial Bernoulli production systems. IEEE Transactions on Systems, Man and Cybernetics: Systems, 45, 97-108.*)

2.1. Introduction

In this chapter, a novel analytical method has been established to model the manufacturing system for both steady-state and transient analyses. This research has overcome the restrictions of existing methods on the number of machines and the capacity of buffers. That is, it has greatly advanced MSM for both steady-state and transient analyses by directly dealing with general serial manufacturing systems with multiple unreliable Bernoulli machines and finite buffer capacities. The proposed MSM is a method derived based on probability theory and fixed-point theory. The solvability of the method is proved theoretically. The transient performance metrics such as second largest eigenvalue modulus, duration of the transients, settling time for work-in-process and production rate, and production loss have been investigated numerically based on the propose MSM method. This research can serve as the base for more complex components such as energy efficiency and TOU based electricity cost to be built on in subsequent chapters.

The remainder of this chapter is organized as follows. Section 2.2 presents the new method for modeling serial manufacturing systems with multiple Bernoulli machines and finite buffers. The core equations of the non-linear, high-dimensional dynamics model are formulated in a fixed-point iteration format. Section 2.3 proves the existence of the model solution using fixed-point theory. The model is used in Section 2.4 to construct several key metrics to characterize the transient performance of the systems. Finally, the overall conclusions of this research are drawn in Section 2.5.

The following notation is used in this chapter.

Boldface:

$\mathbf{q}_i(t)$	a column vector containing the state probabilities of buffer b_i at the end of time slot t
$\mathbf{X}^*$	a fixed point
$\mathbf{X}(t)$	a column vector containing the state probabilities of all the buffers at the end of time slot t

Upper Case:

$\mathcal{A}$, $\mathcal{B}$, $\mathcal{C}$, and $\mathcal{D}$	four sets
$BL_i(t)$	blockage probability of machine m_i during time slot t
$BS_i(t)$	probability of simultaneous blockage and starvation of machine m_i ($i = 1, \ldots, N$) during time slot t
C_i	capacity of buffer b_i (the largest number of parts the buffer can hold)
CP_T	cumulative production of the system during the planning horizon
D	definition domain of $\mathbf{X}$
$ID_i(t)$	probability of machine m_i ($i = 1, \ldots, N$) being idle during time slot t
J_G	Jacobian of $G(\mathbf{X})$

L_{PR}	percent of production loss
N	number of machines in the manufacturing system
$PR_i(t)$	production rate of machine m_i (i = 1, …, N) during time slot t
$PR_{SYS}(t)$	production rate of the system during time slot t
$Q_{i,(j_2\|j_1)}(t)$	transition probability from state j_1 to j_2 during time slot t for buffer b_i
$SLEM$	second largest eigenvalue modulus
$ST_i(t)$	starvation probability of machine m_i during time slot t
T	number of total time slots during the planning horizon
V	number of elements in $\mathbf{X}(t)$
$WIP_i(t)$	work-in-process inventory of buffer b_i at the end of time slot t
$WIP_{SYS}(t)$	total work-in-process of the system at the end of time slot t

Lower Case:

b_i	index of the ith buffer in the system, i = 1, ..., $N - 1$
$h_i(t)$	state (occupancy) of buffer b_i at the end of time slot t
i, j, j_1, j_2, k, t	general indexes
m_i	index of the ith machine in the system, i = 1, ..., N
p_i	probability of machine m_i being up during time slot t (considering machine reliability only)
$q_{i,j}(t)$	probability of buffer b_i in state j (j = 0, …, C_i) at the end of time slot t
t_{ITER}	number of iteration
t_{PR}	settling time of PR
t_{WIP}	settling time of WIP

Greek:

Ω	state sample space of machine m_i

Functions:

$G(\cdot)$	state transition dynamics
$g_i(\cdot)$	element function of $G(\cdot)$
$inf(\cdot)$	infimum function

2.2. Manufacturing System Modeling

2.2.1. Assumptions

The diagram of a typical manufacturing system is shown in Figure 2.1. The following assumptions are adopted for the study in this chapter:

(i) The system consists of N machines (denoted by squares) and $N - 1$ buffers (denoted by circles) connected in series.

(ii) A planning horizon is evenly discretized into T slots, with $t = 1$ being the first slot, and $t = T$ being the last. The slot duration is equal to the cycle time of the machines. The cycle time represents the time needed by a machine to process a product.

(iii) Let the capacity of buffer b_i ($i = 1, ..., N - 1$) be C_i, which is the largest number of products the buffer can hold. Buffer states are defined by the number of products it contains at the end of a time slot. Let $h_i(t)$ be the state (occupancy) of buffer b_i at the end of time slot t. Then $h_i(t)$ ranges from 0 (empty) to C_i (full) and it can change in each time slot at most by one product.

(iv) Due to random failure, machine m_i ($i = 1, ..., N$) is up during time slot t with probability p_i and down with probability $1 - p_i$. Each machine's uptime and downtime are determined independently from the other machines'. Machine states are defined by its working status during a time slot. It is assume that the last machine is never blocked and the first machine is never starved.

(v) The blocked-before-service (Jacob and Meerkov, 1995; Li and Meerkov, 2009) and time-dependent-failure (Gershwin, 1994; Jacob and Meerkov, 1995) conventions are adopted.

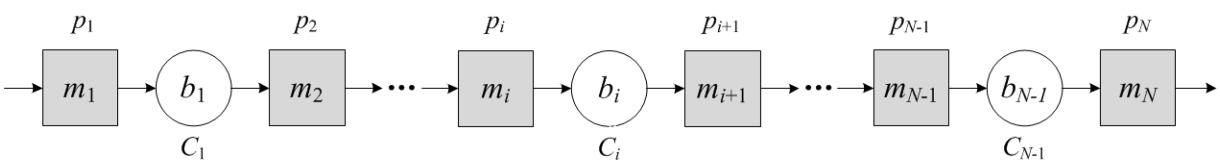

Figure 2.1. Diagram of a typical manufacturing system

2.2.2. Machine and buffer states

For buffer b_i ($i = 1, ..., N - 1$), we define the following states:

$$\{h_i(t) = j\} \equiv \{b_i \text{ contains } j \text{ parts at the end of time slot } t\} \tag{2.1}$$

For machine m_i ($i = 1, ..., N$), during time slot t, we define the following states:

$$\begin{aligned}
&\{m_i \text{ up}\} \equiv \{m_i \text{ is up}\} \\
&\{m_i \text{ dn}\} \equiv \{m_i \text{ is down}\} \\
&\{m_i \text{ pr}\} \equiv \{m_i \text{ is processing a part}\} \\
&\{m_i \text{ id}\} \equiv \{m_i \text{ is idle}\} \\
&\{m_i \text{ st}\} \equiv \{m_i \text{ is starved}\} \\
&\{m_i \text{ bl}\} \equiv \{m_i \text{ is blocked}\}
\end{aligned} \tag{2.2}$$

The decomposition of these machine states are illustrated in Figure 2.2.

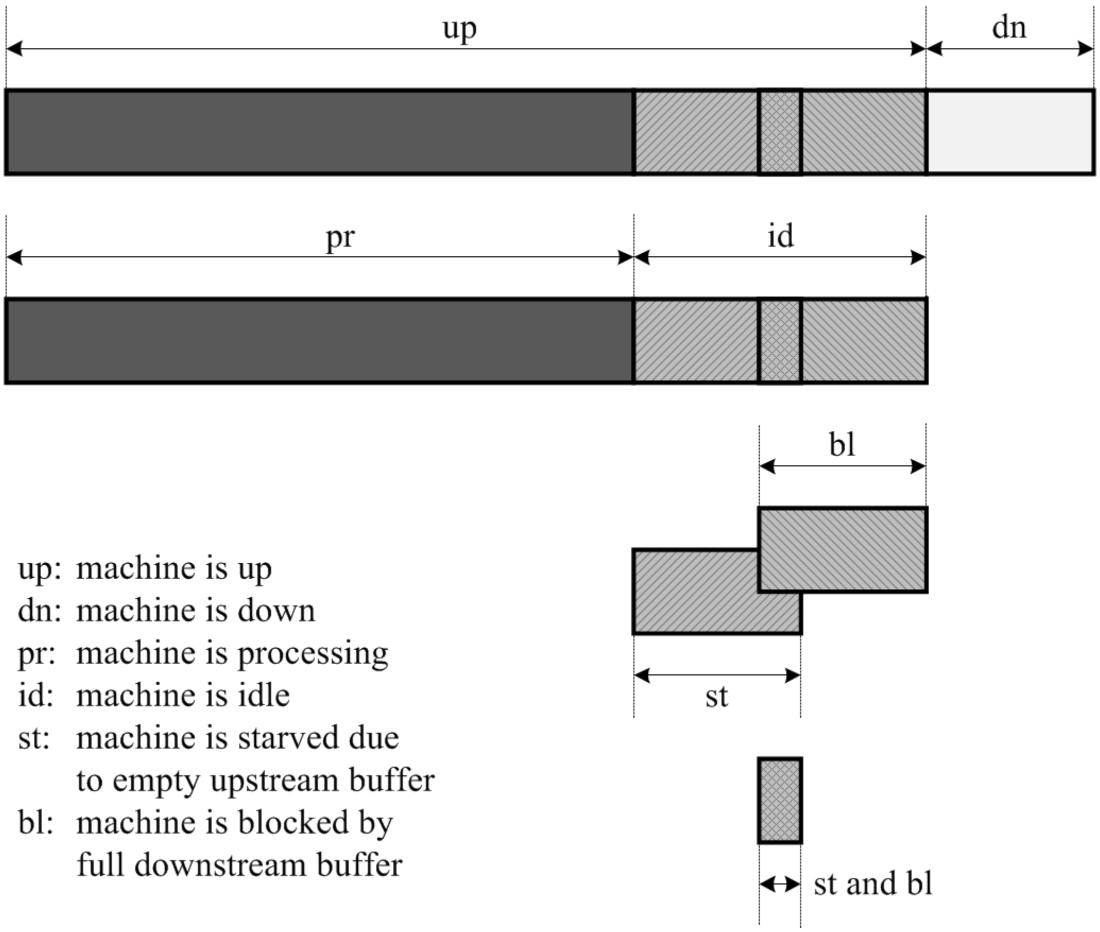

Figure 2.2. Decomposition of machine states

Furthermore, we define the following three negation states for machine m_i:

$$\begin{aligned}
&\{m_i \text{ npr}\} \equiv \{m_i \text{ is not processing any part}\} \\
&\{m_i \text{ nst}\} \equiv \{m_i \text{ is not starved}\} \\
&\{m_i \text{ nbl}\} \equiv \{m_i \text{ is not blocked}\}
\end{aligned} \tag{2.3}$$

The relationships between these machine states can be mathematically interpreted as follows. Let Ω be the state sample space of machine m_i (i = 1, ..., N). Then during time slot t:

$$
\begin{aligned}
&\Omega = \{m_i \text{ up}\} \bigcup \{m_i \text{ dn}\} \\
&\{m_i \text{ up}\} = \{m_i \text{ pr}\} \bigcup \{m_i \text{ st}\} \bigcup \{m_i \text{ bl}\} \\
&\{m_i \text{ up}\} \bigcap \{m_i \text{ dn}\} = \varnothing \\
&\{m_i \text{ pr}\} \bigcap \{m_i \text{ st}\} = \varnothing \\
&\{m_i \text{ pr}\} \bigcap \{m_i \text{ bl}\} = \varnothing \\
&\{m_i \text{ pr}\} = \{m_i \text{ up}\} \bigcap \{m_i \text{ nst}\} \bigcap \{m_i \text{ nbl}\} \\
&\{m_i \text{ npr}\} = \{m_i \text{ dn}\} \bigcup \{m_i \text{ st}\} \bigcup \{m_i \text{ bl}\} \\
&\{m_1 \text{ st}\} = \varnothing \\
&\{m_N \text{ bl}\} = \varnothing
\end{aligned} \tag{2.4}
$$

2.2.3. Buffer state transition probabilities

Let $Q_{i,(j_2|j_1)}(t)$ be the transition probability from state j_1 to j_2 during time slot t for buffer b_i ($i = 1, \ldots, N-1$). Since the occupancy of buffer b_i can change at most by one part in each time slot, the state transition diagram of b_i is shown in Figure 2.3.

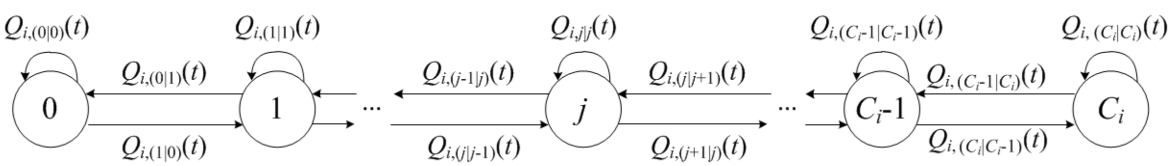

Figure 2.3. State transition diagram of b_i ($i = 1, \ldots, N-1$) during time slot t

During time slot t, the transition matrix of buffer b_i ($i = 1, \ldots, N-1$) can be represented as

$$
\mathbf{Q}_i(t) = \begin{bmatrix}
Q_{i,(0|0)}(t) & Q_{i,(0|1)}(t) & & & & & & \\
Q_{i,(1|0)}(t) & Q_{i,(1|1)}(t) & \ddots & & & & & \\
& \ddots & \ddots & \ddots & & & & \\
& & \ddots & Q_{i,(j|j)}(t) & Q_{i,(j|j+1)}(t) & & & \\
& & & Q_{i,(j+1|j)}(t) & Q_{i,(j+1|j+1)}(t) & \ddots & & \\
& & & & \ddots & \ddots & \ddots & \\
& & & & & \ddots & Q_{i,(C_i-1|C_i-1)}(t) & Q_{i,(C_i-1|C_i)}(t) \\
& & & & & & Q_{i,(C_i|C_i-1)}(t) & Q_{i,(C_i|C_i)}(t)
\end{bmatrix} \tag{2.5}
$$

Before deriving the expression of each transition probability element in the transition matrix, we introduce the following four lemmas.

Lemma 1: Let $\mathcal{A}$, $\mathcal{B}$, and $\mathcal{C}$ be three sets. If $\mathcal{C} \subseteq \mathcal{B}$, then $\Pr(\mathcal{AB} \mid \mathcal{C}) = \Pr(\mathcal{A} \mid \mathcal{C})$.

Proof: According to the conditional probability formula, we have

$$\Pr(\mathcal{AB} \mid \mathcal{C}) = \frac{\Pr(\mathcal{ABC})}{\Pr(\mathcal{C})} = \frac{\Pr(\mathcal{AC})}{\Pr(\mathcal{C})} = \Pr(\mathcal{A} \mid \mathcal{C}) \tag{2.6}$$

■

Lemma 2: Let $\mathcal{A}$, $\mathcal{B}$, and $\mathcal{C}$ be three sets. If $\Pr(\mathcal{A} \mid \mathcal{BC}) = 0$, then $\Pr(\mathcal{AB} \mid \mathcal{C}) = 0$.

Proof: According to the conditional probability formula, we have

$$\Pr(\mathcal{AB} \mid \mathcal{C}) = \frac{\Pr(\mathcal{ABC})}{\Pr(\mathcal{C})} = \frac{\Pr(\mathcal{A} \mid \mathcal{BC})\Pr(\mathcal{BC})}{\Pr(\mathcal{C})} = 0 \tag{2.7}$$

■

Lemma 3: Let $\mathcal{A}$, $\mathcal{B}$, and $\mathcal{C}$ be three sets. If $\Pr(\mathcal{A} \mid \mathcal{BC}) = 1$, then $\Pr(\mathcal{AB} \mid \mathcal{C}) = \Pr(\mathcal{B} \mid \mathcal{C})$.

Proof: According to the conditional probability formula, we have

$$\Pr(\mathcal{AB} \mid \mathcal{C}) = \frac{\Pr(\mathcal{ABC})}{\Pr(\mathcal{C})} = \frac{\Pr(\mathcal{A} \mid \mathcal{BC})\Pr(\mathcal{BC})}{\Pr(\mathcal{C})} = \frac{\Pr(\mathcal{BC})}{\Pr(\mathcal{C})} = \Pr(\mathcal{B} \mid \mathcal{C}) \tag{2.8}$$

■

Lemma 4: Let $\mathcal{A}$, $\mathcal{B}$, $\mathcal{C}$, and $\mathcal{D}$ be four sets. If $\mathcal{CD} \subseteq \mathcal{B}$, then $\Pr(\mathcal{ABC} \mid \mathcal{D}) = \Pr(\mathcal{AC} \mid \mathcal{D})$.

Proof: According to the conditional probability formula, we have

$$\Pr(\mathcal{ABC} \mid \mathcal{D}) = \frac{\Pr(\mathcal{ABCD})}{\Pr(\mathcal{D})} = \frac{\Pr(\mathcal{ACD})}{\Pr(\mathcal{D})} = \Pr(\mathcal{AC} \mid \mathcal{D}) \tag{2.9}$$

■

Based on these lemmas, we can derive the expression of transition probability of buffer b_i from state 0 to state 0 during time slot t:

$$
\begin{aligned}
Q_{i,(0|0)}(t) &= \Pr[\{h_i(t)=0\} \,|\, \{h_i(t-1)=0\}] \\
&= \Pr[\{m_i \text{ npr}\} \cap \cancel{\{m_{i+1} \text{ npr}\}} \,|\, \{h_i(t-1)=0\}] \\
&= \Pr[\{m_i \text{ dn}\} \cup \{m_i \text{ st}\} \cup \cancel{\{m_i \text{ bl}\}} \,|\, \{h_i(t-1)=0\}] \\
&= \Pr[\{m_i \text{ dn}\} \cup \{m_i \text{ st}\}] \\
&= 1 - p_i + ST_i(t), \ (C_i \geq 1)
\end{aligned}
\tag{2.10}
$$

where the deletion of $\cancel{\{m_{i+1} \text{ npr}\}}$ and $\cancel{\{m_i \text{ bl}\}}$ from the equation is due to

$$
\begin{aligned}
&\{h_i(t-1)=0\} \subseteq \{m_{i+1} \text{ npr}\}, \ \text{(Lemma 1)} \\
&\Pr[\{m_i \text{ bl}\} \,|\, \{h_i(t-1)=0\}] = 0
\end{aligned}
\tag{2.11}
$$

The expression of transition probability from state 1 to state 0 is

$$
\begin{aligned}
Q_{i,(0|1)}(t) &= \Pr[\{h_i(t)=0\} \,|\, \{h_i(t-1)=1\}] \\
&= \Pr[\{m_i \text{ npr}\} \cap \{m_{i+1} \text{ pr}\} \,|\, \{h_i(t-1)=1\}] \\
&= \Pr[(\{m_i \text{ dn}\} \cup \{m_i \text{ st}\} \cup \cancel{\{m_i \text{ bl}\}}) \cap \{m_{i+1} \text{ pr}\} \,|\, \{h_i(t-1)=1\}] \\
&= \Pr[(\{m_1 \text{ dn}\} \cup \{m_i \text{ st}\}) \cap (\{m_{i+1} \text{ up}\} \cap \cancel{\{m_{i+1} \text{ nst}\}} \cap \{m_{i+1} \text{ nbl}\}) \,|\, \{h_i(t-1)=1\}] \\
&= \Pr[(\{m_1 \text{ dn}\} \cup \{m_i \text{ st}\}) \cap (\{m_{i+1} \text{ up}\} \cap \{m_{i+1} \text{ nbl}\})] \\
&= [1 - p_i + ST_i(t)][p_{i+1} - BL_{i+1}(t)], \ (C_i \geq 1)
\end{aligned}
\tag{2.12}
$$

where the deletion of $\cancel{\{m_i \text{ bl}\}}$ and $\cancel{\{m_{i+1} \text{ nst}\}}$ from the equation is due to

$$
\begin{aligned}
&\Pr[\{m_i \text{ bl}\} \,|\, \{m_{i+1} \text{ pr}\} \cap \{h_i(t-1)=1\}] = 0, \ \text{(Lemma 2)} \\
&\{h_i(t-1)=1\} \subseteq \{m_{i+1} \text{ nst}\}, \ \text{(Lemma 1)}
\end{aligned}
\tag{2.13}
$$

The expression of transition probability from state 0 to state 1 is

$$
\begin{aligned}
Q_{i,(1|0)}(t) &= \Pr[\{h_i(t)=1\} \,|\, \{h_i(t-1)=0\}] \\
&= \Pr[\{m_i \text{ pr}\} \cap \cancel{\{m_{i+1} \text{ npr}\}} \,|\, \{h_i(t-1)=0\}] \\
&= \Pr[\{m_i \text{ up}\} \cap \{m_i \text{ nst}\} \cap \cancel{\{m_i \text{ nbl}\}} \,|\, \{h_i(t-1)=0\}] \\
&= \Pr[\{m_i \text{ up}\} \cap \{m_i \text{ nst}\}] \\
&= p_i - ST_i(t), \ (C_i \geq 1)
\end{aligned}
\tag{2.14}
$$

where the deletion of $\cancel{\{m_{i+1} \text{ npr}\}}$ and $\cancel{\{m_i \text{ nbl}\}}$ from the equation is due to

$$\begin{aligned}
&\{h_i(t-1)=0\} \subseteq \{m_{i+1} \text{ npr}\}, \text{ (Lemma 1)} \\
&\{h_i(t-1)=0\} \subseteq \{m_i \text{ nbl}\}, \text{ (Lemma 1)}
\end{aligned} \tag{2.15}$$

The expression of transition probability from state j to state j is

$$\begin{aligned}
Q_{i,(j|j)}(t) &= \Pr[\{h_i(t)=j\} \,|\, \{h_i(t-1)=j\}] \\
&= \Pr[(\{m_i \text{ pr}\} \cap \{m_{i+1} \text{ pr}\}) \cup (\{m_i \text{ npr}\} \cap \{m_{i+1} \text{ npr}\}) \,|\, \{h_i(t-1)=j\}] \\
&= \Pr[(\{m_i \text{ pr}\} \cap \{m_{i+1} \text{ pr}\} \,|\, \{h_i(t-1)=j\}) \\
&\quad + \Pr[(\{m_i \text{ npr}\} \cap \{m_{i+1} \text{ npr}\}) \,|\, \{h_i(t-1)=j\}] \\
&= \Pr[\{m_i \text{ up}\} \cap \{m_i \text{ nst}\} \cap \cancel{\{m_i \text{ nbl}\}} \cap \{m_{i+1} \text{ up}\} \cap \cancel{\{m_{i+1} \text{ nst}\}} \cap \{m_{i+1} \text{ nbl}\} \,|\, \{h_i(t-1)=j\}] \\
&\quad + \Pr[(\{m_i \text{ dn}\} \cup \{m_i \text{ st}\} \cup \cancel{\{m_i \text{ bl}\}}) \cap (\{m_{i+1} \text{ dn}\} \cup \cancel{\{m_{i+1} \text{ st}\}} \cup \{m_{i+1} \text{ bl}\}) \,|\, \{h_i(t-1)=j\}] \\
&= \Pr[\{m_i \text{ up}\} \cap \{m_i \text{ nst}\} \cap \{m_{i+1} \text{ up}\} \cap \{m_{i+1} \text{ nbl}\}] \\
&\quad + \Pr[(\{m_i \text{ dn}\} \cup \{m_i \text{ st}\}) \cap (\{m_{i+1} \text{ dn}\} \cup \{m_{i+1} \text{ bl}\})] \\
&= [p_i - ST_i(t)][p_{i+1} - BL_{i+1}(t)] \\
&\quad + [1 - p_i + ST_i(t)][1 - p_{i+1} + BL_{i+1}(t)], \ (j=1,\ldots,C_i-1;\ C_i \geq 2)
\end{aligned} \tag{2.16}$$

where the deletion of $\cancel{\{m_i \text{ nbl}\}}$, $\cancel{\{m_{i+1} \text{ nst}\}}$, $\cancel{\{m_i \text{ bl}\}}$, and $\cancel{\{m_{i+1} \text{ st}\}}$ from the equation is due to

$$\begin{aligned}
&\{h_i(t-1)=j\} \subseteq \{m_i \text{ nbl}\}, \text{ (Lemma 1)} \\
&\{h_i(t-1)=j\} \subseteq \{m_{i+1} \text{ nst}\}, \text{ (Lemma 1)} \\
&\Pr[\{m_i \text{ bl}\} \,|\, \{h_i(t-1)=j\}] = 0 \\
&\Pr[\{m_{i+1} \text{ st}\} \,|\, \{h_i(t-1)=j\}] = 0
\end{aligned} \tag{2.17}$$

The expression of transition probability from state $j + 1$ to state j is

$$\begin{aligned}
Q_{i,(j|j+1)}(t) &= \Pr[\{h_i(t)=j\} \,|\, \{h_i(t-1)=j+1\}] \\
&= \Pr[\{m_i \text{ npr}\} \cap \{m_{i+1} \text{ pr}\} \,|\, \{h_i(t-1)=j+1\}] \\
&= \Pr[(\{m_i \text{ dn}\} \cup \{m_i \text{ st}\} \cup \cancel{\{m_i \text{ bl}\}}) \cap \{m_{i+1} \text{ pr}\} \,|\, \{h_i(t-1)=j+1\}] \\
&= \Pr[(\{m_i \text{ dn}\} \cup \{m_i \text{ st}\}) \cap (\{m_{i+1} \text{ up}\} \cap \cancel{\{m_{i+1} \text{ nst}\}} \cap \{m_{i+1} \text{ nbl}\}) \,|\, \{h_i(t-1)=j+1\}] \\
&= \Pr[(\{m_i \text{ dn}\} \cup \{m_i \text{ st}\}) \cap (\{m_{i+1} \text{ up}\} \cap \{m_{i+1} \text{ nbl}\})] \\
&= [1 - p_i + ST_i(t)][p_{i+1} - BL_{i+1}(t)], \ (j=1,\ldots,C_i-1; C_i \geq 2)
\end{aligned} \tag{2.18}$$

where the deletion of $\cancel{\{m_i \text{ bl}\}}$, and $\cancel{\{m_{i+1} \text{ nst}\}}$ from the equation is due to

$$\begin{aligned}&\Pr[\{m_i\ \text{bl}\}\,|\,\{m_{i+1}\ \text{pr}\}\cap\{h_i(t-1)=j+1\}]=0,\ \text{(Lemma 2)}\\&\{h_i(t-1)=j+1\}\subseteq\{m_{i+1}\ \text{nst}\}=1,\ \text{(Lemma 1)}\end{aligned}\tag{2.19}$$

The expression of transition probability from state j to state j + 1 is

$$\begin{aligned}Q_{i,(j+1|j)}(t)&=\Pr[\{h_i(t)=j+1\}\,|\,\{h_i(t-1)=j\}]\\&=\Pr[\{m_i\ \text{pr}\}\cap\{m_{i+1}\ \text{npr}\}\,|\,\{h_i(t-1)=j\}]\\&=\Pr[\{m_i\ \text{up}\}\cap\{m_i\ \text{nst}\}\cap\cancel{\{m_i\ \text{nbl}\}}\cap(\{m_{i+1}\ \text{dn}\}\cup\cancel{\{m_{i+1}\ \text{st}\}}\cup\{m_{i+1}\ \text{bl}\})\,|\,\{h_i(t-1)=j\}]\\&=\Pr[\{m_i\ \text{up}\}\cap\{m_i\ \text{nst}\}\cap(\{m_{i+1}\ \text{dn}\}\cup\{m_{i+1}\ \text{bl}\})]\\&=[p_i-ST_i(t)][1-p_{i+1}+BL_{i+1}(t)],\ (j=1,...,C_i-1;C_i\ge 2)\end{aligned}\tag{2.20}$$

where the deletion of $\cancel{\{m_i\ \text{nbl}\}}$, and $\cancel{\{m_{i+1}\ \text{st}\}}$ from the equation is due to

$$\begin{aligned}&\{h_i(t-1)=j\}\subseteq\{m_i\ \text{nbl}\},\ \text{(Lemma 1)}\\&\Pr[\{m_{i+1}\ \text{st}\}\,|\,\{h_i(t-1)=j\}]=0\end{aligned}\tag{2.21}$$

The expression of transition probability from state C_i to state C_i is

$$\begin{aligned}Q_{i,(C_i|C_i)}(t)&=\Pr[\{h_i(t)=C_i\}\,|\,\{h_i(t-1)=C_i\}]\\&=\Pr[(\{m_i\ \text{pr}\}\cap\{m_{i+1}\ \text{pr}\})\cup(\{m_i\ \text{npr}\}\cap\{m_{i+1}\ \text{npr}\})\,|\,\{h_i(t-1)=C_i\}]\\&=\Pr[\{m_i\ \text{pr}\}\cap\{m_{i+1}\ \text{pr}\}\,|\,\{h_i(t-1)=C_i\}]\\&\quad+\Pr[\cancel{\{m_i\ \text{npr}\}}\cap\{m_{i+1}\ \text{npr}\}\,|\,\{h_i(t-1)=C_i\}]\\&=\Pr[\{m_i\ \text{up}\}\cap\{m_i\ \text{nst}\}\cap\cancel{\{m_i\ \text{nbl}\}}\cap\{m_{i+1}\ \text{pr}\}\,|\,\{h_i(t-1)=C_i\}]\\&\quad+\Pr[\{m_{i+1}\ \text{dn}\}\cup\cancel{\{m_{i+1}\ \text{st}\}}\cup\{m_{i+1}\ \text{bl}\}\,|\,\{h_i(t-1)=C_i\}]\\&=\Pr[\{m_i\ \text{up}\}\cap\{m_i\ \text{nst}\}\cap(\{m_{i+1}\ \text{up}\}\cap\cancel{\{m_{i+1}\ \text{nst}\}}\cap\{m_{i+1}\ \text{nbl}\})\,|\,\{h_i(t-1)=C_i\}]\\&\quad+\Pr[\{m_{i+1}\ \text{dn}\}\cup\{m_{i+1}\ \text{bl}\}]\\&=\Pr[\{m_i\ \text{up}\}\cap\{m_i\ \text{nst}\}\cap(\{m_{i+1}\ \text{up}\}\cap\{m_{i+1}\ \text{nbl}\})]+\Pr[\{m_{i+1}\ \text{dn}\}\cup\{m_{i+1}\ \text{bl}\}]\\&=[p_i-ST_i(t)][p_{i+1}-BL_{i+1}(t)]+[1-p_{i+1}+BL_{i+1}(t)],\ (C_i\ge 1)\end{aligned}\tag{2.22}$$

where the deletion of $\cancel{\{m_i\ \text{npr}\}}$, $\cancel{\{m_i\ \text{nbl}\}}$, $\cancel{\{m_{i+1}\ \text{st}\}}$, and $\cancel{\{m_{i+1}\ \text{nst}\}}$ is due to

$$\begin{aligned}&\Pr[\{m_i\ \text{npr}\}\,|\,\{m_{i+1}\ \text{npr}\}\cap\{h_i(t-1)=C_i\}]=1,\ \text{(Lemma 3)}\\&\{m_{i+1}\ \text{pr}\}\cap\{h_i(t-1)=C_i\}\subseteq\{m_i\ \text{nbl}\},\ \text{(Lemma 4)}\\&\Pr[\{m_{i+1}\ \text{st}\}\,|\,\{h_i(t-1)=C_i\}]=0\\&\{h_i(t-1)=C_i\}\subseteq\{m_{i+1}\ \text{nst}\},\ \text{(Lemma 1)}\end{aligned}\tag{2.23}$$

2.2.4. Transients and steady state of the manufacturing system

Let $q_{i,j}(t)$ be the probability of buffer b_i ($i = 1, \ldots, N - 1$) in state j ($j = 0, \ldots, C_i$) at the end of time slot t. According to the law of total probability, the evolution of $q_{i,j}(t)$ can be described by the following constrained non-linear dynamics system:

$$q_{i,j}(t) = \sum_{k=0}^{C_i} Q_{i,(j|k)}(t) q_{i,k}(t-1),\ (j = 0, \ldots, C_i) \tag{2.24}$$

After we substitute the transition probabilities $Q_{i,(j|k)}(t)$ with the derived equations in the previous subsection, the dynamics equation (2.24) of buffer b_i ($i = 1, \ldots, N - 1$) are re-written as

$$\begin{aligned}
q_{i,0}(t) &= Q_{i,(0|0)}(t)q_{i,0}(t-1) + Q_{i,(0|1)}(t)q_{i,1}(t-1) \\
&= [1 - p_i + ST_i(t)]q_{i,0}(t-1) + [1 - p_i + ST_i(t)][p_{i+1} - BL_{i+1}(t)]q_{i,1}(t-1),\ (C_i \ge 1) \\
q_{i,1}(t) &= Q_{i,(1|0)}(t)q_{i,0}(t-1) + Q_{i,(1|1)}(t)q_{i,1}(t-1) + Q_{i,(1|2)}(t)q_{i,2}(t-1) \\
&= [p_i - ST_i(t)]q_{i,0}(t-1) \\
&\quad + \{[p_i - ST_i(t)][p_{i+1} - BL_{i+1}(t)] + [1 - p_i + ST_i(t)][1 - p_{i+1} + BL_{i+1}(t)]\}q_{i,1}(t-1) \\
&\quad + [1 - p_i + ST_i(t)][p_{i+1} - BL_{i+1}(t)]q_{i,2}(t-1),\ (C_i \ge 2) \\
&\ldots \\
q_{i,j}(t) &= Q_{i,(j|j-1)}(t)q_{i,j-1}(t-1) + Q_{i,(j|j)}(t)q_{i,j}(t-1) + Q_{i,(j|j+1)}(t)q_{i,j+1}(t-1) \\
&= [p_i - ST_i(t)][1 - p_{i+1} + BL_{i+1}(t)]q_{i,j-1}(t-1) \\
&\quad + \{[p_i - ST_i(t)][p_{i+1} - BL_{i+1}(t)] + [1 - p_i + ST_i(t)][1 - p_{i+1} + BL_{i+1}(t)]\}q_{i,j}(t-1) \\
&\quad + [1 - p_i + ST_i(t)][p_{i+1} - BL_{i+1}(t)]q_{i,j+1}(t-1),\ (j = 2, \ldots, C_i - 1; C_i \ge 3) \\
&\ldots \\
q_{i,C_i}(t) &= Q_{i,(C_i|C_i-1)}(t)q_{i,C_i-1}(t-1) + Q_{i,(C_i|C_i)}(t)q_{i,C_i}(t-1) \\
&= [p_i - ST_i(t)][1 - p_{i+1} + BL_{i+1}(t)]q_{i,C_i-1}(t-1) \\
&\quad + \{[p_i - ST_i(t)][p_{i+1} - BL_{i+1}(t)] + [1 - p_{i+1} + BL_{i+1}(t)]\}q_{i,C_i}(t-1),\ (C_i \ge 2) \\
q_{i,C_i}(t) &= Q_{i,(C_i|C_i-1)}(t)q_{i,C_i-1}(t-1) + Q_{i,(C_i|C_i)}(t)q_{i,C_i}(t-1) \\
&= [p_i - ST_i(t)]q_{i,C_i-1}(t-1) \\
&\quad + \{[p_i - ST_i(t)][p_{i+1} - BL_{i+1}(t)] + [1 - p_{i+1} + BL_{i+1}(t)]\}q_{i,C_i}(t-1),\ (C_i = 1)
\end{aligned} \tag{2.25}$$

The following constraint also applies:

$$\sum_{j=0}^{C_i} q_{i,j}(t) = 1 \tag{2.26}$$

The steady state of the system above is described by the balance equations

$$q_{i,j} = \sum_{k=0}^{C_i} Q_{i,(j|k)} q_{i,k}, \ (j = 0, \ldots, C_i) \tag{2.27}$$

$$\sum_{j=0}^{C_i} q_{i,j} = 1 \tag{2.28}$$

2.2.5. Performance measures

Since the first machine is never starved, the probability of starvation of machine m_1 during time slot t is

$$ST_1(t) = \Pr[\{m_1 \text{ st}\}] = 0 \tag{2.29}$$

The probability of starvation of machine m_i (i = 2, …, N) during time slot t is

$$\begin{aligned} ST_i(t) &= \Pr[\{m_i \text{ st}\}] \\ &= \Pr[\{m_i \text{ up}\} \cap \{h_{i-1}(t-1) = 0\}] \\ &= p_i q_{i-1,0}(t-1) \end{aligned} \tag{2.30}$$

Since the last machine is never blocked, the probability of blockage of machine m_N during time slot t is

$$BL_N(t) = \Pr[\{m_N \text{ bl}\}] = 0 \tag{2.31}$$

The probability of blockage of machine m_i (i = 1, …, $N-1$) during time slot t is

$$\begin{aligned} BL_i(t) &= \Pr[\{m_i \text{ bl}\}] \\ &= \Pr[\{m_i \text{ up}\} \cap \{h_i(\mathrm{t}-1) = C_i\} \cap \{m_{i+1} \text{ npr}\}] \\ &= \Pr[\{m_i \text{ up}\} \cap \{h_i(\mathrm{t}-1) = C_i\} \cap (\{m_{i+1} \text{ dn}\} \cup \cancel{\{m_{i+1} \text{ st}\}} \cup \{m_{i+1} \text{ bl}\})] \\ &= \Pr[\{m_i \text{ up}\} \cap \{h_i(\mathrm{t}-1) = C_i\} \cap (\{m_{i+1} \text{ dn}\} \cup \{m_{i+1} \text{ bl}\})] \\ &= p_i q_{i,C_i}(t-1)[1 - p_{i+1} + BL_{i+1}(t)] \end{aligned} \tag{2.32}$$

The probability of simultaneous blockage and starvation of machine m_i (i = 1 or N) during time slot t is

$$BS_i(t) = \Pr[\{m_i \text{ bl}\} \cap \{m_i \text{ st}\}] = 0 \tag{2.33}$$

The probability of simultaneous blockage and starvation of machine m_i (i = 2, …, $N-1$) during time slot t is

$$\begin{aligned} BS_i(t) &= \Pr[\{m_i \text{ bl}\} \cap \{m_i \text{ st}\}] \\ &= \Pr[\{m_i \text{ up}\} \cap \{h_i(t) = C_i\} \cap \{m_{i+1} \text{ npr}\} \cap \cancel{\{m_i \text{ up}\}} \cap \{h_{i-1}(t-1) = 0\} \\ &= \Pr\{\{m_i \text{ up}\} \cap \{h_i(t) = C_i\} \cap [\{m_{i+1} \text{ dn}\} \cup \cancel{\{m_{i+1} \text{ st}\}} \cup \{m_{i+1} \text{ bl}\}] \cap \{h_{i-1}(t-1) = 0\}\} \\ &= p_i q_{i,C_i}(t-1)[1 - p_{i+1} + BL_{i+1}(t)] q_{i-1,0}(t-1) \end{aligned} \tag{2.34}$$

The probability of machine m_i (i = 1, …, N) being idle during time slot t is

$$ID_i(t) = BL_i(t) + ST_i(t) - BS_i(t) \tag{2.35}$$

The work-in-process of buffer b_i (i = 1, …, N − 1) at the end of time slot t is

$$WIP_i(t) = \sum_{j=0}^{C_i} j q_{i,j}(t) \tag{2.36}$$

The total work-in-process of the system at the end of time slot t is

$$WIP_{SYS}(t) = \sum_{i=1}^{N-1} WIP_i(t) \tag{2.37}$$

The production rate of machine m_i (i = 1, …, N) during time slot t is

$$PR_i(t) = p_i - ID_i(t) \tag{2.38}$$

The production rate of the system during time slot t is equal to the production rate of the last machine m_N, i.e.,

$$PR_{SYS}(t) = PR_N(t) \tag{2.39}$$

The average cumulative production of the system during the planning horizon of T time slots is

$$CP_T = \sum_{t=1}^{T} PR_{SYS}(t) \tag{2.40}$$

2.3. Solving the MSM Dynamics using the Fixed-Point Method

2.3.1. Solution existence of the MSM dynamics equations

For each buffer, the dynamics system (2.25) contains C_i + 1 equations. Therefore, for the N − 1 buffer manufacturing system, the MSM contains a total of $V = \sum_{i=1}^{N-1}(C_i + 1)$ equations.

Define a column vector consisting of the V variables:

$$\mathbf{X}(t) \equiv [q_{1,0}(t),\ \ldots,\ q_{1,C_1}(t),\ \ \ldots\ldots,\ \ q_{i,0}(t),\ \ldots,\ q_{i,C_i}(t),\ \ \ldots\ldots,\ \ q_{N-1,0}(t),\ \ldots,\ q_{N-1,C_{N-1}}(t)]^{\mathrm{T}} \quad (2.41)$$

Let

$$\mathbf{q}_i(t) \equiv [q_{i,0}(t),\ \ldots,\ q_{i,C_i}(t)]^{\mathrm{T}},\ i=1,\ \ldots,\ N-1 \quad (2.42)$$

Then

$$\mathbf{X}(t) \equiv \begin{bmatrix} \mathbf{q}_1(t) \\ \vdots \\ \mathbf{q}_i(t) \\ \vdots \\ \mathbf{q}_{N\text{-}1}(t) \end{bmatrix} \quad (2.43)$$

After substituting ST's and BL's (i.e. equations (2.29)-(2.32)) into MSM dynamics system (2.25), the dynamics of the system is formulated in a fixed-point iteration format:

$$\mathbf{X}(t) = G[\mathbf{X}(t-1)] \quad (2.44)$$

where $G(\boldsymbol{X}) = [g_1(\boldsymbol{X}), \ldots, g_V(\boldsymbol{X})]^{\mathrm{T}}$ are the right-hand side of the equal signs in equation (2.25) in order from top to bottom and from the first buffer to the last. The solution (i.e. the fixed point) of the formulation satisfies $\mathbf{X}^* = G(\mathbf{X}^*)$. Let D be the definition domain of **X**, i.e.

$$\begin{aligned} D \equiv \{[q_{1,0},\ \ldots,\ q_{1,C_1},\ \ \ldots\ldots,\ \ q_{i,0},\ \ldots,\ q_{i,C_i},\ \ \ldots\ldots,\ \ q_{N-1,0},\ \ldots,\ q_{N-1,C_{N-1}}]^{\mathrm{T}} \mid 0 \le q_{i,j} \le 1, \\ \textstyle\sum_{j=0}^{C_i} q_{i,j} = 1,\ \text{for } i=1,\ldots,N-1;\ j=1,\ldots,C_i\} \end{aligned} \quad (2.45)$$

We introduce Brouwer fixed-point theorem and the following three lemmas.

Theorem 1 (Brouwer Fixed-Point Theorem): Every continuous function from a convex compact subset of a Euclidean space to the subset itself has a fixed point.

Proof: See (Border, 1985, p29). ■

Lemma 5: Function G(**X**) is continuous and Fréchet differentiable in D.

Proof: It is easy to see that each element g_i(**X**) (i = 1, …, V) in G(**X**) is a continuous and

Fréchet differentiable function in D, which is a necessary and sufficient condition for $G(\mathbf{X})$ being continuous and Fréchet differentiable in D. ■

Lemma 6: D is a convex compact set in $\mathbb{R}^V$.

Proof: Let

$$\begin{aligned}\mathbf{X} &\equiv [q_{1,0}^x,\ \ldots,\ q_{1,C_1}^x,\ \ \ldots\ldots,\ \ q_{i,0}^x,\ \ldots,\ q_{i,C_i}^x,\ \ \ldots\ldots,\ \ q_{N-1,0}^x,\ \ldots,\ q_{N-1,C_{N-1}}^x]^{\mathrm{T}} \in D \\ \mathbf{Y} &\equiv [q_{1,0}^y,\ \ldots,\ q_{1,C_1}^y,\ \ \ldots\ldots,\ \ q_{i,0}^y,\ \ldots,\ q_{i,C_i}^y,\ \ \ldots\ldots,\ \ q_{N-1,0}^y,\ \ldots,\ q_{N-1,C_{N-1}}^y]^{\mathrm{T}} \in D\end{aligned} \tag{2.46}$$

For $0 \le \lambda \le 1$, we have

$$\begin{aligned}\mathbf{Z} &= \lambda\mathbf{X} + (1-\lambda)\mathbf{Y} \\ &= \lambda[q_{1,0}^x,\ \ldots,\ q_{1,C_1}^x,\ \ \ldots\ldots,\ \ q_{i,0}^x,\ \ldots,\ q_{i,C_i}^x,\ \ \ldots\ldots,\ \ q_{N-1,0}^x,\ \ldots,\ q_{N-1,C_{N-1}}^x]^{\mathrm{T}} \\ &\quad + (1-\lambda)[q_{1,0}^y,\ \ldots,\ q_{1,C_1}^y,\ \ \ldots\ldots,\ \ q_{i,0}^y,\ \ldots,\ q_{i,C_i}^y,\ \ \ldots\ldots,\ \ q_{N-1,0}^y,\ \ldots,\ q_{N-1,C_{N-1}}^y]^{\mathrm{T}} \\ &= [\lambda q_{1,0}^x + (1-\lambda)q_{1,0}^y,\ \ldots,\ \lambda q_{1,C_1}^x + (1-\lambda)q_{1,C_1}^y,\ \ \ldots\ldots, \\ &\qquad \lambda q_{i,0}^x + (1-\lambda)q_{i,0}^y,\ \ldots,\ \lambda q_{i,C_i}^x + (1-\lambda)q_{i,C_i}^y,\ \ \ldots\ldots, \\ &\qquad \lambda q_{N-1,0}^x + (1-\lambda)q_{N-1,0}^y,\ \ldots,\ \lambda q_{N-1,C_{N-1}}^x + (1-\lambda)q_{N-1,C_{N-1}}^y]^{\mathrm{T}}\end{aligned} \tag{2.47}$$

We denote

$$\mathbf{Z} \equiv [q_{1,0}^z,\ \ldots,\ q_{1,C_1}^z,\ \ \ldots\ldots,\ \ q_{i,0}^z,\ \ldots,\ q_{i,C_i}^z,\ \ \ldots\ldots,\ \ q_{N-1,0}^z,\ \ldots,\ q_{N-1,C_{N-1}}^z]^{\mathrm{T}} \tag{2.48}$$

where $q_{i,j}^z = \lambda q_{i,j}^x + (1-\lambda)q_{i,j}^y$ ($i = 1, \ldots, N-1$; $j=1, \ldots, C_i - 1$). It is obvious that $q_{i,j}^z \ge 0$ and

$$\sum\nolimits_{j=0}^{C_i} q_{i,j}^z = \lambda \sum\nolimits_{j=0}^{C_i} q_{i,j}^x + (1-\lambda)\sum\nolimits_{j=0}^{C_i} q_{i,j}^y = \lambda + (1-\lambda) = 1 \tag{2.49}$$

This leads to $q_{i,j}^z \le 1$. Therefore, $\mathbf{Z} \in D$, which proves D is a convex compact set in $\mathbb{R}^V$. ■

Lemma 7: Function $G(\boldsymbol{X})$ maps D to itself.

Proof: Let

$$\mathbf{X} \equiv [q_{1,0}^x,\ \ldots,\ q_{1,C_1}^x,\ \ \ldots\ldots,\ \ q_{i,0}^x,\ \ldots,\ q_{i,C_i}^x,\ \ \ldots\ldots,\ \ q_{N-1,0}^x,\ \ldots,\ q_{N-1,C_{N-1}}^x]^{\mathrm{T}} \in D \tag{2.50}$$

$$\mathbf{Y} = G(\mathbf{X}) \tag{2.51}$$

We denote

$$\mathbf{Y} \equiv [q^y_{1,0},\ ...,\ q^y_{1,C_1},\ \ ......,\ \ q^y_{i,0},\ ...,\ q^y_{i,C_i},\ \ ......,\ \ q^y_{N-1,0},\ ...,\ q^y_{N-1,C_{N-1}}]^{\mathrm{T}} \tag{2.52}$$

where $q^y_{i,j}$ (i = 1, …, N − 1; j=1, …, C_i − 1) are the corresponding expression on the right-hand side of the equal signs in equation (2.25). It is easy to see that $q^y_{i,j} \geq 0$ and

$$\begin{aligned}\sum\nolimits_{j=0}^{C_i} q^y_{i,j} &= (Q^x_{i,(0|0)} + Q^x_{i,(1|0)})q^x_{i,0} + ... \\ &\quad + (Q^x_{i,(j-1|j)} + Q^x_{i,(j|j)} + Q^x_{i,(j+1|j)})q^x_{i,j} + ... \\ &\quad + (Q^x_{i,(C_i-1|C_i)} + Q^x_{i,(C_i|C_i)})q^x_{i,C_i} \\ &= \sum\nolimits_{j=0}^{C_i} q^x_{i,j} \\ &= 1\end{aligned} \tag{2.53}$$

This leads to $q^y_{i,j} \leq 1$. Therefore, $\mathbf{Y} = G(\mathbf{X}) \in D$. ■

The following theorem addresses the existence of the fixed point (i.e. steady-state solution) of the MSM dynamics equations in D.

Theorem 2: Function $G(\boldsymbol{X})$ has a fixed point in $D \subset \mathbb{R}^V$. That is, there exists a point $\boldsymbol{X}^* \in D$, such that $\mathbf{X}^* = G(\mathbf{X}^*)$.

Proof: This is true considering Theorem 1 (Brouwer Fixed-Point Theorem) and Lemmas 5 through 7. ■

2.3.2. Numerical solution of the MSM dynamics equations

The steady state of the dynamics equations is numerically solved using the fixed-point iteration (2.44). The iteration starts when all buffers are empty at the beginning of time slot t = 1, i.e.,

$$\mathbf{X}(t-1)=\mathbf{X}(0)=\begin{bmatrix}\mathbf{q}_1(0)\\ \vdots\\ \mathbf{q}_i(0)\\ \vdots\\ \mathbf{q}_{N\text{-}1}(0)\end{bmatrix} \tag{2.54}$$

where

$$\mathbf{q}_i(0)=[q_{i,0}(0),\ q_{i,1}(0),\ ...,\ q_{i,C_i}(0)]^{\mathrm{T}}=[1,\ 0,\ ...,\ 0]^{\mathrm{T}},\ i=1,\ ...,\ N-1 \tag{2.55}$$

Therefore, every machine except the first one is starved, and no machine is blocked. The iteration stops when $\|\mathbf{X}(t)-\mathbf{X}(t-1)\|\le 10^{-10}$. We have tested this method on three example manufacturing systems whose parameters are given in Table 2.1.

Table 2.1. Parameters of three example serial Bernoulli manufacturing systems

Example	Number of machines N	Machine reliabilities $\boldsymbol{p}$	Buffer capacities $\boldsymbol{C}$
1	2	[0.9 0.8]	[3]
2	4	[0.9 0.8 0.8 0.9]	[3 2 3]
3	10	[0.9 0.8 0.9 0.8 0.9 0.8 0.9 0.8 0.9 0.8]	[5 4 5 4 5 4 5 4 5]

After the iteration stops, we take the last $\mathbf{X}(t)$ as the approximate fixed point $\mathbf{X}^*$. Then we plot the norm $\|\mathbf{X}(t)-\mathbf{X}^*\|$ over time t in Figure 2.4. We observe the following result.

Numerical Result 1: The dynamics equations converge approximately linearly for a major portion of the fixed-point iteration. It converges faster towards the end of the iteration.

Remark 1: It is worth mentioning that Numerical Result 1 is observed for serial Bernoulli manufacturing systems on a general basis and not only for the three example systems. The same is true for Numerical Results 2 through 5.

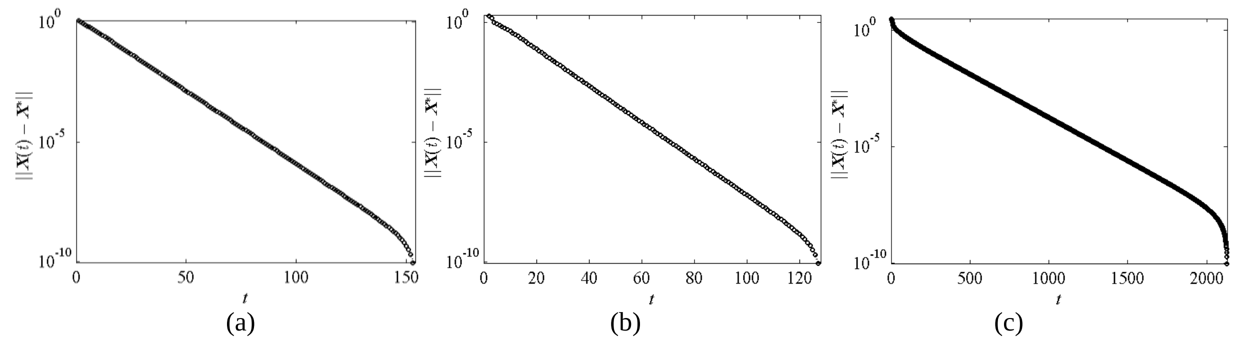

Figure 2.4. Norm $\left\|\mathbf{X}(t)-\mathbf{X}^{*}\right\|$ over time t for the (a) two-, (b) four-, and (c) ten-machine systems with parameters in Table 2.1

In order to see the detailed evolution of each buffer's state probabilities, we pick the four-machine system in Table 2.1 and plot the elements in $\mathbf{X}(t)$ over time t in Figure 2.5. The following result is observed.

Numerical Result 2: The probability of a buffer being empty, i.e. $q_{i,0}$ ($i = 1, \ldots, N - 1$) is monotonically decreasing; The probability of a buffer being full, i.e. q_{i,C_i} ($i = 1, \ldots, N - 1$) is monotonically increasing.

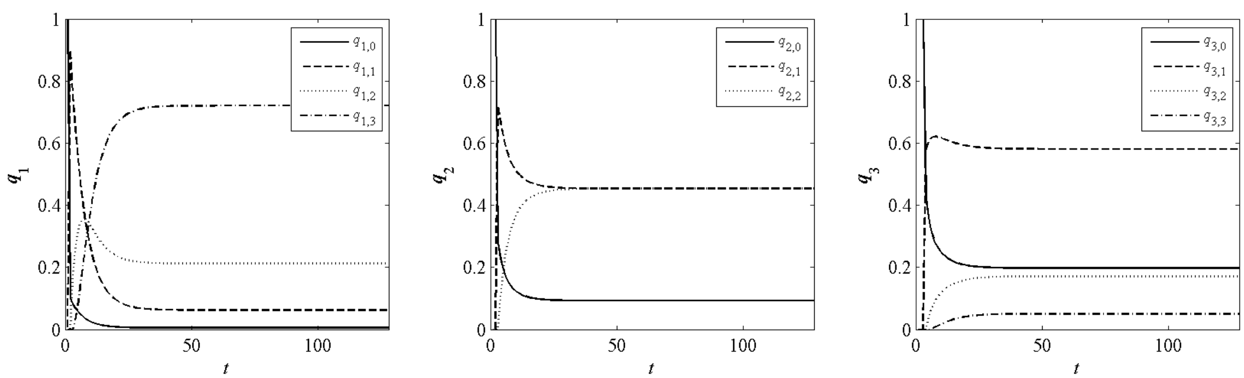
Figure 2.5. Evolution of elements in $\mathbf{X}(t)$ over time t for the four-machine system with parameters in Table 2.1

The evolution of the probabilities of each machine being starved, blocked, and producing a part as well as the work-in-process of each buffer for the four-machine system is plotted in Figure 2.6. The following result is observed.

Numerical Result 3: The probability of a machine being starved, i.e. ST_i ($i = 1, \ldots, N$) is monotonically decreasing; The probability of a machine being blocked, i.e. BL_i ($i = 1, \ldots, N$) is monotonically increasing. The production rate of the first machine, i.e. PR_1 is monotonically decreasing; The production rate of the last machine, i.e. $PR_N = PR_{SYS}$ is monotonically increasing. The work-in-process of a buffer, i.e. WIP_i ($i = 1, \ldots, N - 1$) and the total work-in-process of the system, i.e. WIP_{SYS} are both monotonically increasing.

Remark 2: The result shows that during transients, the system production rate PR_{SYS} is constantly smaller than the steady counterpart. This is the cause of production loss, which will be analyzed in Section 2.4.4.

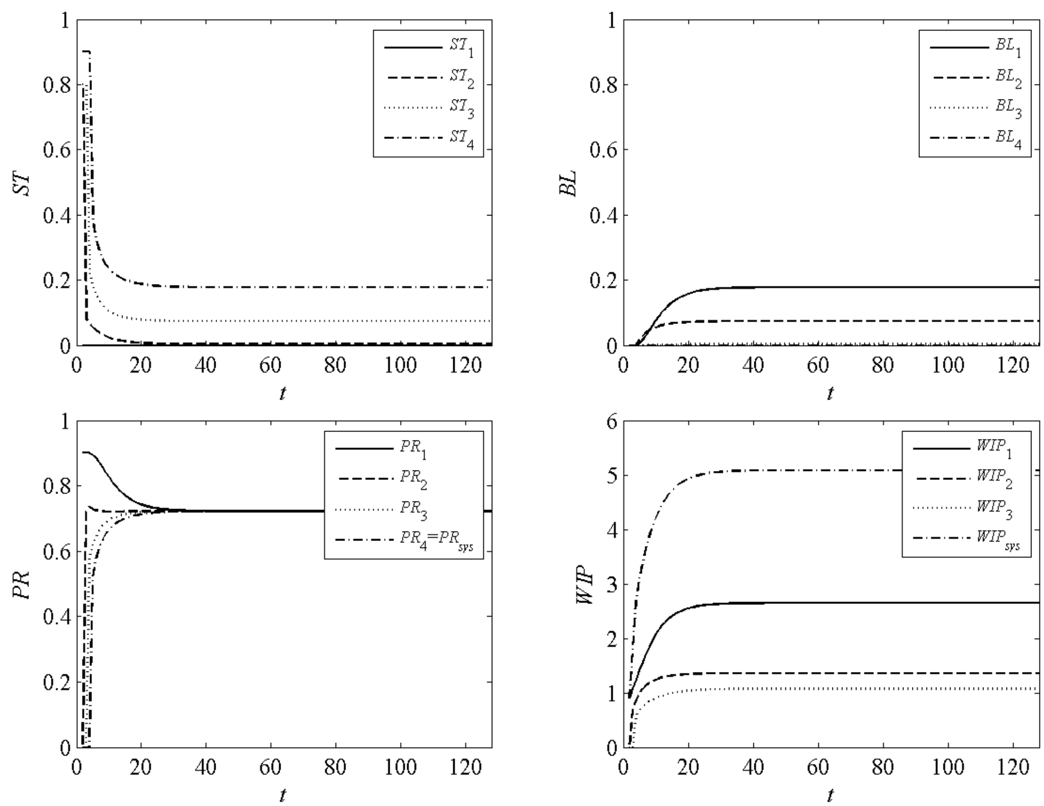

Figure 2.6. Evolution of performance measures over time t for the four-machine system with parameters in Table 2.1

We have also implemented the aggregation algorithm proposed in (Jacob and Meerkov, 1995; Li and Meerkov, 2009). After comparing the steady-state performance measures with the calculation result of the aggregation algorithm, we observe

Numerical Result 4: The steady-state performance measures ST_i, BL_i ($i = 1, \ldots, N$), PR_1, PR_N, PR_{SYS}, WIP_i ($i = 1, \ldots, N - 1$), and WIP_{SYS} are the same as the results calculated by the aggregation algorithm.

2.4. Transient Metrics

2.4.1. Second largest eigenvalue modulus (*SLEM*)

The transients of a longer manufacturing system may not last longer than a shorter manufacturing system. This phenomenon can be seen in Figure 2.4. The two-machine system needs 153 cycle times to reach the steady state after a fresh start, while the four-machine system needs 127 cycle times. It turns out that the duration of the transients is a complex function of machine reliabilities, buffer capacities, and number of machines. It would be more practical to use only one metric to characterize the duration of the transients. For the two-machine cases, the metric is the second largest eigenvalue of the transition matrix (Meerkov and Zhang, 2008). We will generalize this to the multiple-machine cases.

According to Lemma 5, $G(\mathbf{X})$ is differentiable. The Jacobian of $G(\mathbf{X})$ is

$$J_G = G'(\mathbf{X}) \equiv \begin{pmatrix} \frac{\partial g_1}{\partial x_1} & \cdots & \frac{\partial g_1}{\partial x_V} \\ \vdots & \ddots & \vdots \\ \frac{\partial g_V}{\partial x_1} & \cdots & \frac{\partial g_V}{\partial x_V} \end{pmatrix} \tag{2.56}$$

J_G is a V by V matrix. We first calculate all the eigenvalues of J_G, and then plotted the second largest eigenvalue modulus (*SLEM*) as well as the norm $\left\|\mathbf{X}(t)-\mathbf{X}^*\right\| / \left\|\mathbf{X}(t-1)-\mathbf{X}^*\right\|$ of the three example systems in Figure 2.7. We observe

Numerical Result 5: The largest eigenvalue modulus of J_G is one. The *SLEM*, which is between zero and one, determines the slope (i.e., convergence rate) for a major portion of the iteration curves. The relationship $SLEM \approx \dfrac{\left\|\mathbf{X}(t)-\tilde{\mathbf{X}}^*\right\|}{\left\|\mathbf{X}(t-1)-\tilde{\mathbf{X}}^*\right\|}$ holds, i.e., the rate of convergence is approximately characterized by *SLEM*. Smaller *SLEM* indicates faster convergence and shorter duration of transients.

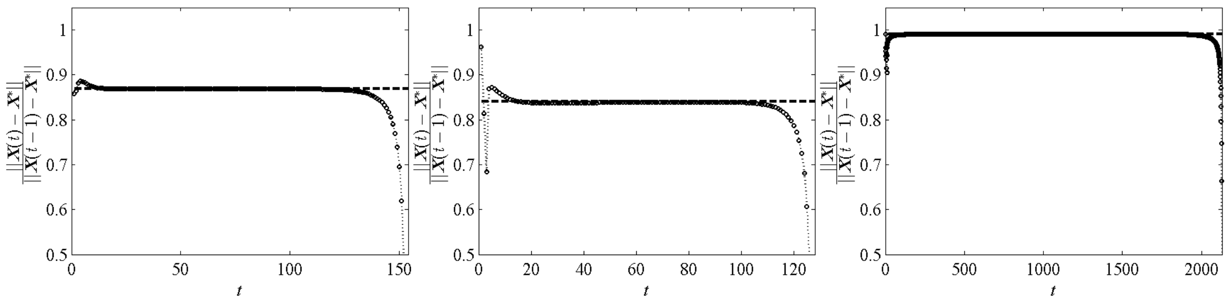

(a) (b) (c)

Figure 2.7. Norm $\left\|\mathbf{X}(t)-\tilde{\mathbf{X}}^*\right\| / \left\|\mathbf{X}(t-1)-\tilde{\mathbf{X}}^*\right\|$ (circle-dotted curve) and *SLEM* (dashed line) over time *t* for the (a) two-, (b) four-, and (c) ten-machine systems with parameters in Table 2.1

In an attempt to numerically characterize *SLEM* as a function of machine reliabilities p_i, buffer capacities C_i, and number of machines N, we have investigated the following three groups of manufacturing systems. The first, second, and third groups contains two-, four-, and ten-machine systems, respectively. The machines in each system have identical reliability p_i. The reliability p_i in each group ranges from 0.50 to 0.99 with an interval of 0.02 (reliabilities smaller than 0.5 are of little value in practice). The buffers in each system have identical capacity C_i. The capacity C_i in each group ranges from 1 to 15 with an interval of 1.

The values of *SLEM* are plotted in Figure 2.8 for the three groups of systems. The solid curve with circles in the C_i-p_i-*SLEM* space indicates the positions of the smallest *SLEM* values (denoted by min(*SLEM*)) corresponding to each buffer capacity. This curve is projected in the C_i-*SLEM* plane (represented by the dotted line with squares) and the C_i-p_i plane (represented by the dashed line with triangles).

Numerical Result 6: *SLEM* and min(*SLEM*) are both monotonically increasing functions of buffer capacity C_i and machine number N. On the C_i-p_i plane, the optimal p_i corresponding to min(*SLEM*) is a monotonically decreasing function of capacity C_i.

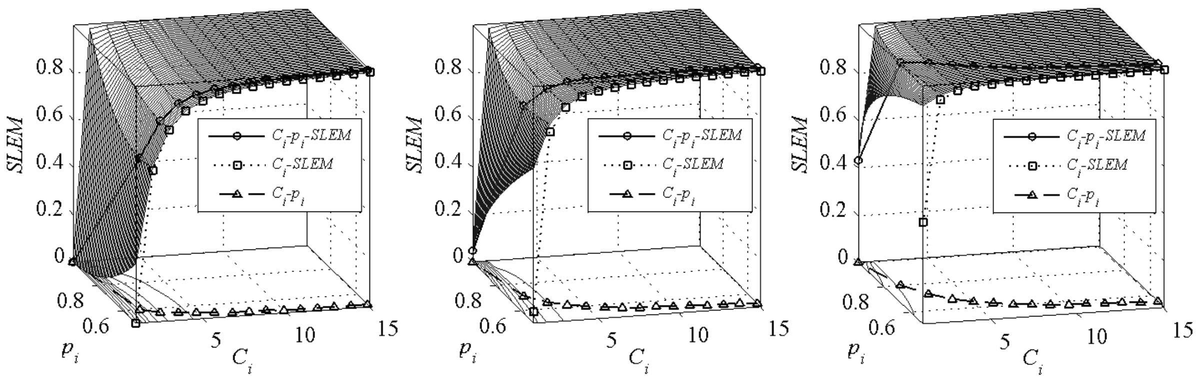

(a) (b) (c)

Figure 2.8. *SLEM* as a function of machine reliabilities p_i, buffer capacities C_i for the (a) two-, (b) four-, and (c) ten-machine systems

Remark 3: It is worth mentioning that Numerical Result 6 is observed for serial Bernoulli manufacturing systems with identical machine reliabilities and buffer capacities on a general basis and not only for the three groups of systems demonstrated. The same is true for Numerical Results 7 through 10.

2.4.2. Number of iteration

Similarly, the total number of iteration t_{ITER} needed to reach the steady state can also be numerically characterized as a function of machine reliabilities p_i, buffer capacities C_i, and the number of machines N. The values of t_{ITER} are plotted in Figure 2.9 for the three groups of systems. The solid curve with circles in the C_i-p_i-*SLEM* space indicates the positions of the smallest t_{ITER} values (denoted by min(t_{ITER})) corresponding to each buffer capacity. This curve is projected in the C_i-*SLEM* plane (represented by the dotted line with squares) and the C_i-p_i plane (represented by the dashed line with triangles).

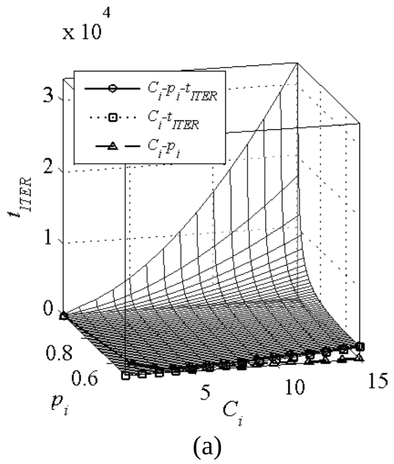

Figure 2.9. t_{ITER} as a function of machine reliabilities p_i, buffer capacities C_i for the (a) two-, (b) four-, and (c) ten-machine systems

Numerical Result 7: t_{ITER} and min(t_{ITER}) are both monotonically increasing functions of buffer capacity C_i and machine number N. On the C_i-p_i plane, the optimal p_i corresponding to min(t_{ITER}) is approximately a monotonically decreasing function of capacity C_i.

2.4.3. Settling time

For the two-machine systems, Meerkov and Zhang (2008) have introduced the concept of settling time to describe the time needed for a performance measure to reach and remain within ±5% of its steady-state value. This concept can be generalized to longer manufacturing systems. We define the settling time of *WIP*

$$t_{WIP} = \inf\left(t \left| \frac{\tilde{WIP}^* - WIP(t+\Delta)}{\tilde{WIP}^*} \le 5\%,\ \forall \Delta \in \{0,\ \ldots,\ t_{ITER} - t\} \right. \right) \tag{2.57}$$

The values of t_{WIP}'s are plotted in Figure 2.10 for the three groups of systems.

Numerical Result 8: t_{WIP} and min(t_{WIP}) are both monotonically increasing functions of buffer capacity C_i and machine number N. On the C_i-p_i plane, the optimal p_i corresponding to min(t_{WIP}) is approximately a monotonically decreasing function of capacity C_i.

Remark 4: Based on Figure 2.9 and Figure 2.10, it appears t_{ITER} has a strong correlation with t_{WIP}.

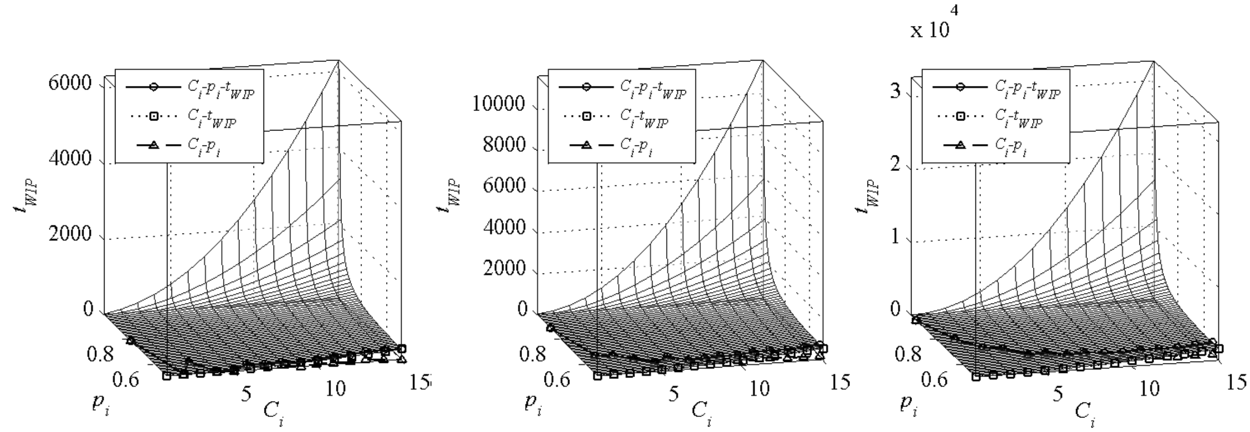

(a) (b) (c)

Figure 2.10. t_{WIP} as a function of machine reliabilities p_i, buffer capacities C_i for the (a) two-, (b) four-, and (c) ten-machine systems

Similarly, we can also define the settling time of *PR*

$$t_{PR} = \inf\left(t \left| \frac{P\tilde{R}^* - PR(t+\Delta)}{P\tilde{R}^*} \le 5\%,\ \forall \Delta \in \{0,\ ...,\ t_{ITER} - t\} \right. \right) \qquad (2.58)$$

The values of t_{PR}'s are plotted in Figure 2.11 for the three groups of systems.

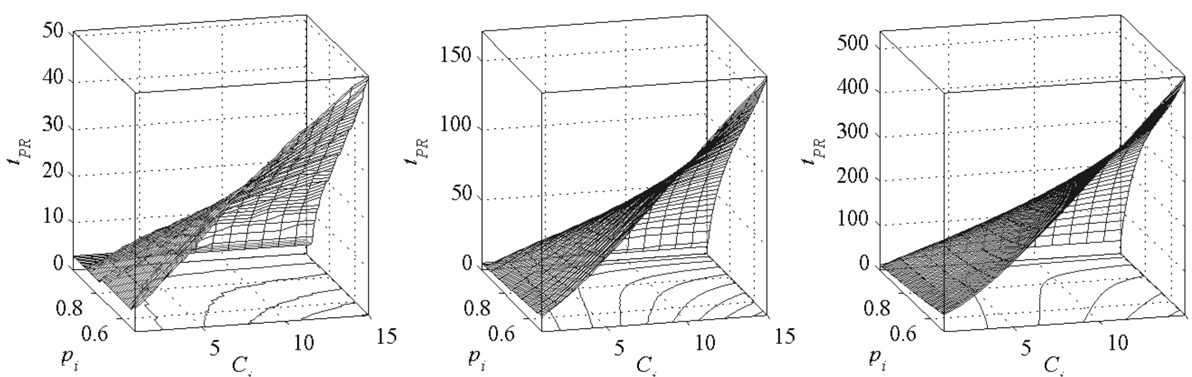

(a) (b) (c)

Figure 2.11. t_{PR} as a function of machine reliabilities p_i, buffer capacities C_i for the (a) two-, (b) four-, and (c) ten-machine systems

Numerical Result 9: t_{PR} is a monotonically increasing function of buffer capacity C_i and machine number N. It is a monotonically decreasing function of machine reliability p_i.

Remark 5: Based on Figure 2.10 and Figure 2.11, it appears t_{WIP} is in general much larger than t_{PR}. This is true especially when the machines are highly reliable ($p_i > 0.9$).

2.4.4. Production loss

As a generalization, we analyze the production loss due to transients following a fresh start for a study period of T = 500 cycle times (an 8-hour shift with each cycle time being around one minute). This is typical for automotive assembly plants. The percent of production loss is defined as

$$L_{PR} = \frac{\sum_{t=1}^{T}[PR^* - PR(t)]}{T \cdot PR^*} \tag{2.59}$$

The values of L_{PR} are plotted in Figure 2.12 for the three groups of systems.

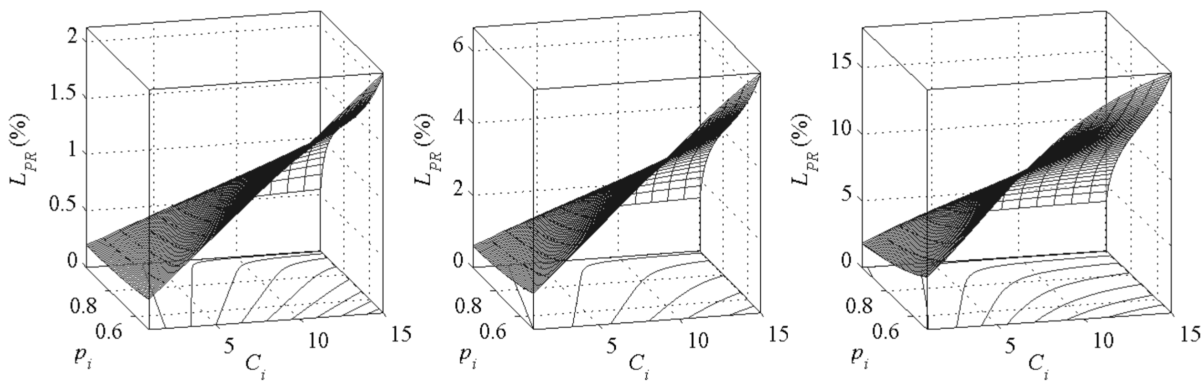

Figure 2.12. L_{PR} as a function of machine reliabilities p_i, buffer capacities C_i for the (a) two-, (b) four-, and (c) ten-machine systems

Numerical Result 10: L_{PR} is a monotonically increasing function of buffer capacity C_i and machine number N. It is a monotonically decreasing function of machine reliability p_i.

Remark 6: From Figure 2.11 and Figure 2.12, it appears L_{PR} has a strong correlation with t_{PR}. This can be explained by the fact that longer duration of transients cause greater loss of production.

2.5. Conclusions

The complicated interrelations between component-level characteristics and system-level characteristics have been modeled in this chapter. Detailed analysis of the model generates valuable information that is helpful for understanding the steady-state and transient behaviors of the system. The transient performance metrics such as duration of transients t_{ITER}, settling time for work-in-process t_{WIP}, settling time for production rate t_{PR}, and percent of production loss L_{PR} due to transients have been thoroughly investigated. Numerical exploration also reveals that the transient behaviors are largely attributed to the second largest eigenvalue modulus *SLEM* of the Jacobian matrix J_G.

The research outcome of this chapter forms the basis for the modeling and monotonicity analysis of per-product energy efficiency and electricity cost in the next chapter.

CHAPTER 3

TOU BASED ELECTRICITY ENERGY EFFICIENCY AND COST OF MANUFACTURING A PRODUCT

(Parts of this chapter were previously published as: *Wang, Y., Li, L., 2014. Time-of-use based electricity cost of manufacturing systems: Modeling and monotonicity analysis. International Journal of Production Economics, 156, 246-259.*)

3.1. Introduction

In this chapter, the per-product electricity cost as a function of manufacturing system parameters and the TOU rates is modeled. The contributions of both electricity energy consumption and peak demand are analyzed and combined to formulate the electricity cost of manufacturing a product. The model of the complex interrelations and dynamics established in Chapter 2 for the system with multiple machines and buffers is integrated. New knowledge of the effects of various modeling parameters on the electricity cost is acquired through monotonicity analysis. The formulated model is utilized to answer the following two questions facing manufacturers: With the availability of TOU rates in mind, is switching from the flat rates to the TOU rates economically sound? What changes can be made on electric use routines to take advantage of the TOU rates? The findings based on case studies show that by adopting the TOU rates: energy efficiency is unaffected; with appropriate adjustment of production routines, a significant saving of up to 24.8% of the per-product electricity cost can be achieved.

The remainder of this chapter is organized as follows. Section 3.2 models the electricity energy consumption, peak demand, and cost for typical manufacturing systems. Section 3.3 introduces the monotonicity analysis on machine and buffer parameters such as buffer capacities, machine reliabilities, cycle time, and machine number. Section 3.4 examines the energy efficiency and economic impacts of switch from flat rates to TOU rates to guide the decision making process for manufacturers. Finally, conclusions of this chapter are drawn in Section 3.5.

The following notation is used in this chapter.

Upper Case:

C_i	capacity of buffer b_i (the largest number of parts the buffer can hold)
CP_T	average cumulative production of the system during the planning horizon
$ID_i(t)$	probability of machine m_i (i = 1, ..., N) being idle during time slot t
H	number of hours in the finite planning horizon
H_1, H_2	number of hours of the off- and on-peak periods, respectively, within the planning horizon
N	number of machines in the manufacturing system
$PR_i(t)$	production rate of machine m_i (i = 1, ..., N) during time slot t
$PR_N(t)$	production rate of the last machine during time slot t
T	number of total time slots during the planning horizon
T_1, T_2	numbers of time slots of the off- and on-peak periods, respectively, during the planning horizon

Lower Case:

$b(t)$	billable cost indicator
$c_D(t)$	TOU demand rate (\$/kW) during time slot t
c_{DT}	cost of the billable power demand of the system during the planning

horizon

$\overline{c_E}$ defined as $T_1 \cdot c_{E,1} + T_2 \cdot c_{E,2}$

$c_E(t)$ TOU energy rate ($/kWh) during time slot t

$c_{E,1}$, $c_{E,2}$ off- and on-peak energy rates, respectively

c_{ET} cost of the total electricity energy consumption of the system during the planning horizon

c_{Fixed} fixed charge during the planning horizon

c_T total electricity cost during the planning horizon

c_{UNIT} per-product electricity cost of the system during the planning horizon

$c_{UNIT,SUM}$, $c_{UNIT,WIN}$, $c_{UNIT,YW}$ summer-month, winter-month, and yearly-weighted per-product electricity costs, respectively

$c_{UNIT,YW}^{Scenario\ 0 \to i}$ per-product electricity cost saving by switching from Scenario 0 to Scenario i (i = 1 or 2)

$d_i(t)$ expected electric demand (in kW) of machine m_i during time slot t

$d_{i,2}$, $d_{i,1}$, $d_{i,0}$ electric power (in kW) drawn by machine m_i during time slot t when it is up & processing, up & idle, and down, respectively

$d_{SYS}(t)$ electric power demand of the system during time slot t

d_T billable power demand of the system (the highest average kW measured in any on-peak 15-minute interval during the planning horizon)

$d_{T,A}$, $d_{T,B}$ highest average demands found by sliding from left to right with an interval t_C and sliding from right to left with an interval t_C, respectively

$e_i(t)$ expected electric energy (in kWh) consumed by machine m_i during time slot t

$e_{i,2}$, $e_{i,1}$, $e_{i,0}$ — electric energy (in kWh) consumed by machine m_i during time slot t when it is up & processing, up & idle, and down, respectively

$e_{SYS}(t)$ — electricity energy consumption of the system during time slot t

e_T — total electricity energy consumption of the system during the planning horizon

e_{UNIT} — per-product electricity energy consumption of the system during the planning horizon

i, t, t_1, t_2 — general indexes

t_C — cycle time (the time needed by a machine to process a product)

t_D — length of time interval (usually 15 minutes) used to find peak demand

l — the ceiling integer number of the time slots in any interval of length t_D (15 minutes)

m_i — index of the ith machine in the manufacturing system, i = 1, ..., N

p_i — probability of machine m_i being up during time slot t (considering machine reliability only)

w_{SUM}, w_{WIN} — proportional weights of the summer and winter months

Functions:

$\lceil \cdot \rceil$ — ceiling function

3.2. TOU Based Electricity Energy Efficiency and Cost Modeling

3.2.1. Assumptions

In order to model the TOU based electricity energy efficiency and cost, more assumptions as follows are adopted.

(vi) A finite planning horizon of H hours during a workday is evenly discretized into T slots. The slot duration is equal to the cycle time t_C of the machines, i.e., $t_C = H/T$.

(vii) For machine m_i, when it is up and processing during time slot t, it draws on average $d_{i,2}$ kW of electric power and consumes $e_{i,2} = d_{i,2}t_C$ kWh of electric energy; when it is up and idle during time slot t, it draws on average $d_{i,1}$ kW of electric power and consumes $e_{i,1} = d_{i,1}t_C$ kWh of electric energy; when it is down, it draws no power and consumes no energy, which are represented by $d_{i,0} = 0$ kW and $e_{i,0} = 0$ kWh.

(viii) We assume that $d_{i,2} \geq d_{i,1} \geq d_{i,0} = 0$ and $e_{i,2} \geq e_{i,1} \geq e_{i,0} = 0$. Based on the analysis of typical energy (or power) profiles of machine tools, it has been reported that the energy $e_{i,1}$ (or power $d_{i,1}$) for maintaining machine readiness in the idle state may account for up to 85% of the full energy $e_{i,2}$ (or power $d_{i,2}$) needed (Dietmair and Verl, 2009; Fysikopoulos et al., 2012; Gutowski et al., 2005; Li and Sun, 2013).

(ix) Buffers do not consume energy or draw any power.

3.2.2. Modeling of electricity energy

The expected electricity energy consumption of machine m_i during time slot t is

$$\begin{aligned} e_i(t) &= e_{i,2}PR_i(t) + e_{i,1}ID_i(t) + e_{i,0}(1-p_i) \\ &= e_{i,2}PR_i(t) + e_{i,1}[p_i - PR_i(t)] \\ &= (e_{i,2} - e_{i,1})PR_i(t) + e_{i,1}p_i \end{aligned} \tag{3.1}$$

The expected electricity energy consumption of the N-machine system shown in Figure 2.1 during time slot t is

$$e_{SYS}(t) = \sum_{i=1}^{N} e_i(t) \tag{3.2}$$

The total electricity energy consumption of the system during the planning horizon is

$$e_T = \sum_{t=1}^{T} e_{SYS}(t) \tag{3.3}$$

The electricity energy consumption per product during the planning horizon is

$$e_{UNIT} = e_T / CP_T \tag{3.4}$$

The per-product electricity energy consumption is actually an indicator of energy efficiency: the smaller the value of e_{UNIT}, the more energy efficient the manufacturing system.

3.2.3. Modeling of electricity demand

The expected electricity demand of machine m_i during time slot t is

$$\begin{aligned} d_i(t) &= d_{i,2} PR_i(t) + d_{i,1} ID_i(t) + d_{i,0} [1 - p_i] \\ &= d_{i,2} PR_i(t) + d_{i,1} [p_i - PR_i(t)] \\ &= (d_{i,2} - d_{i,1}) PR_i(t) + d_{i,1} p_i \end{aligned} \tag{3.5}$$

The power demand of the system during time slot t is

$$d_{SYS}(t) = \sum_{i=1}^{N} d_i(t) \tag{3.6}$$

The charge for demand is determined based on the peak demand, which is defined as the highest average kW measured in any on-peak interval of length t_D (usually 15 minutes) during the monthly billing period (Orange and Rockland Utilities, 2013b). We denote this peak demand by d_T. A sliding window of length t_D can be used to find d_T.

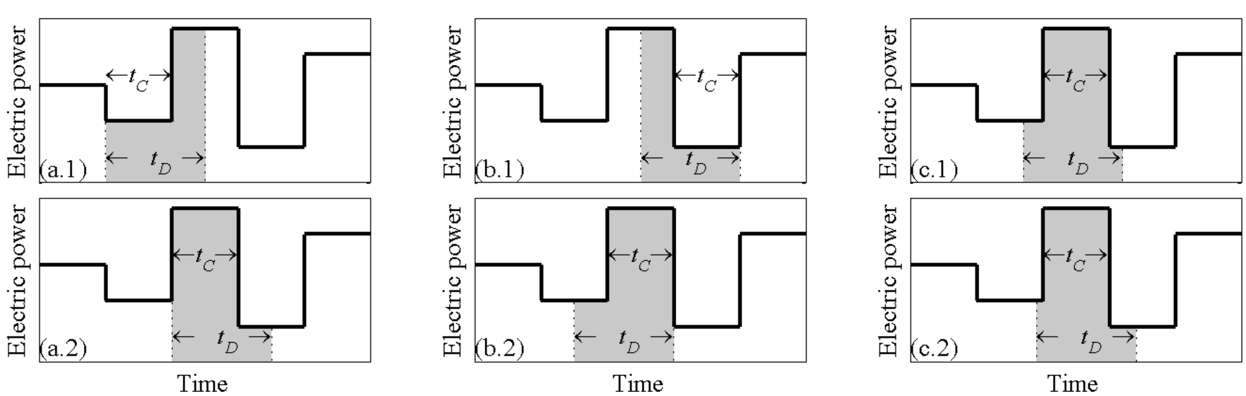

Figure 3.1. Peak demand determination by (a) sliding from left to right *with an interval* t_C; (b) sliding from right to left *with an interval* t_C; and (c) sliding *continuously* from left to right or from right to left

For example, in the case where $1 < t_D/t_C \leq 2$ as shown in Figure 3.1, three methods can be adopted to slide the window. In Figure 3.1(a), it is slid from the start to the end with an interval t_C (i.e., the left side of the window is always aligned with the start of a cycle time). In Figure 3.1(b), it is slid from right to left with an interval t_C (i.e., the right side of the window is always aligned with the end of a cycle time); and in Figure 3.1(c), it is slid continuously from the start to the end or from the end to the start. The highest average demand found by the third method is actually d_T. The highest average demands found by the first and the second methods are denoted by $d_{T,A}$ and $d_{T,B}$, respectively. It is obvious that d_T is always equal to the larger one of the two. Similarly, for the cases where $0 < t_D/t_C \leq 1$ and $2 < t_D/t_C$, this rule also applies.

Formally, let l be the ceiling integer number of the time slots in any interval of length t_D (15 minutes), i.e.,

$$l = \left\lceil t_D / t_C \right\rceil \tag{3.7}$$

Then $d_{T,A}$ and $d_{T,B}$ are

$$d_{T,A} = \max_{t \in \{1,2,\ldots,T-l+1\}} \frac{\sum_{t_1=t}^{t+l-1} e_{SYS}(t_1)b(t_1) - \left(l - t_D/t_C\right) e_{SYS}(t+l-1)b(t+l-1)}{t_D} \tag{3.8}$$

$$d_{T,B} = \max_{t \in \{l,l+1,\ldots,T\}} \frac{\sum_{t_2=t-l+1}^{t} e_{SYS}(t_2)b(t_2) - \left(l - t_D/t_C\right) e_{SYS}(t-l+1)b(t-l+1)}{t_D} \tag{3.9}$$

where

$$b(t) = \begin{cases} 1, & \text{if slot } t \text{ is within on-peak period} \\ 0, & \text{if slot } t \text{ is within off-peak period} \end{cases} \tag{3.10}$$

The peak demand is

$$d_T = \max(d_{T,A}, d_{T,B}) \tag{3.11}$$

3.2.4. Modeling of TOU based electricity cost

The electricity energy cost of the system during the planning horizon is

$$c_{ET} = \sum_{t=1}^{T} c_E(t) e_{SYS}(t) \tag{3.12}$$

where $c_E(t)$ is the TOU energy rate ($/kWh) during time slot *t*. The electricity demand cost of the system during the planning horizon is

$$c_{DT} = c_D d_T \tag{3.13}$$

where c_D is the TOU demand rate ($/kW) during the on-peak period. The total cost can be formulated as

$$c_T = c_{DT} + c_{ET} + c_{Fixed} \tag{3.14}$$

where c_{Fixed} represents the account and other fixed charges during the planning horizon. The total TOU based electricity cost per product during the planning horizon is

$$c_{UNIT} = c_T / CP_T \tag{3.15}$$

3.3. Monotonicity Analysis

From the perspective of improving energy efficiency and cost effectiveness, it is desirable to make both e_{UNIT} and c_{UNIT} as low as possible. It is observed from Section 3.2 that many parameters are utilized to model these two indexes. How the change of one parameter will affect e_{UNIT} and c_{UNIT} is not always intuitive or straightforward. This motivates us to conduct a monotonicity analysis to further investigate the effects of these parameters on e_{UNIT} and c_{UNIT}.

After substitution, e_{UNIT} and c_{UNIT} can be represented by

$$e_{UNIT} = \frac{\sum_{t=1}^{T}\sum_{i=1}^{N}\left[(e_{i,2} - e_{i,1})PR_i(t) + e_{i,1}p_i\right]}{\sum_{t=1}^{T} PR_N(t)} \tag{3.16}$$

$$c_{UNIT} = \frac{c_D \cdot \max(d_{T,A}, d_{T,B}) + \sum_{t=1}^{T}\left\{c_E(t) \cdot \sum_{i=1}^{N}\left[(e_{i,2} - e_{i,1})PR_i(t) + e_{i,1}p_i\right]\right\} + c_{Fixed}}{\sum_{t=1}^{T} PR_N(t)} \tag{3.17}$$

Equations (3.16) and (3.17) describe the electricity energy consumption and the TOU based electricity cost of manufacturing a product when the system dynamics involve transients. One of the most commonly observed transient behaviors occurs after a fresh start (i.e, when all the buffers are empty, every machine except the first one is starved, and no machine is blocked) of the manufacturing system.

If the manufacturing system starts from the steady state (all buffers have been properly filled to some level and machine state probabilities keep unchanged over time) instead, the time slot index t can be dropped, and $PR_N(t) = PR_i(t) = PR_N$, ($i = 1, \ldots, N$). We have $e_{SYS}(t) = e_{SYS}$, $d_T = d_{T,A} = d_{T,B}$, and

$$d_{T,A} = \frac{e_{SYS}}{t_D} \cdot \max_{t \in \{1,2,\ldots,T-l+1\}} \left[\sum_{t_1=t}^{t+l-1} b(t_1) - \left(l - t_D/t_C\right) b(t+l-1)\right] \tag{3.18}$$

Also at the steady state, $c_E(t)$ can be divided into two parts: off-peak price $c_{E,1}$ and on-peak price $c_{E,2}$, which are both constant. The T time slots (corresponding to the planning horizon H) can also be divided into two parts, T_1 and T_2, being the numbers of time slots of the off- and on-peak periods, respectively. Let

$$\overline{c_E} = T_1 \cdot c_{E,1} + T_2 \cdot c_{E,2} \tag{3.19}$$

Then (3.16) and (3.17) can be reformulated as

$$e_{UNIT} = \frac{T \cdot \sum_{i=1}^{N} \left[(e_{i,2} - e_{i,1}) PR_N + e_{i,1} p_i \right]}{T \cdot PR_N} = \sum_{i=1}^{N} (e_{i,2} - e_{i,1}) + \frac{\sum_{i=1}^{N} e_{i,1} p_i}{PR_N} \tag{3.20}$$

$$\begin{aligned} c_{UNIT} &= \frac{\frac{c_D}{t_D} \cdot \sum_{i=1}^{N} \left\{ (e_{i,2} - e_{i,1}) PR_N + e_{i,1} p_i \right\} \cdot \max_{t \in \{1,2,\ldots,T-l+1\}} \left[\sum_{t_1 = t}^{t+l-1} b(t_1) - \left(l - t_D / t_C \right) b(t+l-1) \right]}{T \cdot PR_N} \\ &\quad + \frac{\overline{c_E} \cdot \sum_{i=1}^{N} \left[(e_{i,2} - e_{i,1}) PR_N + e_{i,1} p_i \right] + c_{Fixed}}{T \cdot PR_N} \\ &= \frac{\left\{ \frac{c_D}{t_D} \cdot \max_{t \in \{1,2,\ldots,T-l+1\}} \left[\sum_{t_1 = t}^{t+l-1} b(t_1) - \left(l - t_D / t_C \right) b(t+l-1) \right] + \overline{c_E} \right\} \cdot \sum_{i=1}^{N} (e_{i,2} - e_{i,1})}{T} \\ &\quad + \frac{\left\{ \frac{c_D}{t_D} \cdot \max_{t \in \{1,2,\ldots,T-l+1\}} \left[\sum_{t_1 = t}^{t+l-1} b(t_1) - \left(l - t_D / t_C \right) b(t+l-1) \right] + \overline{c_E} \right\} \cdot \sum_{i=1}^{N} e_{i,1} p_i + c_{Fixed}}{T \cdot PR_N} \end{aligned} \tag{3.21}$$

In the rest of this section, the monotonicity of e_{UNIT} and c_{UNIT} with respect to buffer capacities C_i, machine reliabilities p_i, cycle time t_C, and machine number N are investigated. For steady-state cases, both theoretical analysis and numerical results on the monotonicity are provided. For the cases that involve transients, the theoretical monotonicity analysis is still a challenge, and therefore only scalable numerical results are presented. The ranges of the parameters for the numerical investigation are given in Table 3.1. The power demand values of machines are given in Table 3.2. The plots of the numerical examples are summarized in Table 3.3 through Table 3.6. In order to obtain these plots, the TOU rates in Table 1.2 is adopted. It should be noted that the TOU demand rates c_D and the fixed charge c_{Fixed} should be divided by 21, the number of working days in a month, to obtain the daily equivalents. The planning horizon is H = 16 hours (two shifts), starting from 8am to 12 midnight. However, the propositions and numerical results obtained in this section are general and not limited to the scenario examined in this section.

Table 3.1. Parameters and ranges for numerical investigation on monotonicity

Parameters	**Numerical ranges**	**Note**
Buffer capacities C_i	{1, 2, …, 15}	Assume all the buffers have identical capacity
Machine reliabilities p_i	{0.50, 0.51, …, 0.99}	Assume all the machines have identical reliability; Reliability values under 0.50 are impractical for real applications and thus not studied
Cycle time t_C	{1, 5, 15}	In minutes
Machine numbers N	{2, 4, 10}	Corresponding buffer numbers are {1, 3, 9}

Table 3.2. Power demand (in kW) of machines in the form $[d_{i,2}\ d_{i,1}\ d_{i,0}]$

	$i = 1$	$i = 2$	$i = 3$	$i = 4$	$i = 5$	$i = 6$	$i = 7$	$i = 8$	$i = 9$	$i = 10$
$N = 2$	[20 4 0]	[30 8 0]								
$N = 4$	[20 4 0]	[30 8 0]	[15 5 0]	[35 3 0]						
$N = 10$	[20 4 0]	[30 8 0]	[15 5 0]	[35 3 0]	[25 3 0]	[20 7 0]	[23 10 0]	[32 5 0]	[30 8 0]	[20 5 0]

3.3.1. Effects of buffer capacities C_i

Numerical result 1 (Transient): For the manufacturing system defined by assumptions (i) through (ix), both e_{UNIT} and c_{UNIT} decrease first and then increase as C_i increases.

Proposition 1 (Steady): For the manufacturing system defined by assumptions (i) through (ix), both e_{UNIT} and c_{UNIT} are strictly monotonically decreasing in C_i, $i = 1, 2, \ldots, N - 1$.

Proof: According to (Li and Meerkov, 2009), in Bernoulli serial lines, PR_N is strictly monotonically increasing in C_i, $i = 1, 2, \ldots, N - 1$. Therefore, in (3.20) and (3.21), with other variables being fixed, e_{UNIT} and c_{UNIT} are both strictly monotonically decreasing in C_i. ■

Remark 1: For the transient case, it is desirable to select the optimal C_i so that the per-product electricity energy e_{UNIT} and TOU based per-product electricity cost c_{UNIT} can both be minimized. For the steady case, due to the saturation effect, it may not be economically sound to increase C_i indefinitely because such actions will raise the cost of inventory, which, although important, is not in the research scope of this dissertation.

3.3.2. Effects of machine reliabilities p_i

Numerical result 2 (Transient): For the manufacturing system defined by assumptions (i) through (ix), both e_{UNIT} and c_{UNIT} decrease as p_i increases.

For the steady-state case, the effect of p_i in general is difficult to prove. However, the following proposition holds for a special case.

Proposition 2 (Steady): For the manufacturing system defined by assumptions (i) through (ix), when $N = 2$ and $p_1 = p_2 = p$, both e_{UNIT} and c_{UNIT} are strictly monotonically decreasing in p.

Proof: When $N = 2$ and $p_1 = p_2 = p$, according to (Li and Meerkov, 2009),

$$PR_N = p\left(1-\frac{1-p}{C_1+1-p}\right) \tag{3.22}$$

In (3.20), only the second item involves PR_N and p_i, and it can be reformulated as

$$\frac{\sum_{i=1}^{N} e_{i,1}p_i}{PR_N} = \frac{e_{1,1}+e_{2,1}}{1-\dfrac{1-p}{C_1+1-p}} = \frac{(e_{1,1}+e_{2,1})(C_1+1-p)}{C_1} \tag{3.23}$$

Similarly, in (3.21), only the second item involves PR_N and p_i, and it can be reformulated as

$$\begin{aligned}
&\frac{\left\{\dfrac{c_D}{t_D}\cdot\max\limits_{t\in\{1,2,\ldots,T-l+1\}}\left[\sum_{t_1=t}^{t+l-1} b(t_1)-\left(l-t_D/t_C\right)b(t+l-1)\right]+\overline{c_E}\right\}\cdot\sum_{i=1}^{N}e_{i,1}p_i+c_{Fixed}}{T\cdot PR_N}\\
&=\frac{\left\{\dfrac{c_D}{t_D}\cdot\max\limits_{t\in\{1,2,\ldots,T-l+1\}}\left[\sum_{t_1=t}^{t+l-1} b(t_1)-\left(l-t_D/t_C\right)b(t+l-1)\right]+\overline{c_E}\right\}\cdot(e_{1,1}+e_{2,1})p+c_{Fixed}}{T\cdot p\left(1-\dfrac{1-p}{C_1+1-p}\right)}\\
&=\frac{\left\{\dfrac{c_D}{t_D}\cdot\max\limits_{t\in\{1,2,\ldots,T-l+1\}}\left[\sum_{t_1=t}^{t+l-1} b(t_1)-\left(l-t_D/t_C\right)b(t+l-1)\right]+\overline{c_E}\right\}\cdot(e_{1,1}+e_{2,1})\cdot\left(C_1+1-p\right)}{T\cdot C_1}\\
&\quad+\frac{c_{Fixed}\cdot\left(C_1+1-p\right)}{T\cdot p\cdot C_1}
\end{aligned} \tag{3.24}$$

It is obvious that, with other variables being fixed, e_{UNIT} and c_{UNIT} are both strictly monotonically decreasing in p. ■

Remark 2: For both the transient and steady cases, it is desirable to increase p_i so that the per-product electricity energy e_{UNIT} and TOU based per-product electricity cost c_{UNIT} can both be reduced. The monotonicity in p_i does not seem to suffer from the saturation effect.

3.3.3. Effects of cycle time t_C

Numerical result 3 (Transient): For the manufacturing system defined by assumptions (i) through (ix), both e_{UNIT} and c_{UNIT} increase as t_C increases.

The following proposition holds for a special case in the steady state.

Proposition 3 (Steady): For the manufacturing system defined by assumptions (i) through (ix), e_{UNIT} is strictly monotonically increasing in t_C; when $l = \lceil t_D / t_C \rceil = t_D / t_C$ (i.e., t_D is a multiple of t_C), if there exist a $t \in \{1, 2, \ldots, T - l + 1\}$ such that all $b(t_1) = 1$ or all $b(t_1) = 0$ for all $t_1 \in \{t, \ldots, t + l - 1\}$ (i.e., $\max_{t \in \{1,2,\ldots,T-l+1\}} \sum_{t_1=t}^{t+l-1} b(t_1) = l$ or $\max_{t \in \{1,2,\ldots,T-l+1\}} \sum_{t_1=t}^{t+l-1} b(t_1) = 0$), then c_{UNIT} is strictly monotonically increasing in t_C.

Proof: Since $d_{i,2}$ is fixed and $e_{i,2} = d_{i,2} t_C$, $e_{i,2}$ is strictly monotonically increasing in t_C. Similarly, $e_{i,1}$ is strictly monotonically increasing in t_C. In (3.20), with other variables being fixed, e_{UNIT} is strictly monotonically increasing in t_C.

Similar to the division of T into T_1 and T_2, we can also divide the planning horizon H into two parts, H_1 and H_2, being the durations of the off- and on-peak periods, respectively. Therefore, equation (3.19) is

$$\overline{c_E} = H_1 c_{E,1} / t_C + H_2 c_{E,2} / t_C \tag{3.25}$$

If $\max_{t \in \{1,2,\ldots,T-l+1\}} \sum_{t_1=t}^{t+l-1} b(t_1) = l$, then (3.21) can be reformulated as

$$c_{UNIT} = \frac{\left(c_D \cdot l/t_D + H_1 c_{E,1}/t_C + H_2 c_{E,2}/t_C\right) \cdot \sum_{i=1}^{N}(d_{i,2} - d_{i,1}) \cdot t_C}{H/t_C}$$
$$+ \frac{\left(c_D \cdot l/t_D + H_1 c_{E,1}/t_C + H_2 c_{E,2}/t_C\right) \cdot \sum_{i=1}^{N} d_{i,1} p_i \cdot t_C + c_{Fixed}}{H \cdot PR_N/t_C}$$
$$= \frac{\left(c_D/t_C + H_1 c_{E,1}/t_C + H_2 c_{E,2}/t_C\right) \cdot \sum_{i=1}^{N}(d_{i,2} - d_{i,1}) \cdot t_C}{H/t_C}$$
$$+ \frac{\left(c_D/t_C + H_1 c_{E,1}/t_C + H_2 c_{E,2}/t_C\right) \cdot \sum_{i=1}^{N} d_{i,1} p_i \cdot t_C + c_{Fixed}}{H \cdot PR_N/t_C}$$
$$= \frac{\left(c_D + H_1 c_{E,1} + H_2 c_{E,2}\right) \cdot \sum_{i=1}^{N}(d_{i,2} - d_{i,1}) \cdot t_C}{H}$$
$$+ \frac{\left(c_D + H_1 c_{E,1} + H_2 c_{E,2}\right) \cdot \sum_{i=1}^{N} d_{i,1} p_i \cdot t_C + c_{Fixed} \cdot t_C}{H \cdot PR_N} \quad (3.26)$$

Similarly, if $\max_{t \in \{1,2,\ldots,T-l+1\}} \sum_{t_1=t}^{t+l-1} b(t_1) = 0$, then (3.21) can be reformulated as

$$c_{UNIT} = \frac{\left(H_1 c_{E,1} + H_2 c_{E,2}\right) \cdot \sum_{i=1}^{N}(d_{i,2} - d_{i,1}) \cdot t_C}{H} + \frac{\left(H_1 c_{E,1} + H_2 c_{E,2}\right) \cdot \sum_{i=1}^{N} d_{i,1} p_i \cdot t_C + c_{Fixed} \cdot t_C}{H \cdot PR_N} \quad (3.27)$$

Therefore, with other variables being fixed, c_{UNIT} is strictly monotonically increasing in t_C.

■

Remark 3: As an example, the condition "$l = \lceil t_D/t_C \rceil = t_D/t_C$ and $\max_{t \in \{1,2,\ldots,T-l+1\}} \sum_{t_1=t}^{t+l-1} b(t_1) = l$" is satisfied in Scenario 1 described in Section 3.4; the condition "$l = \lceil t_D/t_C \rceil = t_D/t_C$ and $\max_{t \in \{1,2,\ldots,T-l+1\}} \sum_{t_1=t}^{t+l-1} b(t_1) = 0$" is satisfied in Scenarios 0 and 2 described in Section 3.4. For both the transient and steady cases, it is desirable to reduce t_C so that the per-product electricity energy e_{UNIT} and TOU based per-product electricity cost c_{UNIT} can both be reduced.

3.3.4. Effects of machine number N

Numerical result 4 (Transient): For the manufacturing system defined by assumptions (i) through (ix), both e_{UNIT} and c_{UNIT} increase as N increases.

Proposition 4 (Steady): For the manufacturing system defined by assumptions (i) through (ix), both e_{UNIT} and c_{UNIT} are strictly monotonically increasing in N.

Proof: It can be easily proven by induction that PR_N is strictly monotonically decreasing in N. In addition, as N increases (decreases), the numerators in (3.20) and (3.21) also increases (decreases), which completes the proof. ■

Remark 4: Numerical result 4 and Proposition 4 imply that when more machining processes are involved to manufacture a product, per-product electricity energy e_{UNIT} and TOU based per-product electricity cost c_{UNIT} both increase.

Table 3.3. Transient-state numerical examples (summer)

	t_C = 1 minute	t_C = 5 minutes	t_C = 15 minutes
N = 2	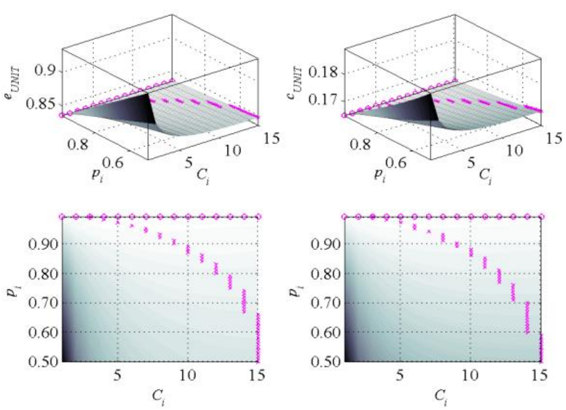	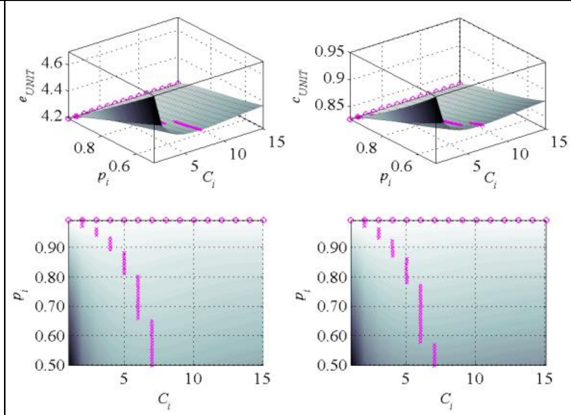	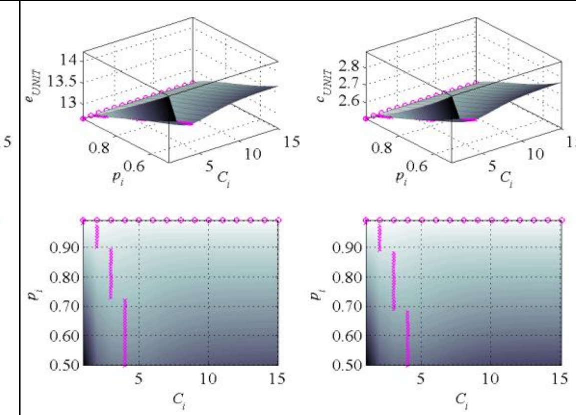
N = 4	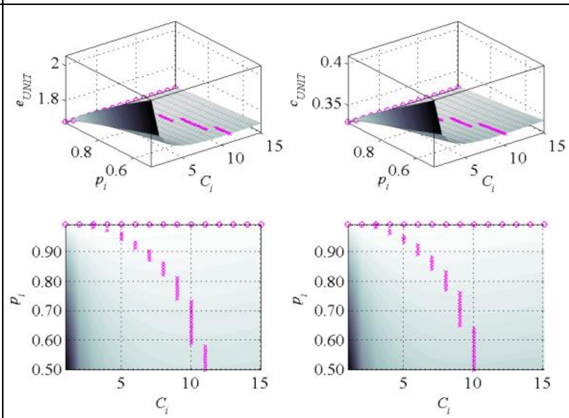	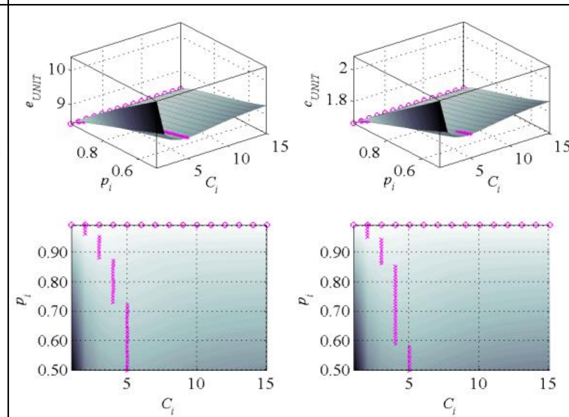	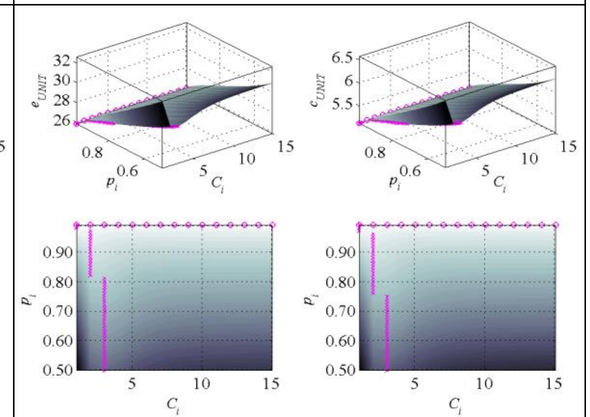
N = 10	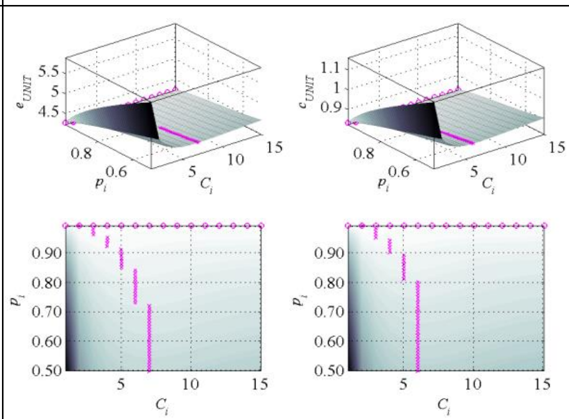	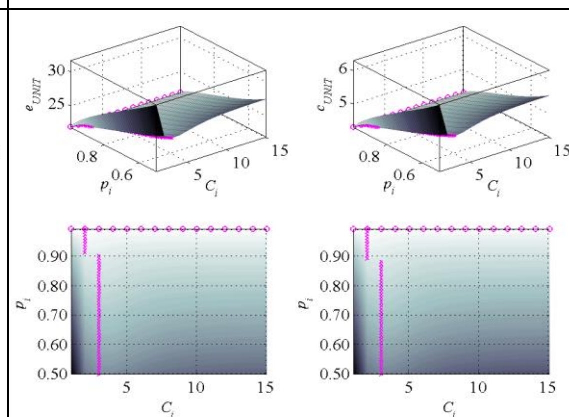	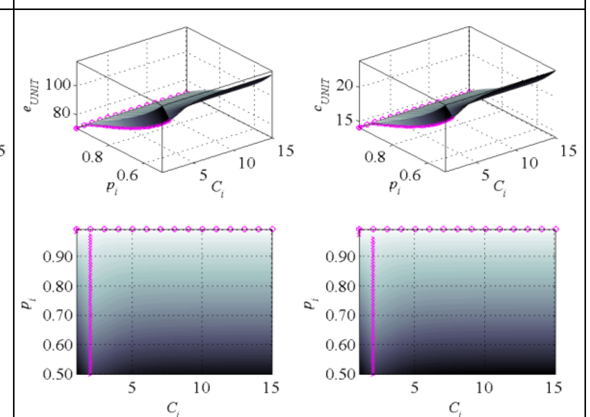

Table 3.4. Transient-state numerical examples (winter)

	t_C = 1 minute	t_C = 5 minutes	t_C = 15 minutes
N = 2	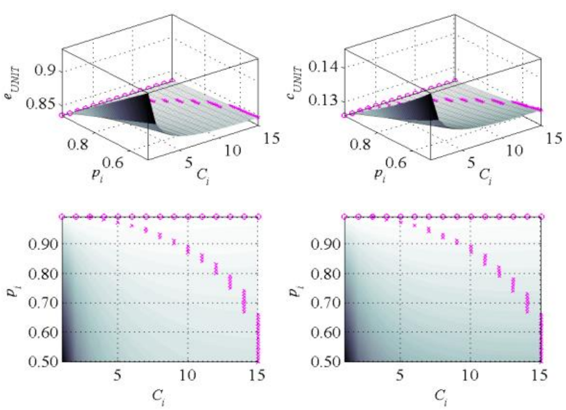	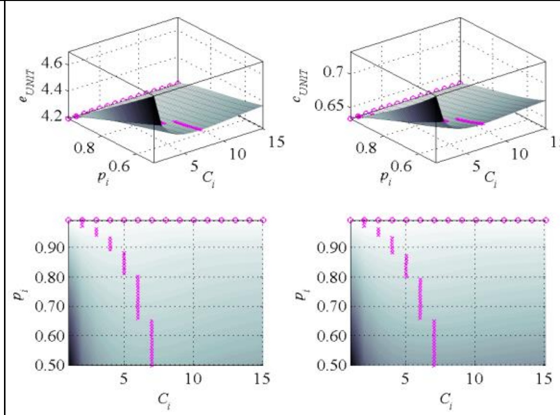	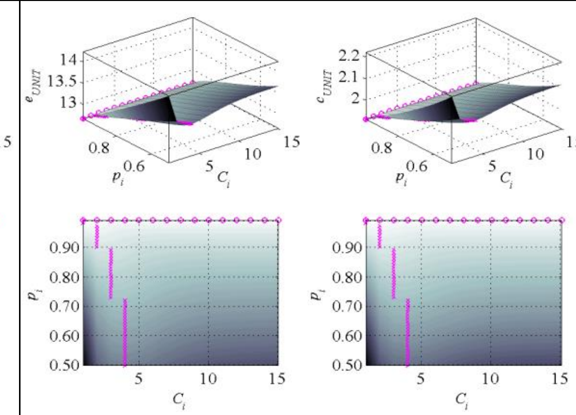
N = 4	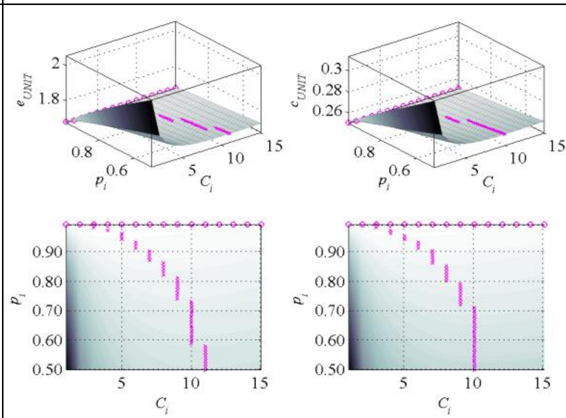	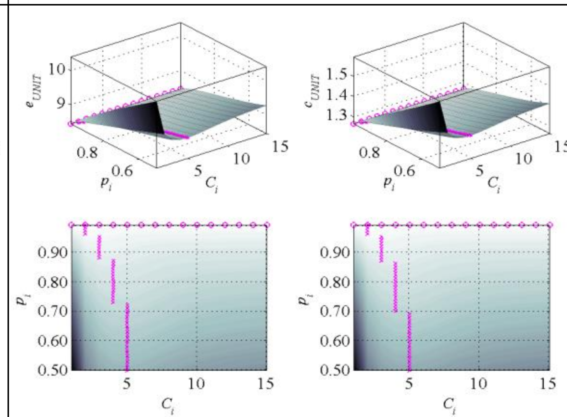	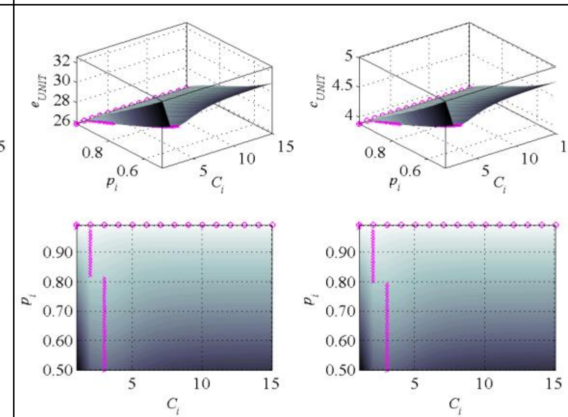
N = 10	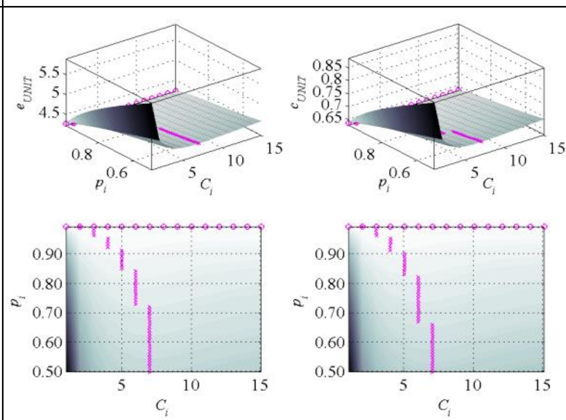	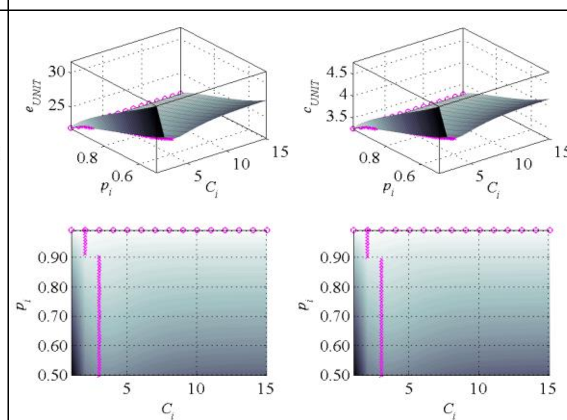	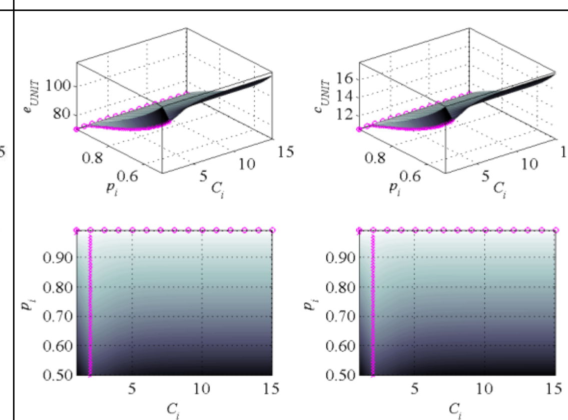

Table 3.5. Steady-state numerical examples (summer)

	t_C = 1 minute	t_C = 5 minutes	t_C = 15 minutes
$N = 2$	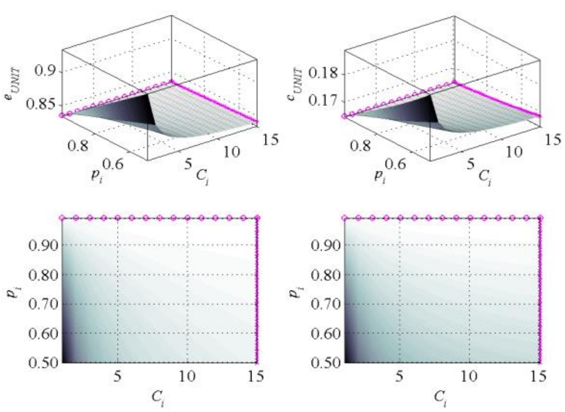	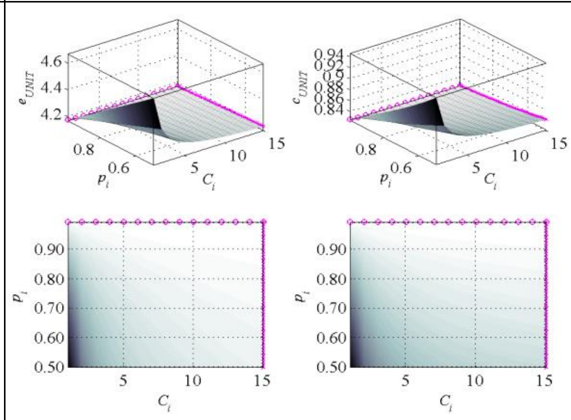	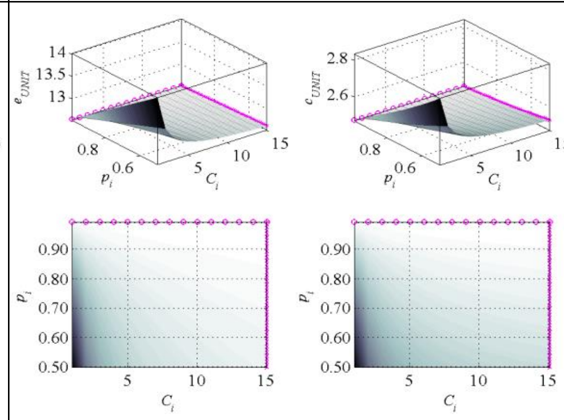
$N = 4$	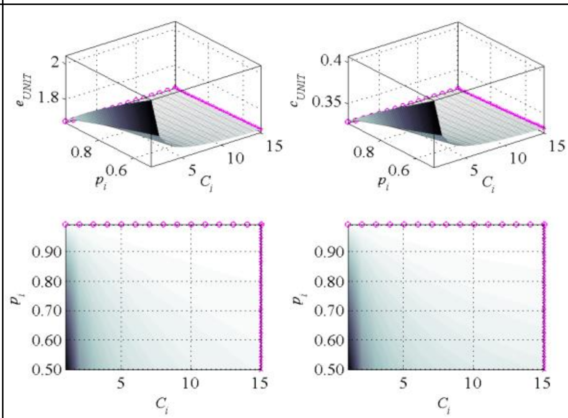	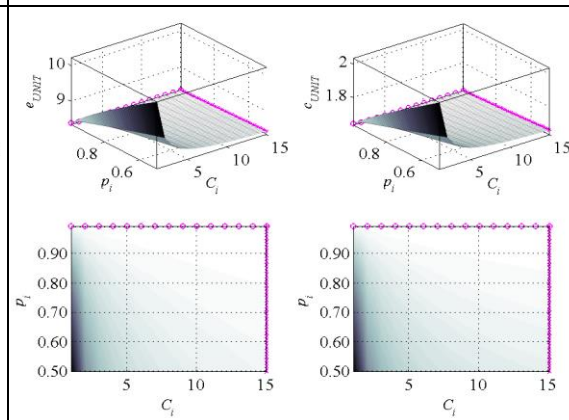	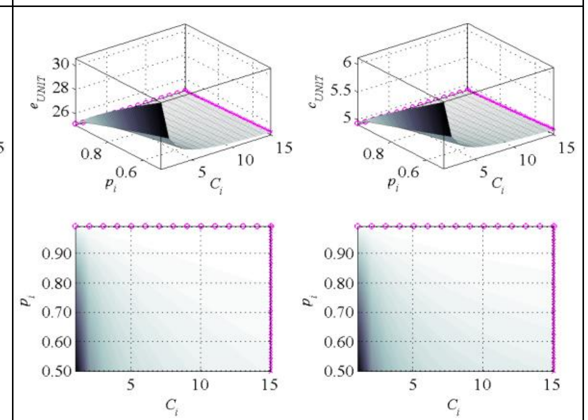
$N = 10$	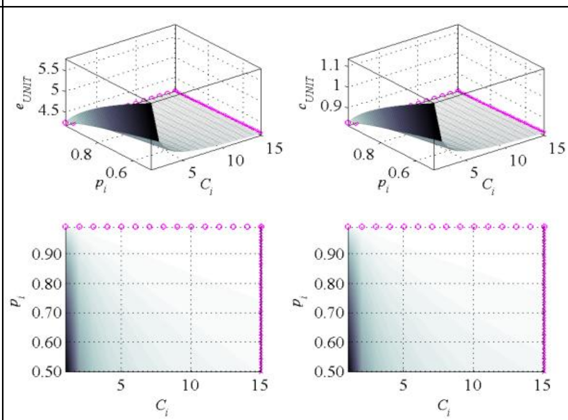	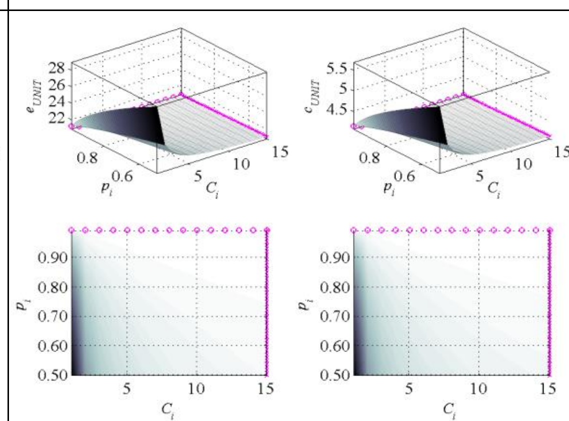	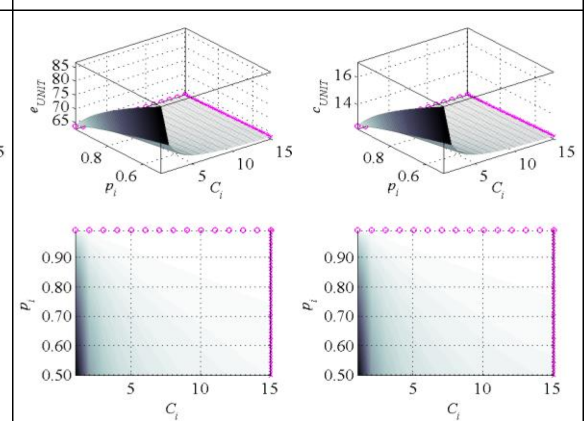

Table 3.6. Steady-state numerical examples (winter)

	t_C = 1 minute	t_C = 5 minutes	t_C = 15 minutes
N = 2	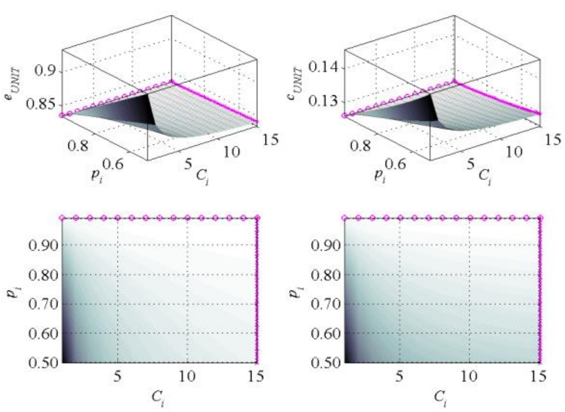	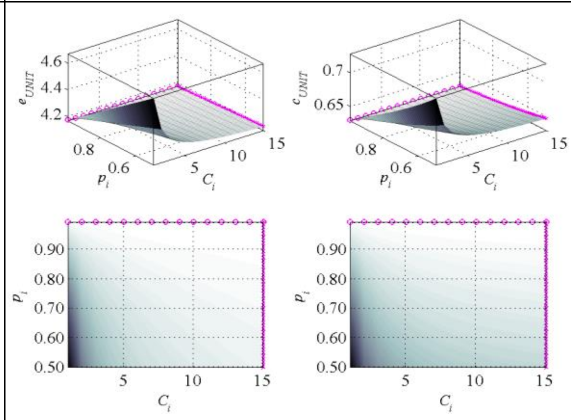	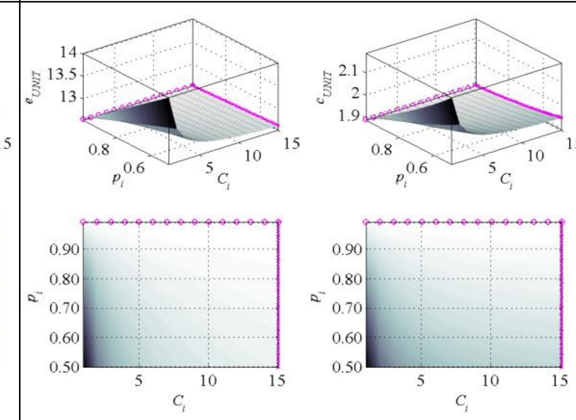
N = 4	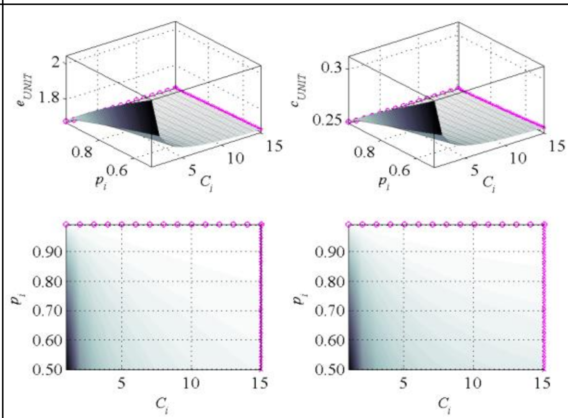	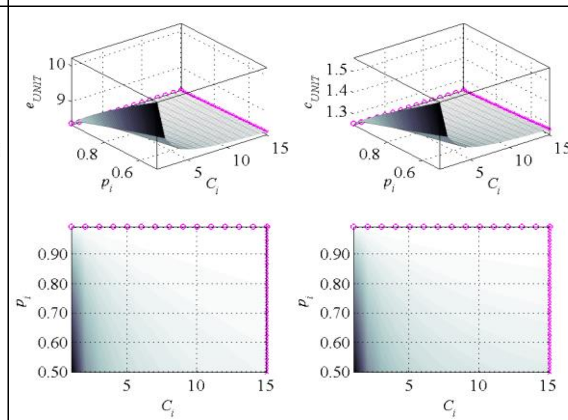	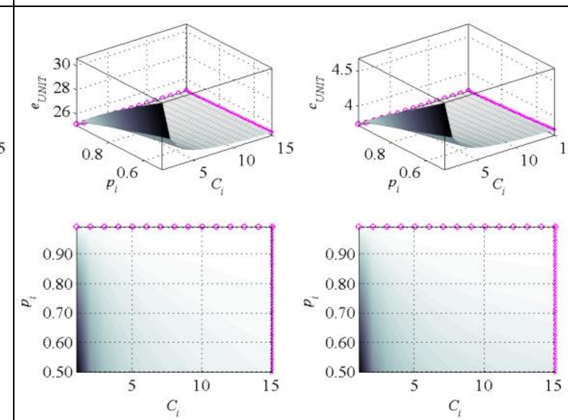
N = 10	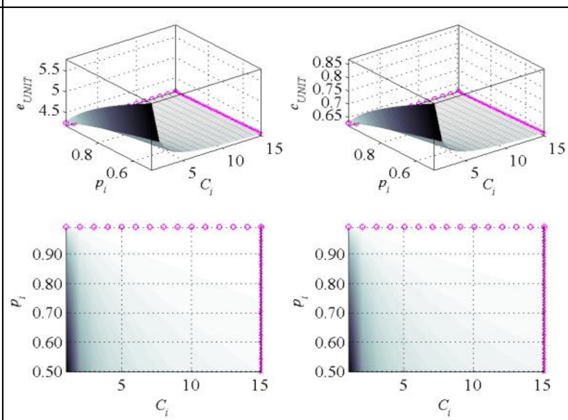	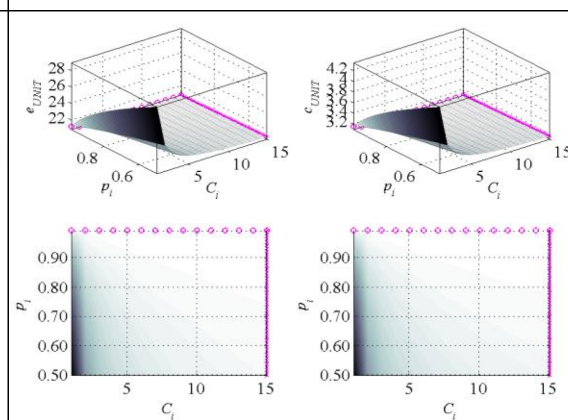	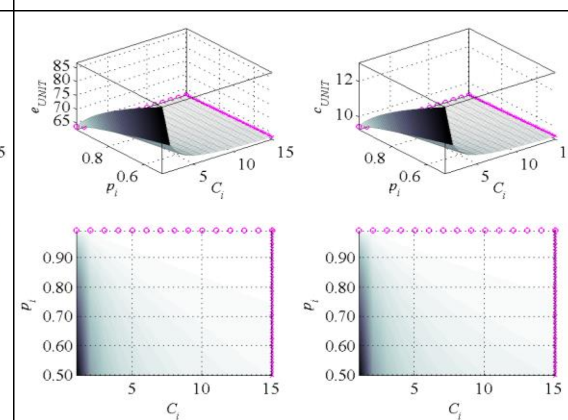

3.4. Decision Making on Rate Plan Switching

In this section, we define three scenarios as shown in Table 3.7 and determine whether it is economically sound to switch from the traditional flat rates to the TOU rates.

Table 3.7. Three different scenarios

Scenario	Rate plan	Planning horizon
Scenario 0	Flat rates in Table 1.1	H=16 hours (two shifts), starting from 8am to 12 midnight
Scenario 1	TOU rates in Table 1.2	H=16 hours (two shifts), starting from 8am to 12 midnight
Scenario 2	TOU rates in Table 1.2	H=16 hours (two shifts), starting from 7pm to 11am (next day)

3.4.1. Effects of seasons

Let $c_{UNIT,SUM}$ and $c_{UNIT,WIN}$ be the per-product electricity cost for the summer and winter months, respectively.

Numerical result 5 (Transient and steady): For the manufacturing system defined by assumptions (i) through (ix), c_{UNIT} is higher in summer than in winter (i.e., $c_{UNIT,SUM} > c_{UNIT,WIN}$) for Scenario 0 and Scenario 1; it is higher in winter than in summer (i.e., $c_{UNIT,SUM} < c_{UNIT,WIN}$) for Scenario 2.

Proposition 5 (Transient and steady): For the manufacturing system defined by assumptions (i) through (ix), e_{UNIT} is not affected by the seasonal difference in the flat or TOU rates.

Proof: The summer pricing profile differs the winter profile in the c_E and/or c_D values. Since there is no pricing item such as c_E or c_D involved in any mathematical expressions of e_{UNIT}, the seasonal rate profiles have no effect on e_{UNIT}. ■

Remark 5: Numerical result 5 can be explained as follows. For Scenario 0, this is because the $\overline{c_E}$ value in summer is higher than that in winter, and $c_D = 0$ because there is no demand charge; for Scenario 1, this is because both $\overline{c_E}$ and c_D values in summer are higher than those in winter; For Scenario 2, this is because the planning horizon is entirely within the off-peak period in summer, while it consists of both on- and off-peak periods in winter.

3.4.2. Effects of rate plans and shift time

Since $c_{UNIT,SUM}$ and $c_{UNIT,SUM}$ can be significantly different, it is reasonable to take a weighted average to obtain a yearly weighted per-product electricity cost, which is denoted by $c_{UNIT,YW}$. Let w_{SUM} and w_{WIN} be the weights for the summer and winter months, respectively. Then

$$c_{UNIT,YW} = w_{SUM} \cdot c_{UNIT,SUM} + w_{WIN} \cdot c_{UNIT,WIN} \tag{3.28}$$

For all the three scenarios, the weights are the proportions of the seasons to a year, i.e., w_{SUM} = 4 / 12, w_{WIN} = 8 / 12. The per-product electricity cost saving by switching from Scenario 0 to Scenario 1 or 2 is defined as

$$c_{UNIT,YW}^{Scenario\ 0\to i} = \left(c_{UNIT,YW}^{Scenario\ 0} - c_{UNIT,YW}^{Scenario\ i} \right) \Big/ c_{UNIT,YW}^{Scenario\ 0} \times 100\%, \quad i = 1,\ 2 \tag{3.29}$$

The plots of the numerical examples are summarized in Table 3.8 and Table 3.9.

Numerical result 6 (Transient and steady): For the manufacturing system defined by assumptions (i) through (ix), the relationship $c_{UNIT,YW}^{Scenario\ 0\to 2} > c_{UNIT,YW}^{Scenario\ 0\to 1} \approx 0$ holds.

Proposition 6 (Transient and steady): For the manufacturing system defined by assumptions (i) through (ix), e_{UNIT} is not affected by switching from one scenario to another.

Proof: Similar to the proof of Proposition 5. ■

Remark 6: Numerical result 6 shows **s**imply switching from Scenario 0 to Scenario 1, without any change in production routine, will not significantly influence the per-product electricity cost. The $c_{UNIT,YW}^{Scenario\ 0\to 1}$ values range from −1.9% to 2.2% in the numerical examples. A further change of production routine, reducing day hours and adding night hours as shown in Scenario 2, can lead to significant savings. The $c_{UNIT,YW}^{Scenario\ 0\to 2}$ values range from 22.5% to 24.8%.

Table 3.8. Transient-state numerical examples (yearly weighted)

	t_C = 1 minute	t_C = 5 minutes	t_C = 15 minutes
N = 2	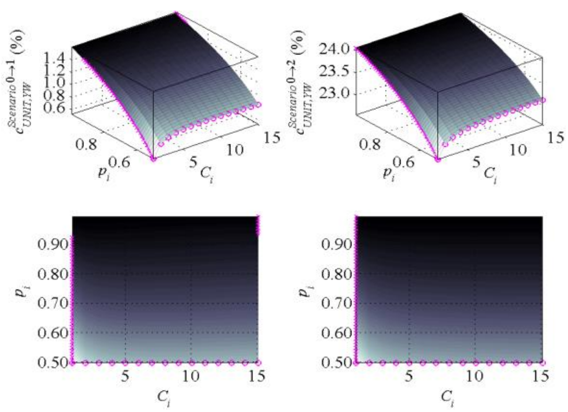	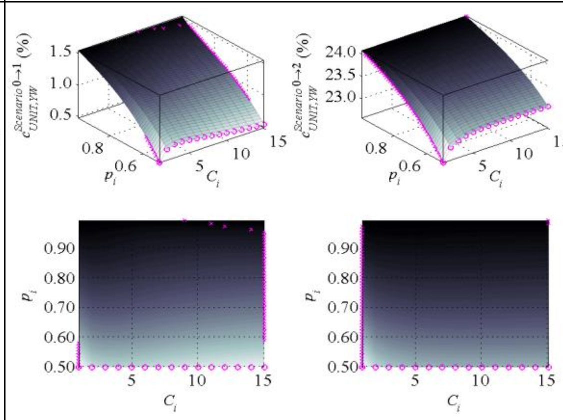	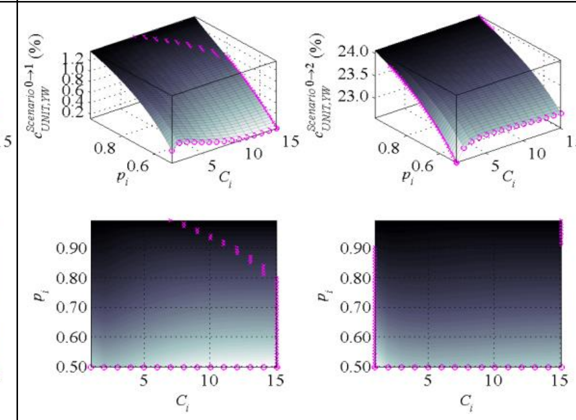
N = 4	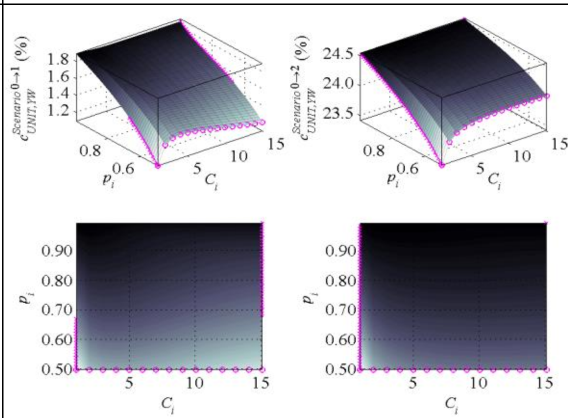	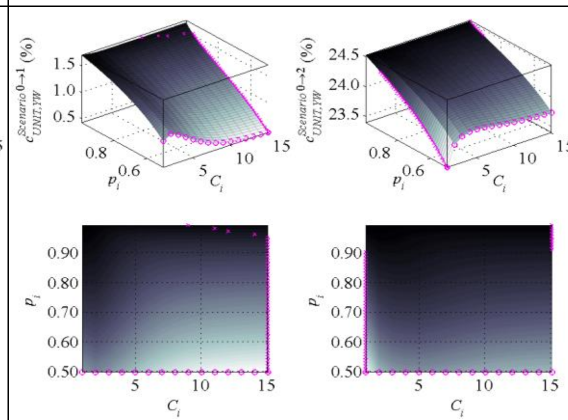	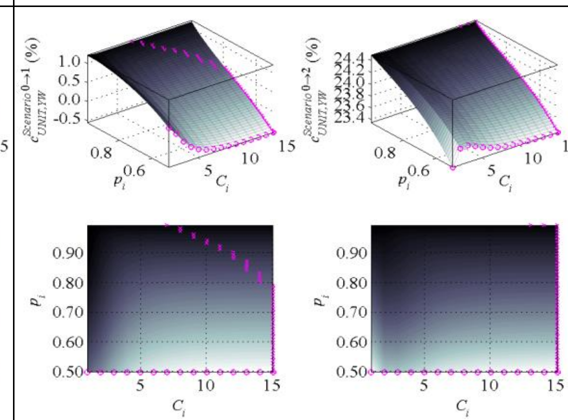
N = 10	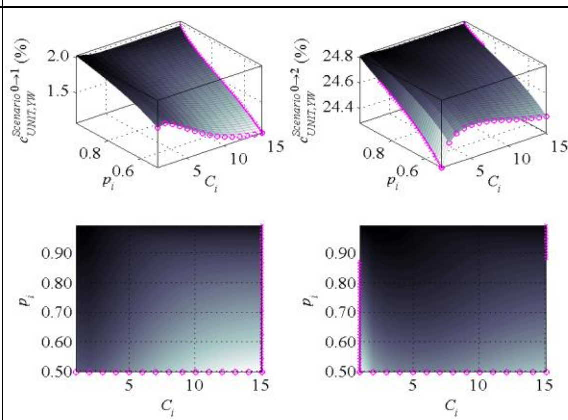	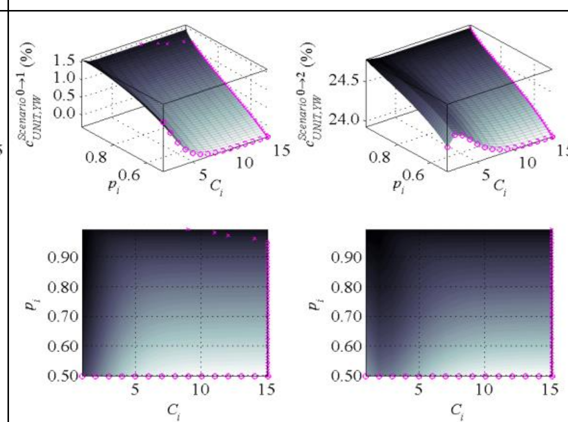	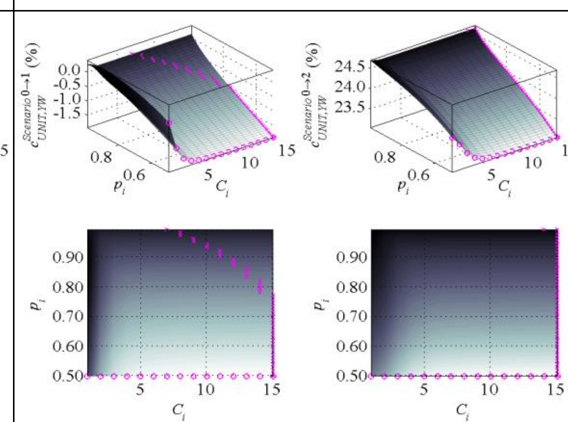

Table 3.9. Steady-state numerical examples (yearly weighted)

	t_C = 1 minute	t_C = 5 minutes	t_C = 15 minutes
N = 2	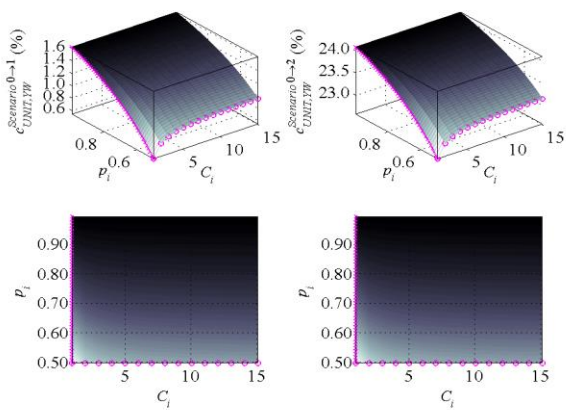	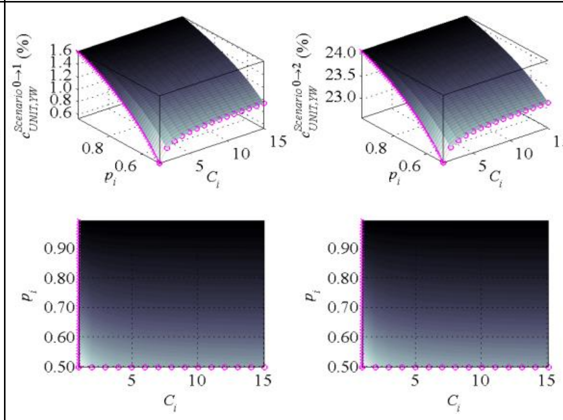	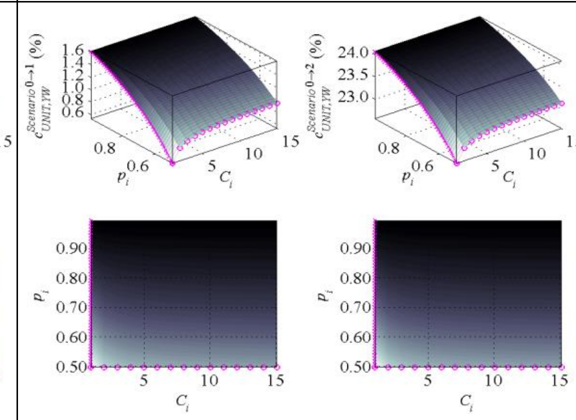
N = 4	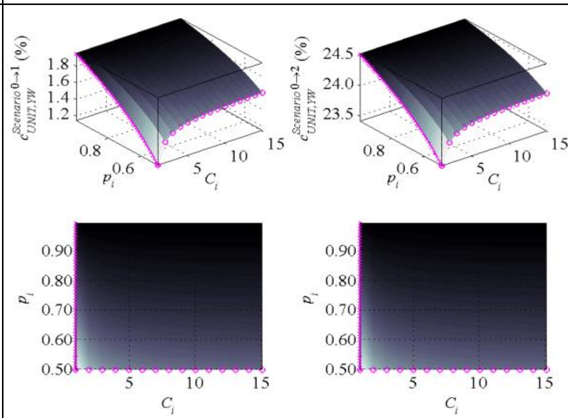	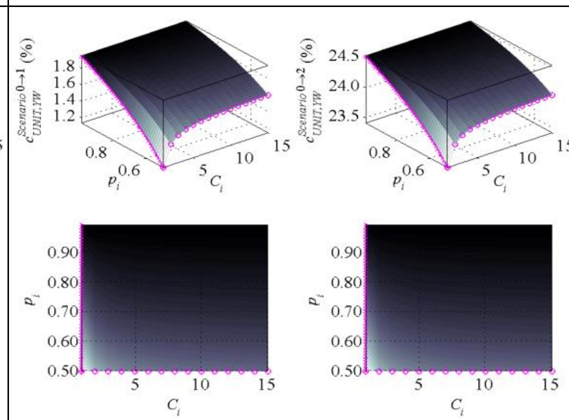	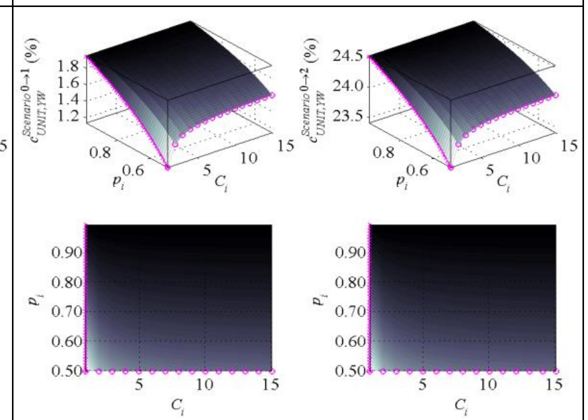
N = 10	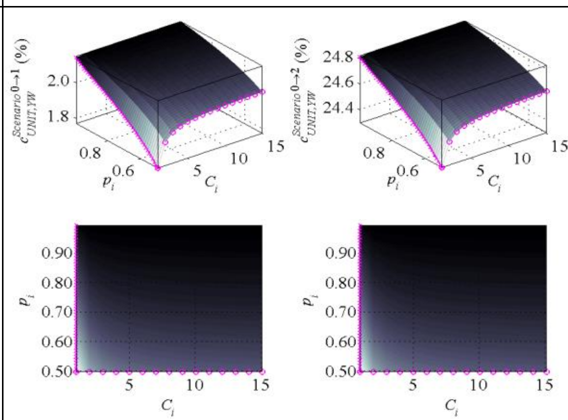	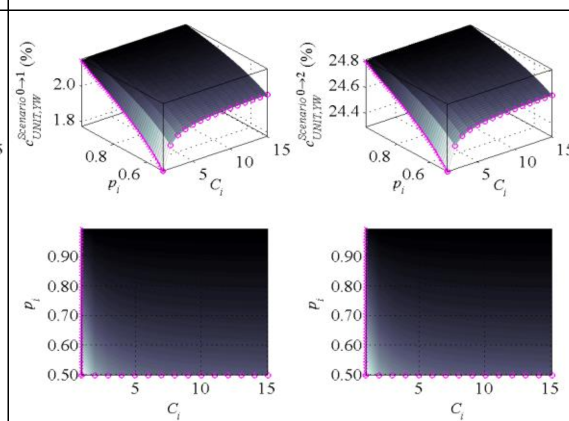	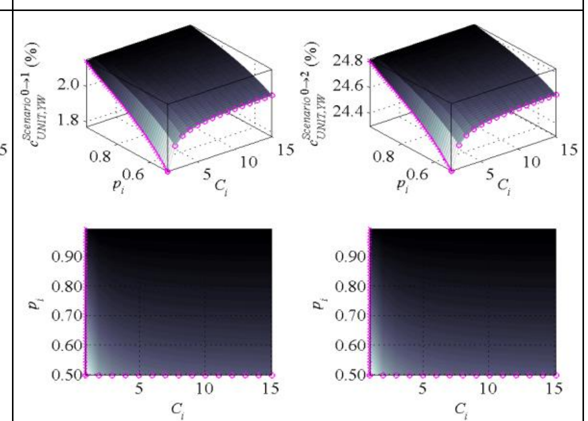

3.5. Conclusions

This chapter proposes a novel method for modeling the TOU based electricity energy efficiency and cost of manufacturing a product. The method integrates both electricity energy consumption and peak demand with varying rates into the production model at the system level. Such issues are previously unaddressed in the manufacturing literature. The model is used to perform monotonicity analysis on machine and buffer parameters such as buffer capacities C_i, machine reliabilities p_i, cycle time t_C, and machine number N. Further analysis on the seasonal differences in the TOU rates and production routine change has also been conducted. The main research outcomes are presented in the six numerical results and six propositions. From the design perspective, the findings can be used to provide guidance on how to select machine and buffer parameters so that per-product energy consumption e_{UNIT} and per-product electricity cost c_{UNIT} can be both maintained at a low level. From the operation perspective, they can be used to justify whether it is economically sound to switch from the flat rates to the TOU rates.

CHAPTER 4

TOU ELECTRICITY PRICING FOR INDUSTRIAL CUSTOMERS: A SURVEY OF U.S. UTILITIES

(Parts of this chapter were previously published as: *Wang, Y., Li, L., 2015. Time-of-use electricity pricing for industrial customers: A survey of U.S. utilities. Applied Energy, 149, 89-103.*)

4.1. Introduction

Customer participation is critical to the success of TOU pricing programs. To fulfill the potential of such programs, customers must be able to access electricity tariffs and understand their terms. This chapter reports a survey of 43 TOU pricing programs targeting industrial customers offered by U.S. utilities. This work is inspired by and complements the Federal Energy Regulatory Commission (FERC) surveys of demand response in the electric power industry, highlighting the interpretation of key pricing components and specific characteristics of TOU tariff sheets collected from public sources. The case studies examine various industrial scenarios to predict electricity cost savings when customers are facing the transition from flat rates to TOU pricing. The analysis results show that the cost savings vary enormously, ranging from -72.0% to 82.6%, depending on specific utility programs and switching strategies involved. Such information is useful for customers to determine whether to participate in a TOU pricing program. Key findings and implications for industrial customers, utilities, and regulatory agencies are also discussed.

The remainder of this chapter is organized as follows. A brief literature review is conducted in Section 4.2. In Section 4.3, we start with analyzing the latest nationwide large-scale demand response survey conducted by the FERC, with a particular focus on TOU pricing programs. In Section 4.4, we proceed to conduct our own survey by collecting and interpreting the TOU tariffs of 43 largest utilities in the U.S. in terms of the numbers of customers enrolled in these TOU programs. These programs represent a wide range of TOU tariff designs. Such TOU tariffs are compared with the otherwise applicable traditional flat rates in Section 4.5, so the customers can estimate the benefits of switching from the flat rate to the TOU rate and ultimately the dollar value of these benefits. Section 4.6 gives our key findings and implications for industrial customers, utilities, and regulatory agencies. Finally, conclusions of this chapter are drawn in Section 4.7.

4.2. A Brief Literature Review

It should be mentioned that related surveys on TOU pricing have been previously conducted by a few researchers and organizations. For example, Faruqui and Malxo (1983) conducted a survey of 12 pilot or experimental TOU pricing programs funded by U.S. Department of Energy in early 1980s that involved about 7,000 customers. A more recent update was accomplished by Faruqui and Sergici (2010) on 15 experimental programs. Similar surveys have also been conducted in other parts of the world. For example, in Great Britain, the nationwide survey of customer experiences with TOU pricing that involved 5,914 interviews was conducted by Ipsos MORI (2012).

However, all these efforts focus on residential programs targeting household applications. The TOU programs targeting industrial customers (Alvarez Bel et al., 2009; Ashok, 2006; Braithwait and Hansen, 2012; Mathieu et al., 2011), who are fundamentally different from residential customers (Gottwalt et al., 2011; Herter et al., 2007; Herter and Wayland, 2010; Rastegar et al., 2012), have been largely neglected. Although commercial and industrial (C&I)

customers own only 12% of all the meters in the U.S., they consume 60% of the electricity in the country (Brief and Davids, 2011). In addition, according to the 2012 FERC survey (U.S. FERC, 2012), the reported potential peak reduction of TOU programs by C&I customers is 6,421MW, while the value by residential customers is only 879MW. Accounting for such facts, utility companies usually create tariffs different from those targeting residential customers, highlighting the benefits specific to the non-residential segment, to attract the interest of industrial customers. Therefore, our survey focuses on the TOU tariffs specifically for industrial customers.

4.3. The FERC Surveys

The FERC has been conducting a series of nationwide voluntary surveys of demand response and advanced metering biennially since 2006 (U.S. FERC, 2006, 2008, 2010, 2012). The survey results serve as a unique database to support utilities and the government for regional and national planning purposes. The latest survey data were released in 2012. A total of 1,978 out of 3,349 entities in all 50 states responded to the 2012 survey, representing a response rate of over 59%. Such data were analyzed in the FERC report (U.S. FERC, 2012) to estimate the "penetration of advanced metering and demand response programs in the electric power industry in the U.S".

Although the 2012 FERC report provided a first-of-its-kind overview of developments of demand response activities as well as advanced metering infrastructure and Smart Grid standards, it did not dig deeper and provide detailed analysis for specific types of demand response programs. For example, the raw data of TOU pricing programs were collected in the survey, but the analysis of such data in the report was limited. Some data mining work is still needed to reveal useful information of this specific type of demand response programs. Such work will be conducted in this section.

We start with mining the raw FERC survey data collected over the years for the trend of TOU pricing programs in potential peak reduction. The graph is shown in Figure 4.1 by customer type. It should be mentioned that many utility companies do not differentiate between commercial and industrial customers. That is, if one tariff is applicable to one type of such customers, it is also applicable to the other type. Therefore, the FERC surveys followed this industry practice, combined these two types of customers into one category, and only collected a total statistic for each question related. The surveys did collect the data of residential customers separately because utility companies usually design residential tariffs differently. The result in Figure 4.1 shows the reported potential peak reduction increases steadily and almost exponentially for the C&I TOU programs. By contrast, the reported potential peak reduction only starts to climb during recent years, and the latest number is only a fraction of that of C&I programs.

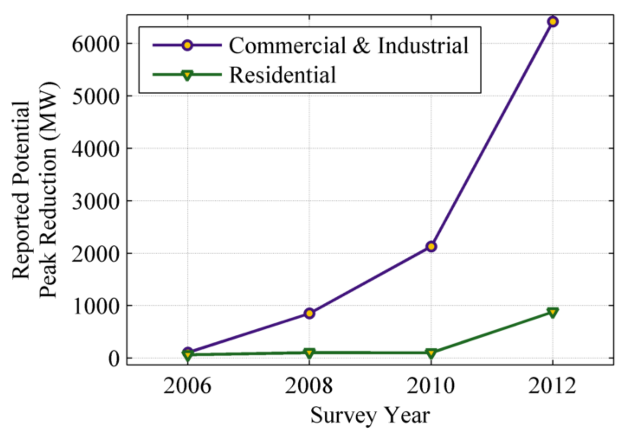

Figure 4.1. Reported potential peak reduction by C&I and residential customers enrolled in TOU programs

The 2012 FERC survey reveals that 149,140 C&I customers enrolled in 408 TOU programs provided by 204 utilities in the U.S., representing a total of 6,421MW potential peak demand reduction. Detailed information by state is shown in Figure 4.2. Figure 4.2(a) indicates out of the 50 states and the District of Columbia, Wisconsin has the greatest number of utilities offering TOU tariffs for C&I customers. It also shows that not every state has utilities that offer TOU tariffs for C&I customers. Figure 4.2(b) indicates that California, North Carolina, and Florida account for more than a half of the total C&I customers enrolled.

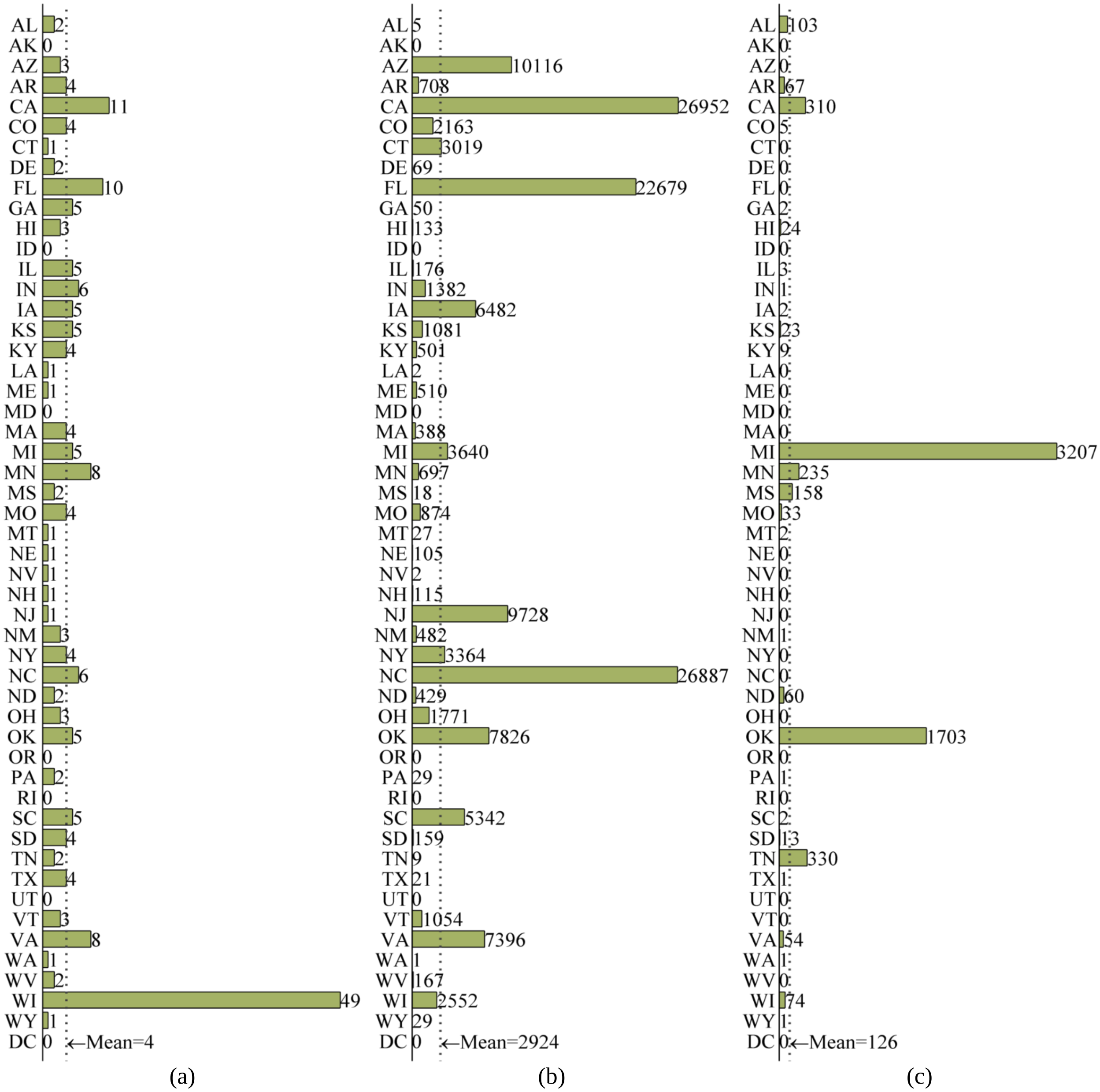

Figure 4.2. (a) Reported number of utilities (total 204) offering TOU programs for C&I customers; (b) Reported number of C&I customers (total 149,140) enrolled in TOU programs; (c) Reported potential peak reduction (in MW, total 6,421MW) by C&I customers enrolled in TOU programs

Figure 4.2(c) indicates that the C&I customers who contribute the most towards the potential peak demand reduction locate in Michigan and Oklahoma. However, some values in Figure 4.2(c) demonstrate great inconsistency with Figure 4.2(a) and Figure 4.2(b). For example, Florida has 22,679 C&I customers in the TOU programs, but its total potential peak reduction is less than 1MW. A similar phenomenon is observed in North Carolina. These discrepancies are because the estimation of potential peak reduction of time-based demand response programs is less straightforward than that of incentive-based ones, for which the tariffs usually specify the detailed amount of demand that can be interrupted/curtailed. Thus, many utility employees who responded to the survey just typed zero in the survey form or left the question unanswered, as revealed in the collected data. In other words, the potential peak reduction information collected by the FERC survey may be incomplete due to its voluntary nature.

We proceed to present the number of utilities offering TOU tariffs for C&I customers by entity type and by NERC (North American Electric Reliability Council) region. Figure 4.3(a) shows that most of the utilities belong to COU, IOU, or MOU. Figure 4.3(b) shows that more than a half of the utilities belong to the MRO and SERC regulatory regions. These regions geographically encompass the Southeastern (excluding Florida) and Midwestern states.

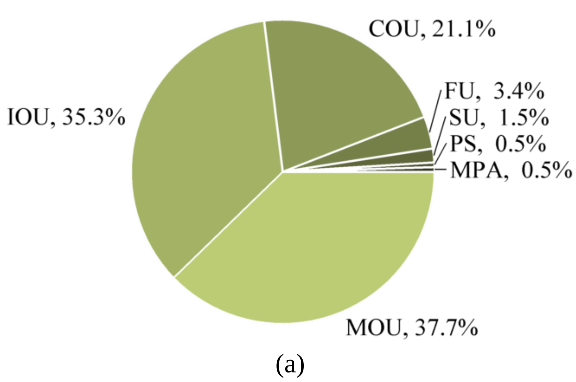

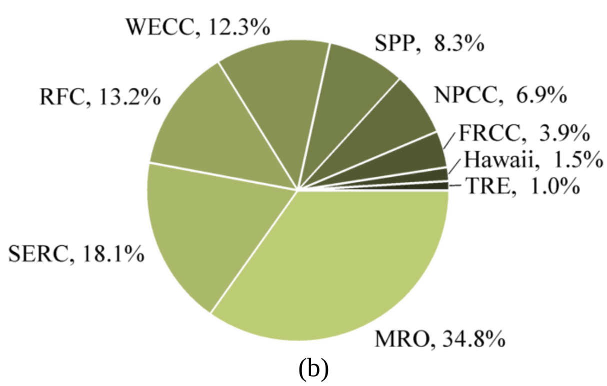

Figure 4.3. Number of utilities (total 204) offering TOU tariffs for C&I customers (a) by entity type (MPA: Municipal Power Agency; PS: Political Subdivision; SU: State Utility; FU: Federal Utility; COU: Cooperatively Owned Utility; IOU: Investor Owned Utility; MOU: Municipally Owned Utility), and (b) by NERC region (TRE: Texas Regional Entity; Hawaii: The State of Hawaii; FRCC: Florida Reliability Coordinating Council; NPCC: Northeast Power Coordinating Council; SPP: Southwest Power Pool RE; WECC: Western Electricity Coordinating Council; RFC: Reliability*First* Corporation; SERC: SERC Reliability Corporation; MRO: Midwest Reliability Organization)

Finally, we display the number of TOU programs for C&I customers in the U.S. by participation exclusion policy and by participation option policy. The participation exclusion policy determines whether the participants enrolled in the TOU programs are excluded from taking part in other demand response programs. Figure 4.4(a) shows only 14.2% of programs enforce this policy. Figure 4.4(b) shows that the majority of the TOU programs adopt the opt-in policy, the mandatory policy is less popular but still accounts for a significant portion in all the programs, and only a small portion of the programs adopt the opt-out policy. It should be mentioned that the exclusion policy and the option policy do not conflict with each other. Some utilities require mandatory participation in the TOU program, but the customers are allowed to enroll in another demand response program such as interruptible load, as long as TOU pricing serves as the base service.

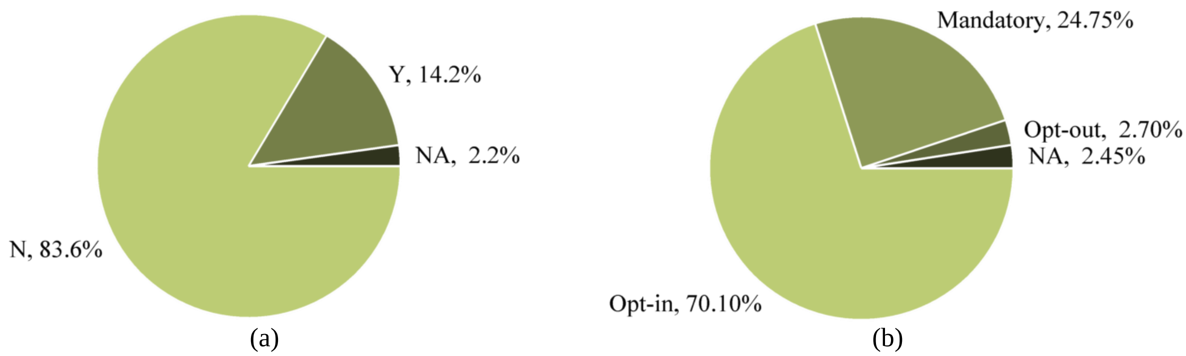

Figure 4.4. Number of TOU programs (total 408) for C&I customers (a) by participation exclusion policy (NA: Not available or no response; Y: Yes; N: No), and (b) by participation option policy (NA: Not available or no response; Opt-out: customers will be enrolled unless they choose not to; Mandatory: Participation will be mandatory based on customers' size or rate class; Opt-in: customers will not be enrolled unless they choose to)

4.4. Survey of TOU Pricing in U.S. Utilities

As mentioned in previous sections, the FERC surveys aim to provide an overall assessment of the development of demand response technologies at the macro level, but it does not collect data of specific pricing information. In addition, the analysis of the FERC survey data is conducted from the perspective of the supply side (i.e., utilities), instead of the perspective of the demand side (i.e., customers). Without such pricing information, the customers are unable to evaluate the benefits of the TOU programs in comparison with their current flat-rate programs. In order to address this issue, we conduct a new survey to gather, analyze, categorize, and summarize information pertinent to TOU programs offered by U.S. utilities targeting industrial customers, highlighting the interpretation of key components and characteristics of detailed tariff information. Since many utility companies do not differentiate between commercial and industrial customers, the insights gained in this section may also be applicable to commercial customers.

4.4.1. Survey approach

As revealed in our FERC survey analysis, there are a total of 204 utilities that offer TOU programs for industrial customers distributed among 44 states. Since surveying all the 204 utilities would impose a significant workload that is too heavy for the authors to manage, we determine to select only the largest utility in terms of the number of enrolled customers from each state as a representative. Ideally, it would be better to select the largest utility in terms of potential peak reduction. However, as mentioned in Section 3, the request for such information is not responded by many surveyed utilities, which renders the collected data incomplete.

After identifying the largest utility in a state, we proceed to collect the rate schedules targeting industrial customers based on publically available information on the Internet. All the data collected in this dissertation originate from the utility's official websites and more specifically, the tariff sheets for regulatory filings in public utility commissions (PUCs), which are the state agencies overseeing retail electric utilities (Scott, 2014; Fremeth, 2014). By surveying only the utilities' websites for tariff sheets, we also test the ease to accessing such information. This is consistent with what customers would usually do to obtain such information. Based on the nationwide FERC survey (U.S. FERC, 2012) of 17 million residential customers and 1.6 million non-residential customers, 92% of the former and 91% of the latter prefer to use the Internet as the communication vehicle to obtain energy usage data and billing information.

We have omitted the utilities that 1) we cannot find the tariff information on their websites, 2) the tariff information is incomplete, 3) the tariffs are canceled or closed, or 4) the tariffs are overly complex and difficult to interpret without direct communication with the utilities. Under such circumstances, we choose the second largest utility in that state as the representative. If none of the utilities' tariff information in the state is accessible, we will do a search and try to identify a substitute utility that did not respond to the FERC survey but actually provides such TOU programs for industrial customers, as well as retrieve the associated tariff information on their websites. This is possible because the response rate of the FERC survey is only 59%.

We have made no attempt to contact the utilities by telephone or via email. This is because according to previous survey efforts (U.S. FERC, 2012; EPRI, 2003; Barbose et al., 2004, 2005), it is not a trivial job to identify relevant personnel, and some utilities are not willing or able to provide specific details other than a response "everything you need to know is on our website". Besides, the survey does not involved reviewing various scattered sources including legislative documents, project reports, case studies, trade press articles, and workshop presentations because the information contained in such sources is minimal and often irrelevant, and as it turns out the pricing information is mostly concentrated in the tariff sheets for PUC filings.

4.4.2. General characteristics of surveyed TOU tariffs

Although the terms of the surveyed rates vary, they share some common characteristics. These general characteristics are summarized in this subsection.

Utilities usually divide industrial customers into several categories based on the customers' monthly peak demand, and design a different tariff for each category. For example, in Progress Energy Carolinas, NC, the flat and TOU tariffs for the customers with monthly peak demand less than 30 kW are SGS-28 and SGS-TOUE-28, respectively; the flat and TOU tariffs for the customers with monthly peak demand between 30 and 1000 kW are MGS-28 and SGS-TOU-28, respectively; the flat and TOU tariffs for the customers with monthly peak demand greater than 1000 kW are LGS-28 and LGS-TOU-28, respectively. Participation in these TOU programs is voluntary since the customers are given the option to switch from the flat rates to such TOU programs. An example of mandatory programs is offered by Flathead Electric Cooperative, Inc., MT. The tariffs applicable to industrial customers with peak demand in the intervals [0, 50) kW, [50, 100) kW, [100, 400) kW, [400, 1000) kW, and [1000, ∞) kW are SGS01, MGS01, LGS01, XGS01, and IND01, respectively. The first two are flat rates and the other three are TOU rates. The participation of the TOU programs is mandatory if the customer's peak demand falls into the associate ranges. Although the category thresholds vary from company to company, the tariff design follows the similar principle: the higher the peak demand, the cheaper the usage unit price of the service.

Most of the surveyed TOU programs require a minimum contract period, which may range from one year to five years. Almost all programs set up a minimum monthly charge, which is usually called the customer charge. It represents part of the fixed cost of providing the electric service and maintaining the customer in the program. Some TOU pricing programs are subject to capacity availability of the utilities. For example, the rate GS-TOU of Delaware Electric Cooperative, Inc., DE is limited to a maximum of 500 members requesting the service.

The electric services provided by the surveyed utilities are either single-phase or three-phase alternating current at 60 hertz. The utilities usually offer services at the secondary and primary voltage levels, and some offer even higher-voltage services. For example, the LGS-TOD program of Kentucky Power Company, KY offers the services at the following voltage levels: secondary (120/208, 120/240, 240, 480, and 277/480 Volts), primary (4,160/2,400, l2,470/7,200, and 34,500/19,900 Volts), subtransmission (19,900, 34,500, 46,000, and 69,000 Volts), and transmission (38,000, 160,000, 345,000, and 765,000 Volts). Similar to the categorization principle of peak power thresholds, the definitions of these voltage levels vary greatly. The tariff design follows the principle: the higher the voltage level, the cheaper the usage unit price of the service but the higher the base customer charge.

In order to help industrial customers to evaluate the benefits of switching from flat rates to TOU rates in Section 5, we only list retail voluntary TOU programs (i.e., those with flat option counterparts) in Table 4.1. To make an apples-to-apples comparison, the applicable peak demand ranges should be approximately the same for the flat and TOU tariffs of the same utility. These listed programs provided industrial customers with the following type of service: one- or three-phase alternating current of 60 Hz at secondary voltage. All the programs provide general services that are not restricted to a specific use.

Of the 44 companies surveyed, we are able to locate voluntary TOU tariffs from 37 of them; we can also locate such tariffs from 6 substitute utilities in the states of AL, GA, NE, NJ, NV, and WY. Most of these tariffs are located on the utilities' websites under the menus "Commercial and Industrial" or "Customer Service" with the title "Rates" or "Tariffs". Some websites also provide a sitemap, which is useful for the authors to quickly navigate to the tariff section. For the state of MT, we can only find the mandatory tariff information of the only utility reported in the FERC survey; we then performed a series of Internet search but still cannot locate a substitute utility in this state that provides voluntary TOU tariffs targeting industrial customers. Therefore, it was omitted from the table and only 43 utilities are listed in Table 4.1.

In Table 4.1, the first two columns list the abbreviations of the 43 states and the representative utilities surveyed. The state abbreviation will be used as the index to represent the utilities in subsequent tables. The third and fourth columns give the names of the flat rate programs and the ranges of the monthly peak demand (in kW) or monthly maximum energy consumption (in kWh). The fifth and sixth columns give the names of the corresponding TOU programs and the ranges of monthly peak demand or monthly maximum energy consumption. The last column lists the websites where these tariffs are retrieved at the time this dissertation is written.

Table 4.1. Surveyed utilities with the corresponding flat and TOU tariffs targeting industrial customers

State	Utility Name	Flat Tariff		TOU Tariff		Website
		Name	Demand or Energy Range	Name	Demand or Energy Range	
AL	Joe Wheeler Electric Membership Corporation	GSA	[50,1000) kW	TGSA	[50,1000) kW	jwemc.org/rate-forms/
AR	Entergy Arkansas Inc	LGS	[100,1000) kW	GST	[0,1000) kW	entergy-arkansas.com/your_business/business_tariffs.aspx
AZ	Salt River Project Agricultural Improvement & Power District	E-36	[5,1500] kW	E-32	[5,1500] kW	srpnet.com/prices/business/
CA	Los Angeles Department of Water and Power	A-1-A	[0,30) kW	A-1-B	[0,30) kW	ladwp.com/ladwp/faces/ladwp/commercial/c-customerservice/c-cs-understandingyourrates/c-cs-uyr-electricrates
CO	Colorado Springs Utilities	E2C	(990,30000) kWh	ETC	(990,30000) kWh	csu.org/pages/electric-tou-b.aspx
CT	Connecticut Light and Power Company	Rate 30	[0,200) kW	Rate 27	[0,350) kW	cl-p.com/rates/rates_and_tariffs
DE	Delaware Electric Cooperative, Inc.	GS	[0,50) kW	GS-TOU	[0,50) kW	delaware.coop/about/rules-regulations-rates
FL	Progress Energy Florida	GS-1	[0,∞) kW	GST-1	[0,∞) kW	duke-energy.com/rates/florida-rates-index.asp
GA	Georgia Power	PLM-9	[30,500) kW	TOU-GSD-8	[30,500) kW	georgiapower.com/pricing/business/home.cshtml?bus=prices
HI	Hawaii Electric Light Company, Inc.	P	[200,∞) kW	TOU-P	[200,∞) kW	hawaiielectriclight.com/helco/residential-services/electric-rates/hawaii-electric-light-rates
IA	Interstate Power and Light Company	Large GS	[20000,∞) kWh	Large GS-TOD	[20000,∞) kWh	alliantenergy.com/aboutalliantenergy/companyinformation/tariffs/030242
IL	MidAmerican Energy Company	Rate 22	[0,∞) kW	Rate 22 - Rider 15	[0,∞) kW	midamericanenergy.com/rates1.aspx
IN	Indiana Michigan Power Company	LGS	[60,1000) kW	LGS-TOD	[0,1000) kW	indianamichiganpower.com/account/bills/rates/iandmratestariffsin.aspx
KS	Kansas Gas & Electric Company	MGS	[200,∞) kW	OPS	[500,∞) kW	westarenergy.com/wcm.nsf/tariff?openview
KY	Kentucky Power Company	LGS	(100,1000] kW	LGS-TOD	(100,1000] kW	kentuckypower.com/account/bills/rates/kentuckypowerratestariffsky.aspx
LA	Southwestern Electric	LP	[0,∞) kW	LPTOD	[800,∞) kW	swepco.com/account/bills/rates/swepcorate

	Power Company					stariffsla.aspx
MA	Western Massachusetts Electric Company	G-0	[0,350) kW	T-0	[0,350) kW	wmeco.com/residential/understandbill/ratesrules/ratestariffs.aspx
ME	Central Maine Power Co	MGS-S	(20,400] kW	MGS-S-TOU	(20,400] kW	cmpco.com/yourbusiness/pricing/pricingschedules/default.html
MI	Indiana Michigan Power Company	MGS	[10,1500] kW	LGS	[100,1500] kW	indianamichiganpower.com/account/bills/rates/iandmratestariffsmi.aspx
MN	Otter Tail Power Company	Rate 10.04	[80,∞) kW	Rate 10.05	[80,∞) kW	otpco.com/rates-and-pricing/minnesota/rates,-rules,-and-regulations/
MO	Union Electric Company	No.3(M)	[100,∞) kW	No.3(M)-TOD	[100,∞) kW	ameren.com/sites/aue/rates/pages/ratesbundledelecfullsrvmo.aspx
MS	Mississippi Power	LGS-LV-6	[500,∞) kW	LGS-TOU-11	[0,∞) kW	mississippipower.com/my-business/our-pricing/rate-and-rider-details
NC	Progress Energy Carolinas	MGS-28	[30,1000) kW	SGS-TOU-28	[30,1000) kW	duke-energy.com/rates/progress-north-carolina.asp
ND	Otter Tail Power Company	Rate 10.03	[80,∞) kW	Rate 10.05	[80,∞) kW	otpco.com/rates-and-pricing/north-dakota/rates,-rules,-and-regulations/
NE	Lincoln Electric System	Large L&P 15	(400,∞) kW	Large L&P 27	(400,∞) kW	les.com/business/rates/rate-schedules
NH	Public Service Company of New Hampshire	G	[0,100] kW	G-OTOD	[0,100] kW	psnh.com/ratestariffs/business/small-business-rates.aspx
NJ	Jersey Central Power & Light Company	GS	[0,∞) kW	GST	(750,∞) kW	firstenergycorp.com/content/customer/customer_choice/new_jersey/new_jersey_tariffs.html
NM	Otero County Electric Cooperative, Inc.	Large Power Reg	[50,∞) kW	Large Power Opt	[50,∞) kW	nmprc.state.nm.us/consumer-relations/company-directory/cooperatives/otero-county-electric-coop/
NV	NV Energy (South)	LGS-1	[0,300) kW	OLGS-1-TOU	[0,300) kW	nvenergy.com/company/rates/index.cfm
NY	Orange & Rockland Utils Inc.	SC02	[0,∞) kW	SC20	[5,∞) kW	oru.com/aboutoru/tariffsandregulatorydocuments/newyork/scheduleforelectricservice.html
OH	Ohio Power Company	GS-3	[10,8000) kW	GS-3 (Opt TOD)	[10,8000) kW	aepohio.com/account/bills/rates/aepohioratestariffsoh.aspx
OK	Public Service Company of Oklahoma	GS	[8000,∞) kWh	GSTOD	[8000,∞) kWh	psoklahoma.com/account/bills/rates/ratesandtariffs.aspx
PA	Adams Electric Cooperative, Inc.	A-1	[0,50] kW	T-1	[0,50] kW	adamsec.com/content/rates
SC	Progress Energy Carolinas	MGS-29	[30,1000) kW	SGS-TOU-29	[0,1000) kW	duke-energy.com/rates/progress-south-carolina.asp
SD	Otter Tail Power Company	Rate 10.04	[80,∞) kW	Rate 10.05	[80,∞) kW	otpco.com/rates-and-pricing/south-dakota/rates,-rules,-and-regulations/
TN	Kingsport Power Company	MGS	[10,100) kW	MGS-TOD	[10,300) kW	appalachianpower.com/account/bills/rates/apcoratestariffstn.aspx
TX	Entergy Texas, Inc.	GS	[5,2500] kW	GS-TOD	[5,2500] kW	entergy-texas.com/your_business/tariffs.aspx
VA	Virginia Electric & Power Co	GS-2	[30,500) kW	GS-2T	[30,500) kW	dom.com/dominion-virginia-power/customer-service/rates-and-tariffs/business-rates-and-tariffs.jsp
VT	Burlington Electric Department	LG	(3000,∞) kWh	LT	(3000,∞) kWh	burlingtonelectric.com/my-business/my-bill/business-rates-and-fees
WA	Snohomish County PUD No 1	Schedule 20	[100,∞) kW	Schedule 24	(500,∞) kW	snopud.com/aboutus/rates.ashx?p=1166
WI	Wisconsin Power and Light Company	GS-1	[0,75] kW	GS-3	[0,75] kW	alliantenergy.com/aboutalliantenergy/companyinformation/tariffs/030306
WV	Appalachian Power Company	GS	[10,1000) kW	GS (Opt TOD)	[10,1000) kW	appalachianpower.com/account/bills/rates/apcoratestariffswv.aspx
WY	Rocky Mountain Power	Schedule 28	(20,∞) kW	Schedule 46	[1000,∞) kW	rockymountainpower.net/about/rar/wri.html

4.4.3. Detailed survey results

There are many variations of the flat rate structures. Detailed pricing information of the flat rates identified in Table 4.1 is summarized in Table 4.2. These results can be explained as follows:

(i) The state abbreviation in the first column is actually an index representing the utility surveyed in that state.

(ii) For the flat rates, some utilities divide the entire year into different seasons. The summer months usually contains June through September. More than a half of the utilities (23) do not make a partition and simply set the prices for the whole year.

(iii) All the flat rates of the surveyed utilities contain the energy charge and the customer charge. Many also contain the demand charge. A customer's monthly bill is rendered by adding up the three components.

(iv) The energy and demand prices in the summer months are usually higher than the other months. Many utilities bill the energy charge and the demand charge on a multi-tier basis. For example, in the flat rate in AL, the first 15,000 kWh of electric energy consumed in a summer month is charged at $0.10791/kWh; the energy consumption higher than 15,000 kWh is charged at $0.06310/kWh. Similarly, if the peak electric demand of a customer in the monthly billing period is less than 50 kW, the demand charge is zero; if the peak demand is greater than 50 kW, the part over 50 kW is charged at $13.97/kW for the month.

(v) The unit kWh/kW used in the energy charge of some utilities has a special meaning. For example, in the summer months of the MO case, it means $0.0997/kWh is charged for all kWh up to a maximum level equal to 150 hours (h) multiplied by the peak demand (kW) in the current month; $0.0752/kWh is charged for the next block of kWh up to a maximum level equal to 200 hours multiplied by the peak demand; $0.0508/kWh for all additional kWh used.

(vi) The values in the last column represent the measurement intervals used by the demand meter to find the monthly peak demand and determine the demand charge. For the tariffs with no demand charge, the cells are empty.

(vii) The rates contained in this table are all bundled rates. Bundled rates are the combination of all the services necessary from generation through transmission to distribution of electric power to retail end-use customers. The sales and other taxes as well as various adjustments are not included.

Table 4.2. Details of the flat tariffs (Note: Empty cells are interpreted as not applicable or the values are zero)

State	Months	Energy Charge ($/kWh)	Demand Charge ($/kW)	Customer Charge ($)	Demand Metering Interval (Minutes)
AL	Jun-Sep	First 15000kWh: 0.10791; Over: 0.06310	First 50kW: 0; Over: 13.97	46.46	30
	Dec-Mar	First 15000kWh: 0.10778; Over: 0.06310	First 50kW: 0; Over: 13.10		
	Apr-May; Oct-Nov	First 15000kWh: 0.10710; Over: 0.06310	First 50kW: 0; Over: 13.10		
AR	Jun-Sep	0.0244	10.56	89.92	15
	Oct-May	0.01736	8.95		
AZ	May-Jun; Sep-Oct	First 350kWh/kW: 0.0989; Over: 0.0988		24.87	
	Nov-Apr	First 350kWh/kW: 0.0785; Over: 0.0778			
	Jul-Aug	First 350kWh/kW: 0.1211; Over: 0.1203			
CA	Jun-Sep	0.07219	5.36	6.5	15
	Oct-May	0.04929	5.36		
CO	Whole year	0.0801		18.972	
CT	Whole year	0.1314	11.96	38.5	30
DE	Jun-Sep	0.098438		8.7	
	Oct-May	First 700kWh: 0.093488; Over: 0.078088			
FL	Whole year	0.07286		11.59	
GA	Whole year	First 200kWh/kW: 0.085880; Next 200kWh/kW: 0.011052; Next 200kWh/kW: 0.008317; Over: 0.007235		19	
HI	Whole year	0.218184	19.5	400	15
IA	Jun 16-Sep 15	0.01971	First 200kW: 15.61; Next 800kW: 15.48	0	15
	Sep 16-Jun 15	0.01073	First 200kW: 8.21; Next 800kW: 7.49		
IL	Jun-Sep	0.0845		8.85	
	Oct-May	First 6000kWh: 0.0677; Over: 0.0571			
IN	Whole year	First 300kWh/kW: 0.06217; Over: 0.04216	4.695	35.3	15
KS	Jun-Sep	0.019261	12.506021	100	15
	Oct-May	0.014627	12.506021		
KY	Whole year	0.07795	4.02	85	15

LA	Whole year	First 500MWh: 0.0196; Next 4500MWh: 0.0126; Over: 0.0118	8.56	0	15
MA	Whole year	0.10099	15.27	30	30
ME	Apr-Nov	0.004398	10.23	37.22	15
	Dec-Mar	0.004398	11.33		
MI	Whole year	0.06615	5.69	17.45	15
MN	Jun-Sep	0.04618	7.22	188.5	15
	Oct-May	0.05	6.07		
MO	Jun-Sep	First 150kWh/kW: 0.0997; Next 200kWh/kW: 0.0752; Over: 0.0508	4.62	88.82	15
	Oct-May	First 150kWh/kW: 0.0628; Next 200kWh/kW: 0.0467; Over: 0.0368	1.71		
MS	Whole year	First 200kWh/kW: 0.02774; Next 200kWh/kW: 0.02425; Over:0.00921	7.85	725	15
NC	Whole year	0.06763	4.81	58.69	15
ND	Jun-Sep	0.05115	7.29	175	15
	Oct-May	0.05165	5.61		
NE	Jun-Sep	0.0285	19.95	275	30
	Oct-May	0.0237	19.95		
NH	Whole year	First 500kWh: 0.18525; Next 1000kWh: 0.12358; Over: 0.10977	13.08	29.04	30
NJ	Jun-Sep	First 1000kWh: 0.061999; Over:0.004958	6.94	11.65	15
	Oct-May	First 1000kWh: 0.057366; Over:0.004958	6.47		
NM	Whole year	0.07188	10.5	75	15
NV	Whole year	0.07165	8.57	21.1	15
NY	Jun-Sep	0.18015		33.15	
	Oct-May	0.16052			
OH	Whole year	0.0012605	13.06	22.79	30
OK	Jun-Oct	First 150kWh/kW: 0.0785; Next 150kWh/kW: 0.0716; Over: 0.0493		58.63	
	Nov-May	First 150kWh/kW: 0.0640; Next 150kWh/kW: 0.0579; Over: 0.0477			
PA	Whole year	0.0939		28.5	
SC	Whole year	0.07353	4.91	18.1	15
SD	Jun-Sep	0.01696	7.29	198.5	15
	Oct-May	0.02046	4.63		
TN	Whole year	First 200kWh/kW: 0.07374; Over: 0.03689		21.5	
TX	Whole year	0.01965	6.58	34.95	30
VA	Jun-Sep	First 150kWh/kW: 0.04634; Next 150kWh/kW: 0.02605; Next 150kWh/kW: 0.01136; Over: 0.00289	7.477	21.17	30
	Oct-May	First 150kWh/kW: 0.04634; Next 150kWh/kW: 0.02605; Next 150kWh/kW: 0.01136; Over: 0.00289	6.039		
VT	Whole year	0.083003	20.03	41.04	15
WA	Apr-Sep	First 30MWh: 0.0772; Over: 0.0592	First 100kW: 0; Over: 4.2	9.9	60
	Oct-Mar	First 30MWh: 0.0860;	First 100kW: 0;		

		Over: 0.0689	Over: 4.2		
WI	Jun-Sep	0.1219		15.339	
	Oct-May	0.11092			
WV	Whole year	First 350kWh/kW: 0.06553; Over: 0.03729	4.24	21	15
WY	Whole year	0.0125	14.29	37	15

Detailed pricing information of the TOU rates is summarized in Table 4.3. These results are further explained as follows:

(i) The TOU rate structures are generally more complicated than the corresponding flat rates. The entire day is mostly divided into the on- and off-peak periods, and some also have a mid-peak period. The on-peak period mainly consists of the hours during daytime, and the off-peak period mainly consists of the hours during nighttime. For example, the on-peak period of the TOU tariff of the NY case is from 13 o'clock (i.e., 1pm) to 19 o'clock (i.e., 7pm) during the summer months June through September, and from 10 o'clock (10am) to 21 o'clock (9pm) during the winter months October through May. The off-peak periods are the remaining hours of the workday plus federal holidays, Saturdays, and Sundays.

(ii) The on-, mid-, and off-peak times are the Local Standard Time or Local Daylight Time, whichever is then in effect in the service area.

(iii) The energy consumed at different periods will be charged at different prices. The on-peak prices are generally higher than the mid- and off-peak prices. This is also true for the demand charge.

(iv) The customer will be billed the on-peak demand charge if their maximum measured kW demand for the billing period occurs during the on-peak period. If the maximum measured kW demand occurs during the mid- or off-peak period, the mid- or off-peak demand charge, respectively, will apply.

(v) The customer charges of the TOU rates are all higher than or equal to those of the corresponding flat rates. The differences compensate the costs of technical upgrades for metering as well as usage and billing information communication.

(vi) The distributions of demand metering intervals for the flat and TOU tariffs are shown in Figure 4.5. The demand-metering interval of a TOU tariff may not always be the same as the interval of the flat rate from the same utility. For example, the intervals of the flat rate and the TOU rate of the MN case are 15 minutes and 60 minutes, respectively. For both the flat and TOU rates, the most popular demand-metering interval is 15 minutes, and the least popular one is 60 minutes.

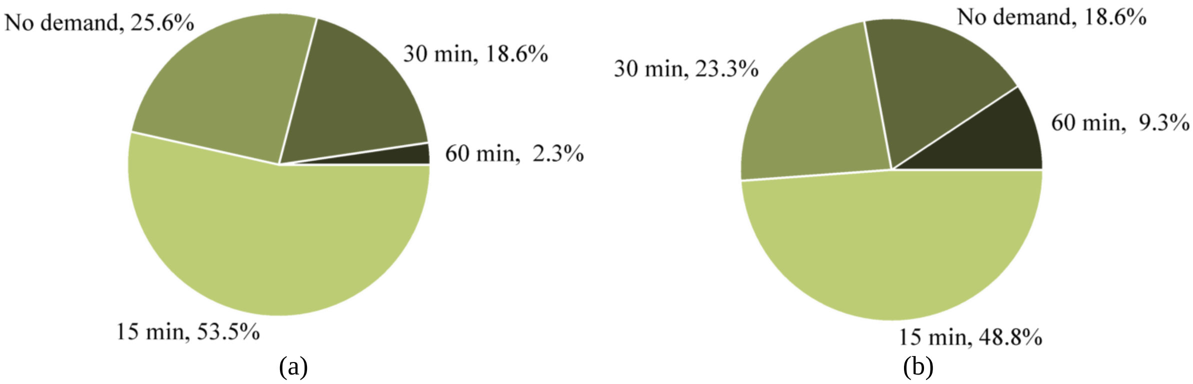

Figure 4.5. Distributions of demand metering intervals among surveyed utilities (total 43) for (a) the flat rates, and (b) the TOU rates

Table 4.3. Details of the TOU tariffs (Note: Empty cells are interpreted as not applicable or the values are zero)

State	Months	On-Peak	Mid-Peak	Off-Peak	Energy Charge ($/kWh)			Demand Charge ($/kW)			Customer Charge ($)	Demand Metering (Minutes)
					On-Peak	Mid-Peak	Off-Peak	On-Peak	Mid-Peak	Off-Peak		
AL	May-Oct	11-21		21-11	0.09715		0.07457	14.1		3.73	46.46	30
	Nov-Apr	2-12		12-2	0.08738		0.07711	13.22		3.73		
AR	Jun-Sep	13-20		20-13	0.01779		0.0127	14.49		4.27	89.92	15
	Oct-May	7-18		18-7	0.00978		0.00838	12.21		3.70		
AZ	May-Jun; Sep-Oct	14-19	11-14;19-23	23-11	0.1649	0.099	0.0518	3.33	3.33	1	24.87	30
	Nov-Apr	5-9	17-21	9-17;21-5	0.1098	0.0982	0.0513	3.33	3.33	1		
	Jul-Aug	14-19	11-14;19-23	23-11	0.2064	0.1101	0.0524	3.33	3.33	1		
CA	Jun-Sep	13-17	10-13;17-20	20-10	0.17089	0.1096	0.03826	5.36	5.36	5.36	15	15
	Oct-May	13-17	10-13;17-20	20-10	0.06558	0.06558	0.03826	5.36	5.36	5.36		
CO	Apr-Sep	16-22		22-16	0.1176		0.0472				20.307	
	Oct-Mar	11-18		18-11	0.1176		0.0472					
CT	Whole year	12-20		20-12	0.19759		0.12123	9.06		9.06	38.5	30
DE	May-Sep	15-18		18-15	0.374538		0.063648				10.7	
	Oct-Apr	6-8;17-21		8-17;21-6	0.175858		0.063648					
FL	Apr-Oct	12-21		21-12	0.17218		0.02714				19.01	
	Nov-Mar	6-10;18-22		22-6;10-18	0.17218		0.02714					
GA	Jun-Sep	14-19	12-14;19-21	21-12;14-19	0.122372	0.060059	0.022592	15.03	5.02	5.02	209	30
	Oct-May			Whole day			0.022592			5.02		
HI	Whole year	17-21	7-17	21-7	0.288184	0.268184	0.168184	24.5	19.5		410	15
IA	Jun 16- Sep 15	7-20		20-7	0.02483		0.01586	First 200kW: 15.61; Next 800kW: 15.48		First 200kW: 15.61; Next 800kW: 15.48	0	15
	Sep 16- Jun 15	7-20		20-7	0.01586		0.00687	First 200kW: 8.21; Next 800kW: 7.49		First 200kW: 8.21; Next 800kW: 7.49		
IL	Jun-Sep	8-20		20-8	0.0924		0.0779				12.85	
	Oct-May	8-20		20-8	First 6000kWh: 0.0756; Over: 0.0650		First 6000kWh: 0.0611; Over: 0.0505					
IN	Whole year	7-21		21-7	0.0871		0.02903	3.727		3.727	35.3	15
KS	Jun-Sep	14-20		20-14	0.01815		0.01815	10.65		2.1	100	15
	Oct-May			Whole day			0.01815			2.1		
KY	Whole year	7-21		21-7	0.09778		0.04116	7.64		7.64	85	15
LA	Jul-Sep	13-19		19-13	First 500MWh: 0.0346; Next 4500MWh: 0.0142; Over: 0.0130		First 500MWh: 0.0179; Next 4500MWh: 0.0114; Over: 0.0110	18.36		5.17	0	15
	Oct-Jun			Whole day			First 500MWh: 0.0179; Next 4500MWh: 0.0114; Over: 0.0110			5.17		
MA	Whole year	12-20		20-12	0.10205		0.09997	17.24		17.24	30	30
ME	Apr-Nov	7-12;16-20	12-16	20-7	0.00579	0.005215	0.003647	9.31	1.98		40.11	15
	Dec-Mar	7-12;16-20	12-16	20-7	0.00579	0.005215	0.003647	10.81	1.98			
MI	Whole year	7-21		21-7	0.08699		0.01796	11.1		11.1	44	15
MN	Jun-Sep	13-19	9-13;19-22	22-9	0.07319	0.05397	0.02437	5.54	1.68		208.5	60
	Oct-May	7-12;17-21	6-7;12-17;21-22	22-6	0.06507	0.04917	0.03665	5.13	0.94			
MO	Jun-Sep	10-22		22-10	First 150kWh/kW: 0.1114; Next 200kWh/kW: 0.0869; Over: 0.0625		First 150kWh/kW: 0.0931; Next 200kWh/kW: 0.0686; Over: 0.0442	4.62		2.31	108.32	15
	Oct-May	10-22		22-10	First 150kWh/kW: 0.0663;		First 150kWh/kW: 0.0608;	1.71		0.855		

					Next 200kWh/kW: 0.0502; Over: 0.0403		Next 200kWh/kW: 0.0447; Over: 0.0348					
MS	Jun-Sep	12-20	10-12;20-22	22-10	0.06488	0.02769	0.0091	13.9	2.7	2.7	1060	15
	Nov-Mar	6-10;18-22		10-18;22-6	0.03699		0.0091	8.25		2.1		
	Apr,May,Oct	12-20		20-12	0.03699		0.0091	8.25		2.1		
NC	Jun-Sep	10-22		22-10	0.05812		0.04636	9.9		1.51	58.69	15
	Oct-Mar	6-13;16-21		13-16;21-6	0.05812		0.04636	7.34		1.51		
	Apr-May	10-22		22-10	0.05812		0.04636	7.34		1.51		
ND	Jun-Sep	13-19	9-13;19-22	22-9	0.0815	0.06247	0.03721	5.75	1.59		195	60
	Oct-May	7-12;17-21	6-7;12-17;21-22	22-6	0.07314	0.05949	0.04199	4.42	1.22			
NE	Jun-Sep	14-20		20-14	0.0285		0.0285	19.95		9.1	305	30
	Oct-May	14-20		20-14	0.0237		0.0237	19.95		9.1		
NH	Whole year	7-20		20-7	0.14838		0.10805	14.88			53.79	30
NJ	Jun-Sep	8-20		8-20	0.004815		0.004815	7.22		7.22	35.25	15
	Oct-May	8-20		8-20	0.004815		0.004815	6.75		6.75		
NM	Whole year	12-22		22-12	0.07825		0.06804	11		5.25	85	15
NV	Jun-Sep	13-19		19-13	0.21007		0.06401	12.47		4.22	24.62	15
	Oct-May			Whole day			0.05314			4.38		
NY	Jun-Sep	13-19		19-13	0.18815		0.10551	19.41		0	51.32	15
	Oct-May	10-21		21-10	0.13065		0.10551	8.38		0		
OH	Whole year	7-21		21-7	0.0012605		0.0012605	13.06		6.97	22.79	30
OK	Jun-Oct	14-19		19-14	0.1189		0.0477				58.63	
	Nov-May			Whole day			First 150kWh/kW: 0.0640; Next 150kWh/kW: 0.0579; Over: 0.0477					
PA	Jun-Aug	7-19		19-7	0.181		0.06				28.5	
	Sep-May	7-19		19-7	0.121		0.06					
SC	Jun-Sep	10-22		22-10	0.06458		0.05123	10.49		1	19.75	15
	Oct-Mar	6-13;16-21		13-16;21-6	0.0628		0.05123	7.77		1		
	Apr-May	10-22		22-10	0.0628		0.05123	7.77		1		
SD	Jun-Sep	13-19	9-13;19-22	22-9	0.04649	0.02761	0.00292	5.59	1.7		218.5	60
	Oct-May	7-12;17-21	6-7;12-17;21-22	22-6	0.03851	0.02289	0.01059	3.91	0.72			
TN	Whole year	6-21		21-6	0.08847		0.02755				23.45	
TX	May-Oct	13-21		21-13	0.04882		0.01682	9.8		9.8	34.95	30
	Nov-Apr	6-10;18-22		10-18;22-6	0.01943		0.01682	5.07		5.07		
VA	Jun-Sep	10-22		22-10	0.03172		0.00541	10.484		2.647	26.17	30
	Oct-May	7-22		22-7	0.03172		0.00541	9.075		2.647		
VT	Jun-Sep	12-18		18-12	0.107754		0.076418	25.47		3.53	43.77	15
	Dec-Mar	6-22		22-6	0.115459		0.076418	25.47		3.53		
	Apr-May; Oct-Nov			Whole day			0.076418			3.53		
WA	Apr-Sep	7-11		11-7	First 30MWh: 0.0787; Over: 0.0607		First 30MWh: 0.0787; Over: 0.0607	First 100kW: 0; Over: 7.36		0	9.9	60
	Oct-Mar	7-11		11-7	First 30MWh: 0.0873; Over: 0.0708		First 30MWh: 0.0873; Over: 0.0708	First 100kW: 0; Over: 7.36		0		
WI	Jun-Sep	8-20		20-8	0.20739		0.05505				15.339	
	Oct-May	8-20		20-8	0.19598		0.05505					
WV	Whole year	7-21		21-7	First 350kWh/kW: 0.06553; Over: 0.03729		First 350kWh/kW: 0.06553; Over: 0.03729	4.24		2.45	21	15
WY	Whole year	7-23		23-7	0.00826		0.00826	16.78		2.26	625	15

4.5. Case Studies

In this section, we evaluate the benefits of switching from flat rates to the corresponding TOU rates using the surveyed results as case studies. The electricity cost models of industrial systems based on both the flat and TOU rates have been established in Chapter 3. The methods developed in Chapter 3 will be used in this section to calculate the total electricity cost c_T during production for both types of rates in the case studies.

Because there are so many differences among these TOU tariffs, it is important to make fair comparisons. We consider three industrial systems with different parameters shown in Table 4.4. The base electricity demand supports lighting and HVAC that maintain the working environment in the facility. The demand of a single machine is divided into three levels based on its working states in the format {*operational*, *idle*, *down*}. There are multiple machines connected in series in the system. The total peak demand is the sum of the base demand and the peak demand of all the machines. Other than the parameters shown in Table 4.4, each machine has a cycle time (time needed to process one part) of 5 minutes. Machines are highly reliable with 99% up time. There is a small buffer area between any two machines connected in sequence. The buffer capacity (maximum number of parts can be held inside the buffer) is 3. The total peak demands of the small, medium, and large systems are 25 kW, 450 kW, and 1200 kW, respectively, so at least one system will fall into the demand range of any utility surveyed in Table 4.1.

Table 4.4. Industrial systems used in the case studies

System Size	Base Demand (kW)	Demand of Single Machine (kW)	Number of Machines	Total Peak Demand (kW)
Small (S)	5	{5, 1, 0}	4	25
Medium (M)	50	{50, 10, 0}	8	450
Large (L)	150	{70, 15, 0}	15	1200

We consider three different scenarios listed in Table 4.5. For each scenario, we consider three different work schedules during a workday: one work shift (8 hours), two work shifts (16 hours), and three work shifts (24 hours). Scenario 0 is the baseline against which the other two scenarios are compared. Under this scenario, the industrial customer adopts the flat rates and the work shift starts at 8 o'clock. Scenario 1 differs from Scenario 0 in that the customer adopts the TOU rates instead of the flat rates. Scenario 3 differs from Scenario 0 in that the customer not only adopts the TOU rates, they also take the initiative in finding the optimal starting time of the work shift to take advantage of the lower prices during the off-peak period. By adopting the optimal starting time, the total electricity cost can be minimized without affecting the total production.

Table 4.5. Three different scenarios

Scenario	Rate Plan	Work Shift Starting Time
Scenario 0	Flat rates in Table 4.2	8 o'clock (8am)
Scenario 1	TOU rates in Table 4.3	8 o'clock (8am)
Scenario 2	TOU rates in Table 4.3	Optimal starting time

After applying the methods developed in Chapter 3, the calculated electricity costs of various scenarios are tabulated in Table 4.6. Only one system (as indicated in the system size column) is selected for the case study of each state's tariffs. Every value represents the total electricity cost of the industrial system in a single workday. We consider 21 workdays in a month. The costs are yearly weighted considering seasonal and monthly differences in the rates.

The results in Table 4.6 shows that increasing the number of work shifts during a workday will undoubtedly also increase the total electricity cost. This is evidenced by comparing the one-shift cost values with the corresponding two-shift and three-shift values. In many states' cases, the total electricity cost of the two-shift production is not doubled in comparison to that of the one-shift production. For example, in the AR case, the cost is \$274.47 for Scenario 0 during one-shift production, while the cost is \$344.36 for Scenario 0 during two-shift production. This is because although the total energy charge is doubled, the total demand charge does not change because the peak demand is kept the same for this case. This rule also applies when comparing three-shift costs with one-shift costs. Therefore, the electricity cost of unit production can be reduced by elongating the production time.

Table 4.6. Total electricity costs of various scenarios

State	System Size	One-Shift c_T ($)			Two-Shift c_T ($)			Three-Shift c_T ($)		
		Scenario 0	Scenario 1	Scenario 2	Scenario 0	Scenario 1	Scenario 2	Scenario 0	Scenario 1	Scenario 2
AL	M	508.15	593.74	349.96	731.96	887.77	843.17	955.77	1170.42	1170.42
AR	M	274.47	318.51	121.24	344.36	357.18	277.09	414.26	392.42	392.42
AZ	M	328.92	357.56	205.49	656.65	711.59	524.43	982.71	933.69	933.69
CA	S	17.86	22.32	14.58	29.11	34.53	24.21	40.36	42.09	42.09
CO	S	16.73	14.64	10.29	32.56	30.92	19.62	48.39	40.25	40.25
CT	S	41.87	43.99	36.44	67.83	75.49	60.4	93.79	99.44	99.44
DE	S	17.52	16.29	13.09	34.29	41.73	28.9	51.06	57.54	57.54
FL	M	258.98	300.8	90.17	517.41	691.8	338.12	775.83	841.65	841.65
GA	M	305.51	342.41	196.07	395.27	477.85	281.74	428.46	557.99	557.99
HI	M	1204.62	1382.44	616.06	1978.5	2341.69	1890.3	2752.38	2982.56	2982.56
IA	M	251.7	271.57	239.7	297.72	319.84	291.95	343.74	356.16	356.16
IL	M	237.33	265.54	214.11	472.26	502.77	451.34	707.18	714.29	714.29
IN	M	321.32	389.3	183.33	526.62	621	440.78	676.16	749.71	749.71
KS	L	861.55	454.98	294.57	1014.46	626.6	466.19	1167.37	798.22	798.22
KY	M	365.4	512.16	311.34	641.88	783.67	607.95	918.36	954.76	954.76
LA	L	667.11	660.63	460.24	852.44	844.69	629.49	1003.36	977.73	977.73
MA	S	39.34	41.67	41.46	59.3	61.63	61.21	79.26	81.38	81.38
ME	S	15.11	14.54	2.63	15.97	15.47	15.14	16.84	16.24	16.24
MI	M	355.59	544.99	300.15	590.22	761.72	547.48	824.84	856.03	856.03
MN	M	318.05	324.14	125.4	490.88	515.39	395.18	663.71	642.97	642.97
MO	M	320	334.38	280.11	519.34	547.16	512.52	670.77	686.06	686.06
MS	L	738.64	869.84	265.97	974.23	1146.35	580.48	1115.49	1259.86	1259.86
NC	M	344.22	377.9	199.11	584.1	571.01	537.12	823.98	740.66	740.66
ND	M	321.2	347.33	152.57	503.81	568.63	445.44	686.42	726.29	726.29
NE	M	524.03	525.46	296.38	613.76	615.19	386.12	703.5	704.93	704.93
NH	S	40.88	49.38	23.91	62.57	74.72	67.75	84.26	97.06	97.06
NJ	L	422.92	435.94	435.94	469.81	481.46	481.46	516.69	526.99	526.99
NM	M	480.2	495.72	356.22	735.16	764.22	728	990.11	1005.55	1005.55
NV	S	25.35	24.32	17.48	39.61	39.14	28.69	53.88	50.36	50.36
NY	M	594.14	712.45	376.68	1186.69	1160.48	891.15	1779.25	1534.71	1534.71
OH	M	281.29	281.29	152.71	285.76	285.76	285.76	290.23	290.23	290.23
OK	M	248.78	230.66	204.35	474.39	460.41	394.64	650.45	631.36	631.36
PA	S	19.91	28.23	13.21	38.47	45.72	32.58	57.02	59.45	59.45
SC	M	365.33	405.2	203.76	626.13	616.7	581.25	886.94	803.54	803.54
SD	M	194.35	214.74	38.9	262.79	313.77	200.19	331.22	354.16	354.16
TN	S	15.59	18.6	6.56	24.27	31.57	22.54	31.56	40.02	40.02
TX	M	210.28	240.73	218.29	279.98	338.18	280.27	349.67	398.99	398.99
VA	M	295.28	307.49	76.32	376.51	396.67	311.13	407.15	423.63	423.63
VT	M	719.24	721.15	347.66	1013.65	1036.08	819.27	1308.05	1318.66	1318.66
WA	L	847.18	1025.64	646.45	1452.81	1647.34	1268.15	2058.44	2269.05	2269.05
WI	S	23.37	40.21	11.61	46.01	65.38	36.79	68.65	76.26	76.26
WV	M	322.95	322.95	285.15	555.37	555.37	555.37	695.99	695.99	695.99
WY	L	924.24	1052.29	235.06	1042.44	1130.4	1130.4	1160.63	1208.5	1208.5

Based on the results in Table 4.6, the electricity cost savings by switching from Scenario

0 to Scenario 1 or Scenario 2 are plotted in Figure 4.6. Careful observation of Figure 4.6 suggests that:

(i) Figure 4.6(a) illustrates the electricity cost savings by switching from Scenario 0 to Scenario 1 for the one-shift cases. The mean value of the 43 cases is -10.9%. In most cases, the cost savings are negative values, which indicate the costs will actually increase due to such a switch. The reason for this is that the 8-hour work shift starting from 8am falls completely into the on-peak period of many of the TOU tariffs. For example, in the WI case, the 8-hour work shift starting from 8am completely falls into the on-peak period (8am-8pm) defined in the TOU tariff. Therefore, the on-peak energy charges \$0.20739/kWh (June-September) and \$0.19598/kWh (October-May) apply, which are both more expensive than the flat rate counterparts, \$0.1219/kWh and \$0.11092/kWh. However, there are still some exceptions. For example, in the KS case, there are only two hours falling into the on-peak period (2pm-8pm) during the summer months (June-September) and the entire work shift falls into off-peak periods (whole day) during the other months. The demand charge during the off-peak periods (\$2.1/kW) is significantly cheaper than the flat rate counterpart (\$12.5/kW).

(ii) Figure 4.6(b) illustrates the electricity cost savings by switching from Scenario 0 to Scenario 2 for the one-shift cases. The mean value of the 43 cases is 37.1%. In most cases, the cost savings are positive values. The reason for this is that the 8-hour work shift is relatively short and can be re-scheduled so that it can completely fall into the off-peak period of many of the TOU tariffs. For example, in the ME case, the off-peak period last for 11 hours (8pm-7am next day). There is no demand charge during the off-peak period in the TOU tariff, while the demand charge is more than \$10/kW in the flat rates.

However, there are still some exceptions. For example, in the MA case, although the off-peak period is relatively long (8pm-12noon next day) in the TOU tariffs, the demand charge $17.24/kW is more expensive than the counterpart $15.27/kW in the flat rate, and there is no significant difference between the energy charges ($0.09997/kWh vs. $0.10099/kWh).

(iii) Similarly, Figure 4.6(c) and Figure 4.6(d) illustrate the electricity cost savings by switching from Scenario 0 to Scenario 1 and Scenario 2, respectively, for the two-shift cases. The two-shift cases show similar patterns to the one-shift cases, except that the magnitudes of most of the positive and negative values are getting smaller. The magnitude decrease is due to the increased working hours (from 8 hours to 16 hours). To explain this more clearly, we extract the on- and non-peak durations of TOU tariffs and tabulate such information in Table 4.7. The durations are also yearly weighted. Table 4.7 shows the mean duration of the non-peak period is about 15 hours, and many of them are separated into different segments during a day. As the non-peak period is shorter than the 16-hour production schedule, a significant portion of the working hours will fall into the on-peak periods of many of the TOU tariffs, the capability of the low prices during off-peak periods cannot be fully utilized.

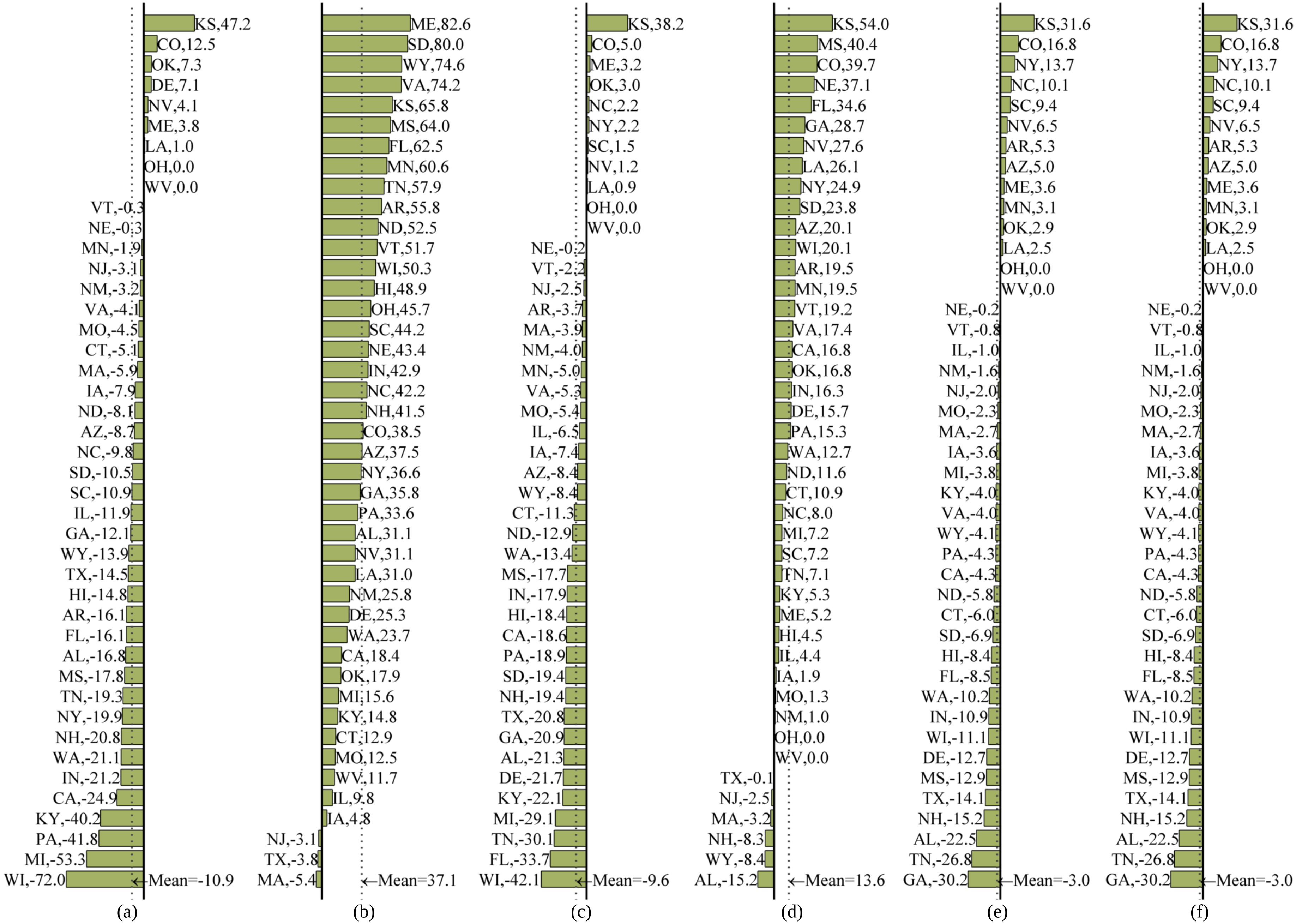

Figure 4.6. Scenario switching savings (%) of the following cases: (a) One-shift, Scenario 0→1; (b) One-shift, Scenario 0→2; (c) Two-shift, Scenario 0→1; (d) Two-shift, Scenario 0→2; (e) Three-shift, Scenario 0→1; (f) Three-shift, Scenario 0→2

(iv) Figure 4.6(e) and Figure 4.6(f) illustrate the electricity cost savings by switching from Scenario 0 to Scenario 1 and Scenario 2, respectively, for the three-shift cases. The magnitudes of most of the positive and negative values are getting even smaller. Figure 4.6(e) and Figure 4.6(f) are actually the same. This is because the three-shift production lasts for a whole day (24 hours) no matter when the production starts, and thus the benefits of the TOU tariffs have been totally lost. The mean value of the 43 cases is -3.0%, which means the overall electricity cost of the TOU tariffs during the day is not significantly different from the flat rates. This result is consistent with the design principle behind the TOU tariffs of many utility companies: they both should reflect the average cost of generating and delivering electricity.

Table 4.7. On- and non-peak durations of TOU tariffs

State	On-peak (hours)	Non-peak (hours)	Note
AL	10	14	
AR	9.67	14.33	
AZ	4.5	19.5	
CA	4	20	
CO	6.5	17.5	
CT	8	16	
DE	4.75	19.25	Separated
FL	8.58	15.42	Separated
GA	1.67	22.33	
HI	4	20	
IA	13	11	
IL	12	12	
IN	14	10	
KS	2	22	
KY	14	10	
LA	1.5	22.5	
MA	8	16	
ME	9	15	Separated
MI	14	10	
MN	8	16	Separated
MO	12	12	
MS	8	16	Separated
NC	12	12	Separated
ND	8	16	Separated
NE	6	18	
NH	13	11	
NJ	12	12	
NM	10	14	
NV	2	22	Separated

NY	9.33	14.67	
OH	14	10	
OK	2.08	21.92	
PA	12	12	
SC	12	12	Separated
SD	8	16	Separated
TN	15	9	
TX	8	16	Separated
VA	14	10	
VT	7.33	16.67	
WA	4	20	
WI	12	12	
WV	14	10	
WY	16	8	
Mean	9.02	14.98	

4.6. Key Findings and Implications

Among the case studies, the cost savings vary enormously, ranging from -72.0% to 82.6%, depending on specific programs and the switching strategies involved. The customers who adopt the Scenario 1 strategy will mostly suffer from the increased electricity cost. These customers simply switch from the flat rate to the TOU rate without taking further actions to adjust the production schedule. The customers who will benefit the most are those whose production runs for one or two shifts a day, and who adopt the Scenario 2 strategy. These customers not only switch from the flat rates to the TOU tariffs, but also take initiative to adjust their production schedule style to optimally match the TOU tariffs closely. This benefit can only be achieved on the basis that they understand the TOU tariffs well. The TOU tariffs may lose their advantages over flat rates for the industrial customers who require 24-hour operation. For such customers, they may get even or suffer from a minor loss. However, exceptions exist for all the above-mentioned scenario-switching cases shown in Figure 4.6. There is no guarantee that the customers switching from one scenario to another will definitely end up with a positive gain. It depends on the rate design of specific programs.

For utilities that are currently offering or considering TOU pricing to generate a meaningful level of demand response capability, attracting more customers to enroll is a key to the success of such programs. Previous research results in (Barbose et al., 2004; He et al., 2012) have shown that most customers are relatively sensitive to price changes and tend to make adjustments in their power usage in response to such changes. However, the TOU tariffs should be carefully designed to balance various factors in the rate structure. The case studies show that the TOU programs with a sufficiently large ratio of on- and off-peak prices, and relatively short on-peak periods are most likely to gain popularity among industrial customers. In addition, once such programs are created, marketing campaigns should focus on the customers who have the ability to shift major electricity use to off-peak lower-price period (e.g., those who run one- or two-shift production). For customers that lack such capabilities (e.g., those who run three-shift production), to achieve a sufficient penetration rate of demand response programs, the mandatory participation policy may have to be enforced. Alternatively, demand response programs other than TOU pricing can also be offered to attract these customers' interests. These alternative demand response programs may include incentive-based programs and other time-based programs.

4.7. Conclusions

In this work, we analyzed the FERC survey data with a specific focus on the TOU pricing programs to extract new information. We then detailed our own efforts in conducting a new survey on the TOU tariffs for industrial customers. The characteristics of the TOU tariffs were summarized. After that, we extended the work to compare the flat tariffs with the TOU tariffs, and used case studies to examine the attractiveness of the TOU pricing to industrial customers. Finally, the key findings of this research and implications for industrial customers, utilities, and regulatory agencies were discussed.

This research is not without limitations. It should be mentioned that the numerical results presented in most of the tables and figures are approximate. The utilities surveyed in this dissertation are identified based on the FERC survey. The FERC survey is voluntary in nature and the response rate of 59% suggests the results may have omitted some important information. In addition, during our own survey, we only consider the most important components in the TOU tariffs, i.e., the energy, demand, and customer charges. In all the utilities we surveyed, the tariff files always contains additional clauses and riders on fuel adjustments, environmental surcharges, various taxes, etc., although these components usually account for only a small proportion of the total customer bills. Also, such TOU tariffs change frequently. Many utility companies update their tariffs yearly and treat devising an appropriate rate structure as an ongoing process. Therefore, the surveyed results may change over time and they should be interpreted with caution considering such factors.

CHAPTER 5

TOU BASED ELECTRICITY DEMAND RESPONSE FOR SUSTAINABLE MANUFACTURING SYSTEMS

(Parts of this chapter were previously published as: *Wang, Y., Li, L., 2013. Time-of-use based electricity demand response for sustainable manufacturing systems. Energy, 63, 233-244.*)

5.1. Introduction

Based on the studies for manufacturing system modeling in Chapter 2 and electricity energy and cost modeling in Chapter 3, we now utilize the model established to control production paces of manufacturing systems for TOU based electricity demand response under the production target constraint. It differs the switching problem in Chapter 3 in that now the decision is more complicated. A detailed schedule with more comprehensive information will be identified. The schedule controls at what time, which machine(s) can be shut down temporarily to lower electricity energy consumption and power demand as long as an average cumulative production target is achieved for the planning horizon.

The remainder of this chapter is organized as follows. Section 5.2 introduces the new problem formulations: energy-efficient and cost-effective scheduling under production constraints. The solution technique for the new problems based on a binary PSO algorithm is presented in Section 5.3. Effects of various factors on the TOU based near-optimal scheduling solutions are examined in Section 5.4. Finally, conclusions of this chapter are drawn in Section 5.5.

The following notation is used in this chapter.

Boldface:

$\mathbf{S}$	position matrix of the binary PSO algorithm
$\mathbf{S}_{PB}$	personal best position matrix of the binary PSO algorithm
$\mathbf{S}_{GB}$	global best position matrix of the binary PSO algorithm
$\mathbf{V}$	velocity matrix of the binary PSO algorithm

Upper Case:

C_i	capacity of buffer b_i (the largest number of parts the buffer can hold)
CP_0	target cumulative production of the system during the planning horizon
CP_T	average cumulative production of the system during the planning horizon
H	number of hours in the finite planning horizon
N	number of machines in the manufacturing system
N_P	swarm size of the binary PSO algorithm
N_T	iteration number of the binary PSO algorithm
$PR_{SYS}(t)$	production rate of the system during time slot t
T	number of total time slots during the planning horizon
$WIP_{SYS}(t)$	work-in-process of the system at the end of time slot t

Lower Case:

$c_D(t)$	TOU demand rate ($/kW) during time slot t
c_{DT}	cost of the billable power demand of the system during the planning horizon
$c_E(t)$	TOU energy rate ($/kWh) during time slot t

c_{ET} — cost of the electricity energy consumption of the system during the planning horizon

c_{Fixed} — fixed charge during the planning horizon

c_T — total electricity cost of the system during the planning horizon

$d_{i,2}$, $d_{i,1}$, $d_{i,0}$ — electric power (in kW) drawn by machine m_i during time slot t when it is up & processing, up & idle, and down, respectively

$d_{SYS}(t)$ — power demand of the system during time slot t

d_T — billable power demand of the system (the highest average kW measured in any on-peak 15-minute interval during the planning horizon)

$e_{SYS}(t)$ — electricity energy consumption of the system during time slot t

e_T — total electricity energy consumption of the system during the planning horizon

i, j, t — general indexes

t_C — cycle time (the time needed by a machine to process a product)

m_i — index of the ith machine in the manufacturing system, $i = 1, ..., N$

p_i' — reliability of machine m_i

$p_i(t)$ — probability of machine m_i being up during time slot t (considering both machine reliability and control signal)

$s_i(t)$ — scheduled control signal ("on" or "off") for machine m_i during time slot t

Greek:

θ_0, θ_1, θ_2 — parameters of the binary PSO algorithm

Functions:

$rand(\cdot, \cdot)$ uniformly distributed random number generator

5.2. Demand Response Problem Formulations

5.2.1. Assumptions

In this chapter, more assumptions as follows are adopted.

(x) Due to internal failure, machine m_i (i = 1, ..., N) is up during time slot t with probability p_i' and down with probability $1 - p_i'$.

(xi) Let $s_i(t)$ be the status of the scheduled control signal for machine m_i during time slot t. It is defined as

$$s_i(t) = \begin{cases} 1, & \text{if the control signal is set to "on"} \\ 0, & \text{if the control signal is set to "off"} \end{cases} \tag{5.1}$$

(xii) Therefore, considering the machine reliability and the control signal together, machine m_i is up during time slot t with probability $p_i(t) = s_i(t)p_i'$ and down with probability $1 - p_i(t) = 1 - s_i(t)p_i'$.

Although this chapter deals with time-dependent up probability $p_i(t)$ instead of only a fixed p_i used in Chapters 2 and 3, the procedure therein can still be followed to derive the system dynamics, performance measures, electricity energy consumption, and power demand, and total electricity cost of the manufacturing system. The only difference is every p_i is replaced by the corresponding $p_i(t)$.

5.2.2. Problem formulations

For the manufacturing system with N machines and $N - 1$ buffers, a production schedule can be created to control at what time, which machine(s) can be shut down temporarily to lower electricity consumption and power demand as long as an average cumulative production target, i.e., CP_0 products, is achieved for the planning horizon. We choose the control signal $s_i(t)$ of each machine m_i ($i = 1, \ldots, N$) to be the decision variables, the following two production scheduling problems with different objectives can be formulated.

Formulation 1: Minimizing the total electricity consumption while maintaining an amount of average cumulative production that is not lower than the required level, i.e.,

$$\min_{s_i(t)} e_T, \text{ subject to: } CP_T \geq CP_0 \tag{5.2}$$

Formulation 2: Minimizing the total electricity cost while maintaining an amount of average cumulative production that is not lower than the required level, i.e.,

$$\min_{s_i(t)} c_T, \text{ subject to: } CP_T \geq CP_0 \tag{5.3}$$

Solving these two problems will provide optimal schedules of control signals for setting each machine in the "on" or "off" status to achieve the corresponding objectives.

5.3. Meta-Heuristic Techniques for Near-Optimal Solutions

The formulated scheduling problems present a huge challenge with regard to finding the optimal solutions. The calculations of electricity consumption e_T and total electricity cost c_T are pretty straightforward as shown in Chapter 3. However, the calculation of the average cumulative production CP_T in Chapter 2 is highly non-linear because it relies on iterative operations to untangle the complex interactions among all the machines and buffers. Besides, the decision variable $s_i(t)$ is binary and not continuous. The formulations are both zero-one nonlinear programming (ZONLP) problems due to these factors.

ZONLP is a special case of mixed integer nonlinear programming (MINLP). Due to the curse of dimensionality, there are still no exact methods that can effectively solve the general MINLP problems. Recently, meta-heuristic methods such as genetic algorithms, particle swarm optimization (PSO), and tabu search have gained popularity in both academia and industrial applications. These methods impose no restrictions such as convexity, continuity, and differentiability on the optimization problems. Among these methods, PSO has been widely studied (Faria et al., 2011; Martens et al., 2011; Poli et al., 2007; Roy et al., 2008; Soares et al., 2012; Thangaraj et al., 2011; Wang and Li, 2012b; Wang et al., 2009). For these reasons, we propose to search for near-optimal solutions to the formulated scheduling problems using a classic binary version of PSO (Kennedy and Eberhart, 1997).

The original binary PSO algorithm is slightly tailored for this research work. The implementation is briefly described in this section. The algorithm randomly generates a large group of members named particles. Each particle is characterized by a position matrix **S** and a velocity matrix **V.** The position matrix **S** represents a potential solution to Formulation 1 or 2 in the encoded form

$$\mathbf{S} \equiv \begin{bmatrix} s_1(1) & s_1(2) & \cdots & s_1(T) \\ s_2(1) & s_2(2) & \cdots & s_2(T) \\ \vdots & \vdots & \ddots & \vdots \\ s_N(1) & s_N(2) & \cdots & s_N(T) \end{bmatrix} \tag{5.4}$$

The velocity matrix **V** is of the same size as **S**, and it modifies the position matrix iteratively during the search process.

Before the search process begins, the position matrixes and the velocity matrixes of the entire swarm are initialized so that the elements in **S**'s and **V**'s are assigned random integer numbers drawn from the set $\{-1, 0, 1\}$. During each search iteration, the position and the velocity of each particle are updated by the following element-by-element operations

$$\mathbf{V}(i,j) = \theta_0 \cdot \mathbf{V}(i,j) + rand(0,\theta_1) \cdot [\mathbf{S}_{PB}(i,j) - \mathbf{S}(i,j)] + rand(0,\theta_2) \cdot [\mathbf{S}_{GB}(i,j) - \mathbf{S}(i,j)] \quad (5.5)$$

$$\mathbf{S}(i,j) = \begin{cases} 1, & \text{if } rand(0,1) < \dfrac{1}{1+e^{-[\mathbf{S}(i,j)+\mathbf{V}(i,j)]}} \\ 0, & \text{otherwise} \end{cases} \quad (5.6)$$

In (5.5) and (5.6), (i, j) means the element in the ith row and jth column in the matrix; $rand(0, \theta_1)$ and $rand(0, \theta_2)$ generate random numbers from the uniform distribution in the ranges $[0, \theta_1]$ and $[0, \theta_2]$, respectively; $\mathbf{S}_{PB}$ is the personal best solution that the particle has found; $\mathbf{S}_{GB}$ is the global best solution of the entire swarm. θ_0 is a scalar inertial weight; A small inertia weight facilitates finer search of the currently focused promising area, while a large inertia weight facilitates the search of new areas. Careful selection of parameters θ_0, θ_1, and θ_2 can ensure a good rate of convergence to the optimum while avoiding premature convergence to a local optimum.

The swarm size (i.e., the number of particles in the swarm) is denoted by N_P. The algorithm terminates after a certain number of PSO iteration N_T. The flowchart of the binary PSO algorithm is illustrated in Figure 5.1.

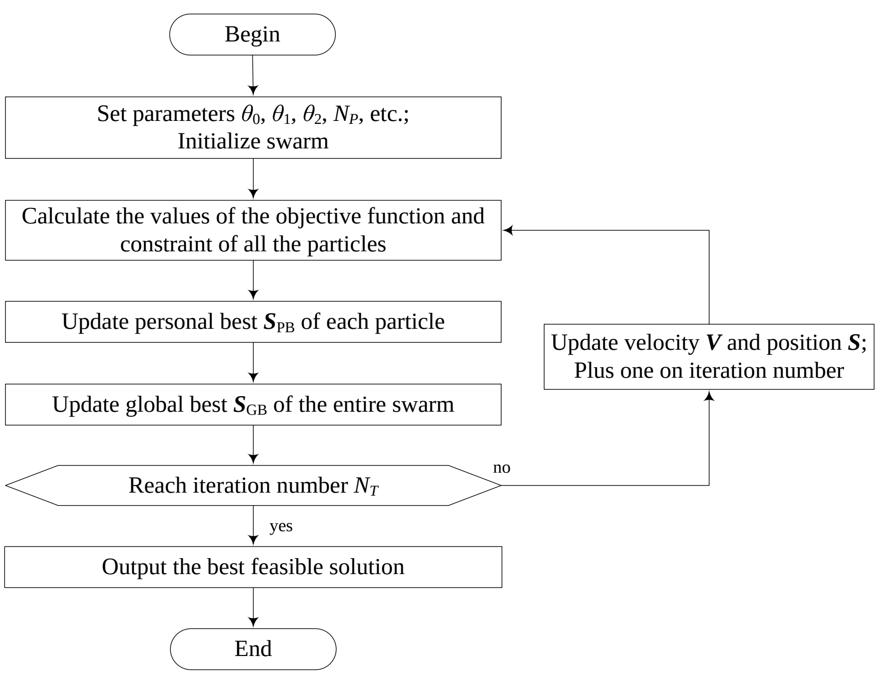

Figure 5.1. Binary PSO algorithm

More details on the near-optimal PSO solutions to the scheduling formulations will be discussed in the next section.

5.4. Effects of Various Factors on the TOU Based Scheduling Solutions

The problem formulations, the TOU pricing profile, and the manufacturing system parameters may all significantly influence the scheduling solutions, and hence the effectiveness and attractiveness of the TOU based demand response program to manufacturing enterprises. Therefore, the effects of these factors should be carefully investigated.

5.4.1. Insights gained from an illustrative case

As an example, we consider a manufacturing system with N = 3 machines and 2 buffers. Suppose the planning horizon is one working day, which consists of two 8-hour shifts (from 8 a.m. to 12 midnight), i.e., H = 16 hours. Suppose the cycle time t_C = 0.25 hours (i.e., 15 minutes) for each machine. Thus, the planning horizon is divided into $T = H/t_C$ = 64 slots. The following parameters of the machines and buffers are given: machine electric power $d_{i,2} = d_{i,1}$ = 25 kW, $d_{i,0}$ = 0 kW, i =1, 2, 3; machine reliabilities p_i' = 0.95, i =1, 2, 3; and buffer capacities C_i = 5, i =1, 2. The parameters are set to be identical for illustration purposes. However, the applicability of the approach proposed in this chapter is not limited to manufacturing systems with identical machine or buffer parameters. The task is to find near-optimal production schedules regarding Formulations 1 and 2, respectively. The schedules will be repeated every working day with targeted average cumulative production of CP_0 = 45 products following a fresh start. The TOU consumption rates $c_E(t)$ for different time periods are provided in Table 1.2. The TOU demand rates $c_D(t)$ and the fixed charge c_{Fixed} are also provided in Table 1.2 but they should be divided by 21, the number of working days in a month, to obtain the daily equivalents.

Parameter selection research for the PSO algorithm has been previously conducted in (Clerc, 2007; Clerc and Kennedy, 2002; Rezaee Jordehi and Jasni, 2013; Shi and Eberhart, 1998; Trelea, 2003). In this dissertation we set swarm size N_P = 1000 and iteration number N_T = 2000. The parameters $\theta_0 = 1$, $\theta_1 = 2$, and $\theta_2 = 2$ reported in (Clerc, 2007) perform generally well and they are also adopted in the implemented binary PSO algorithm.

For Formulation 1, we run 20 trials of the binary PSO program first based on the summer TOU pricing profile. The time consumption of the implemented binary PSO algorithm for each trial is approximately 5 seconds on a computer equipped with a processor of Intel (R) Xeon(R) CPU (W3550 @ 3.07GHz 3.06GHz) and a memory of 4GB. Multiple best solutions have been obtained. Although the exact schedules for these solutions are different, they all correspond to the same minimal e_T out of the 20 trials. We randomly pick one best solution $s_i(t)$ (i = 1, 2, 3) and plot it in Figure 5.2(a). Then we run 20 trials of the binary PSO program based on the winter TOU pricing profile and plot the best solution in Figure 5.2(b). Also plotted are the trajectories of some important measures over time t. These measures are $WIP_{SYS}(t)$, $PR_{SYS}(t)$, $e_{SYS}(t)$, and $d_{SYS}(t)$. The pre-specified TOU energy and demand rates $c_E(t)$ and $c_D(t)$ are shown for reference only. The detailed information of the best summer and winter schedules for Formulation 1 is provided in Table 5.1. The objective and constraint values corresponding to the schedules for Formulation 1 are listed in Table 5.2. These results can be explained as follows:

1) The control signals for the three machines are represented by s_1, s_2, and s_3. These signals are all changing over time. Their changing leads to the changing of the expected values of the performance measures WIP_{SYS}, PR_{SYS}, e_{SYS}, and d_{SYS}.
2) At the beginning (about 8 am) of the production, the three machines are turned "on" (i.e., $s_i = 1$) sequentially. The first one is turned on immediately, while the second and third

ones are turned on with gradually increasing delays. This schedule is meant to conserve electricity on the second and third machines, because the first and the second buffers are all empty after a fresh start and some time is needed for the inventory (i.e., WIP_{SYS}) to build up.

3) At the end (about 12 midnight) of the production, the three machines are turned "off" (i.e., $s_i = 0$) sequentially. The first one is turned off first, while the second and third ones are turned off with gradually increasing delays. This schedule is meant to conserve electricity on the first and second machines, because the built-up inventory (i.e., WIP_{SYS}) in the first and the second buffers takes some time to be depleted.

4) The on-peak period in the summer season is much short than the on-peak period in the winter season. This is represented in the plots of c_E and c_D. Other than the beginning and ending periods of the production, the machines are controlled so that the energy consumption are reduced intermittently and randomly throughout the entire planning horizon as seen in the plots of e_{SYS}, no matter it is in the on-peak period or the off-peak period.

5) Although d_{SYS} can be as low as 0 kW (i.e., all the three machines are turned off during the same time slot) in the figure, the power demand d_T of the system that counts towards the demand charge is still 75 kW as shown in Table 5.2. This is because it is based on the *highest* average kW measured in any 15-minute interval during the on-peak period.

6) Demand charges can be a significant part of the utility bill. In Table 5.2, the demand charge c_{DT} accounts for 36.4% of the total electricity cost c_T in the summer season. This is due to the fact that Formulation 1 does not take demand into consideration, and thus no effort is put into lowering this portion of the cost.

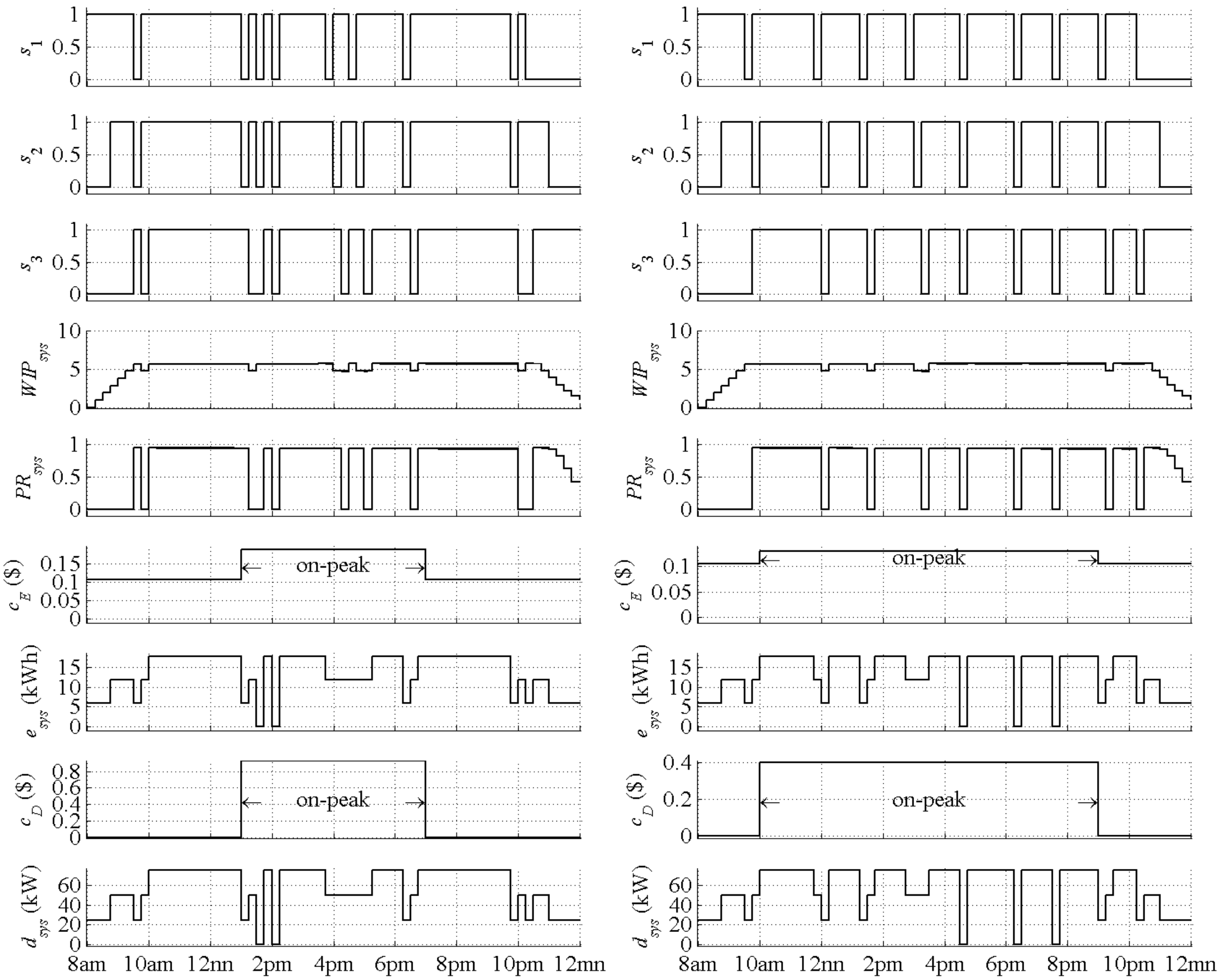

(a) (b)

Figure 5.2. Best schedules for Formulation 1 based on (a) the summer and (b) the winter TOU rates

Table 5.1. Best schedules for Formulation 1

Formulation	Solutions $s_i(t)$
Formulation 1 (Summer)	$s_1(t)$ = [1111110111111111111101010111111011011111101111111111111010000000] $s_2(t)$ = [0001110111111111111101010111111101101111101111111111111011110000] $s_3(t)$ = [0000001011111111111110010111111110110111110111111111111100111111]
Formulation 1 (Winter)	$s_1(t)$ = [1111110111111110111110111110111111011111101111011111011110000000] $s_2(t)$ = [0001111011111111011110111111011111011111101111011111011111110000] $s_3(t)$ = [0000000111111111011111011111101111011111101111011111101110111111]

Table 5.2. Objective and constraint values corresponding to the best schedules for Formulation 1

Formulation	e_T (kWh)	d_T (kW)	$c_{ET} + c_{Fixed}$ ($)	c_{DT} ($)	c_T ($)	CP_T
Formulation 1 (Summer)	872.813	75	121.031	69.321	190.352	45.217
Formulation 1 (Winter)	872.813	75	111.550	29.929	141.479	45.217

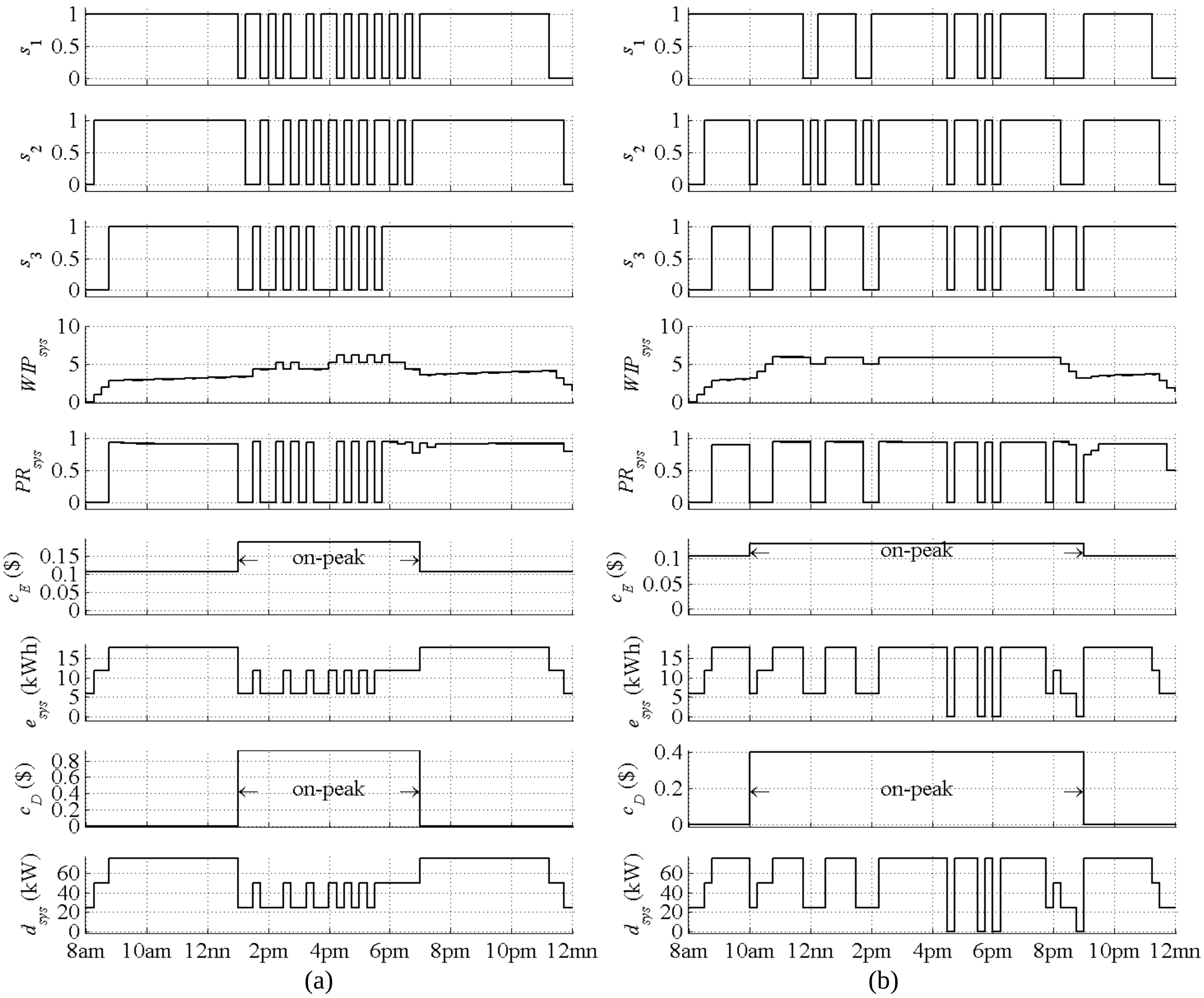

Figure 5.3. Best schedules for Formulation 2 based on (a) the summer and (b) the winter TOU rates

Table 5.3. Best schedules for Formulation 2

Formulation	Solutions $s_i(t)$
Formulation 2 (Summer)	$s_1(t)$ = [11111111111111111111011010100101101010101010111111111111111111000] $s_2(t)$ = [01111111111111111111110010010101010101011010111111111111111111110] $s_3(t)$ = [00011111111111111111100100101010001010101111111111111111111111111]
Formulation 2 (Winter)	$s_1(t)$ = [11111111111111110011111001111111111011101011111110000011111111000] $s_2(t)$ = [00111111011111101011110101111111110111010111111110001111111111100] $s_3(t)$ = [00011111000111110011111001111111110111010111111011101111111111111]

Table 5.4. Objective and constraint values corresponding to the best schedules for Formulation 2

Formulation	e_T (kWh)	d_T (kW)	$c_{ET} + c_{Fixed}$ (\$)	c_{DT} (\$)	c_T (\$)	CP_T
Formulation 2 (Summer)	878.750	50	112.825	46.214	159.039	45.017
Formulation 2 (Winter)	872.813	75	109.013	29.929	138.942	45.012

For Formulation 2, the same procedure is followed. The best solutions together with the measures are plotted in Figure 5.3. The detailed information of the best summer and winter schedules for Formulation 2 is provided in Table 5.3. The objective and constraint values corresponding to the schedules are listed in Table 5.4. Compared to Figure 5.2, the results in Figure 5.3 show different patterns. These results are further explained as follows:

1) The control signals of the machines during the beginning and ending periods of the production are very similar to the ones for Formulation 1.
2) Other than the beginning and ending periods, the machines are controlled so that the electricity consumption is reduced only in the on-peak period when the consumption rate is higher, as seen in the plots of e_{SYS}. This is different from the solutions to Formulation 1. Evidently, Formulation 2 has the capability of tracking the TOU pricing profile.
3) The power demand d_T for the summer season is 50 kW, which is significantly reduced due to the avoidance of the simultaneous operation of all the three machines during the on-peak period. As a result, the demand charge c_{DT} is also reduced, as shown in Table 5.4.
4) The power demand d_T for the winter season is still 75 kW, which is the same as Formulation 1. This is because the winter on-peak period is much longer than the summer on-peak period. Due to the limited capability of the manufacturing system, it is unable to avoid the concurrent operation of all the three machines during the long on-peak period while satisfying the production constraint.
5) For the summer season, although the total electricity consumption e_T is slightly increased compared to Formulation 1, the total electricity related cost c_T is significantly reduced. This is because the primary goal of Formulation 2 is to minimize c_T, and the consumption charge is only one component of c_T. Consequently, Formulation 2 jointly responds to both electricity consumption and power demand while Formulation 1 responds to electricity consumption only.

5.4.2. Insights gained from more cases

We further vary the identical machine reliability p_i' (i = 1, 2, and 3) from 0.91 to 0.99 with an interval of 0.02 and identical buffer capacity C_i (i = 1 and 2) from 1 to 9 with an interval of 2 to create 25 cases. Again, twenty trials of the binary PSO program have been run for each case. The objective values corresponding to the best solutions to these cases are provided in Figure 5.4 and Figure 5.5.

It should be noted that the circles in Figure 5.4 and Figure 5.5 mark the smallest objective function values e_T or c_T along the axis of buffer capacity C_i for each machine reliability p_i' value. For example, the 3-dimentianal coordinates (p_i', C_i, e_T) of the bottom row of Figure 5.4 (a) are (0.99, 1, 872.438), (0.99, 3, 860.063), (0.99, 5, 860.063), (0.99, 7, 860.063), and (0.99, 9, 860.063). Therefore, the last four points with the same lowest e_T value 860.063 kWh are marked.

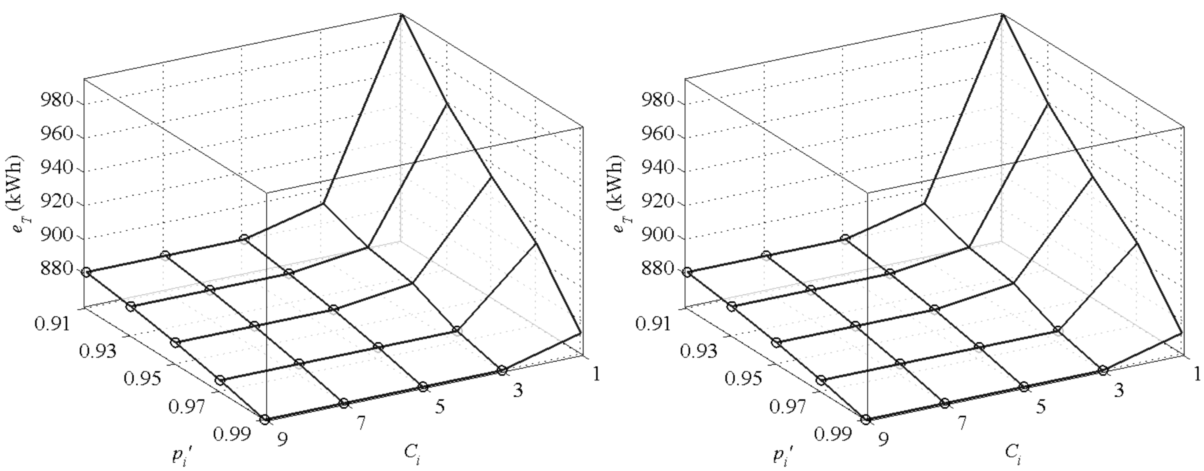

(a) (b)

Figure 5.4. Objective values corresponding to the best solutions to Formulation 1 cases based on (a) the summer and (b) the winter TOU rates

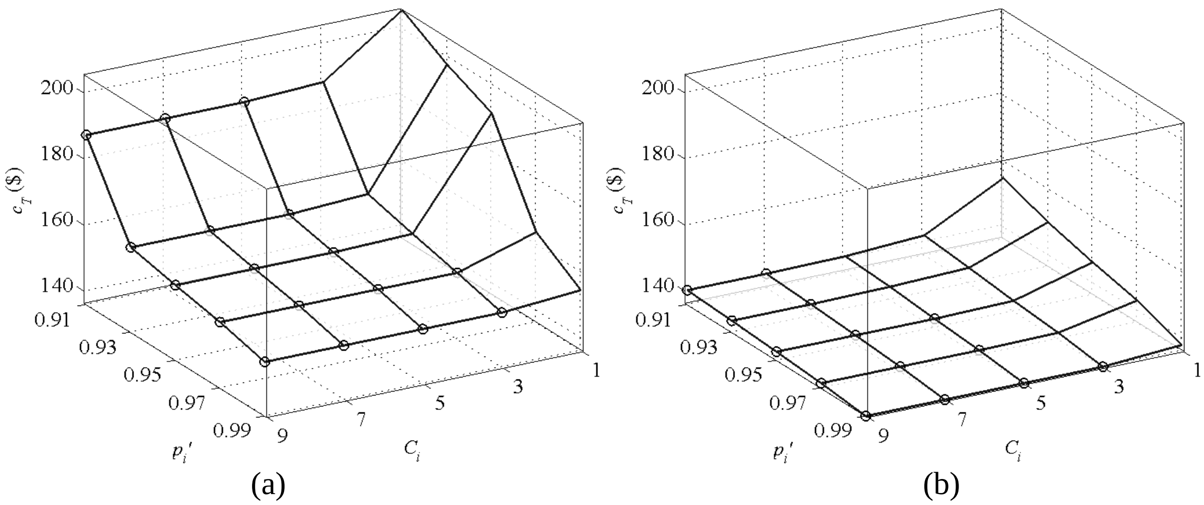

Figure 5.5. Objective values corresponding to the best solutions to Formulation 2 cases based on (a) the summer and (b) the winter TOU rates

Careful observation of Figure 5.4 and Figure 5.5 suggests that:

1) Since Formulation 1 responds to the electricity consumption only, the differences in the TOU rates for the summer and winter seasons have no effect on the best solutions. Therefore, Figure 5.4 (a) and (b) are exactly the same.

2) Since Formulation 2 tracks the TOU pricing profile with regard to both electricity consumption and demand, the best solutions for the summer months shown in Figure 5.5 (a) are quite different from those for the winter months in Figure 5.5 (b). For every case examined, the total electricity cost c_T in the summer months is higher than that of the corresponding winter months.

3) As machine reliabilities p_i' increases, the electricity consumption e_T and the total electricity cost c_T corresponding to the best scheduling solutions of Formulations 1 and 2 respectively both decrease. Clearly, it is desirable to improve machine reliabilities.

4) As buffer capacities C_i increases, the electricity consumption e_T and the total electricity cost c_T corresponding to the best scheduling solutions of Formulations 1 and 2 respectively both decrease first, and then reach a flat zone where they both keep constant.

Therefore, it is not always better to have larger buffer capacities; rather an appropriate buffer size is preferred regarding lowering e_T and c_T.

5.5. Conclusions

This chapter investigates the TOU based electricity demand response problems aiming at minimizing the total electricity energy consumption and cost under the constraint of the production target. The proposed approach fills the gaps in the literature concerning TOU electricity demand response of manufacturing systems and helps reduce the carbon footprints generated by producing a product, which can meaningfully lead to energy-efficient, demand-responsive, and cost-effective manufacturing. The binary PSO algorithm has been applied to pursuit near-optimal scheduling solutions. Although these solutions are not necessarily optimal, they can still provide remarkable insights into the nature of these problems.

As shown in this chapter, many factors may influence the scheduling solutions as well as the effectiveness and attractiveness of the TOU based demand response program to manufacturing enterprises. We have carefully studied the effects of factors such as problem formulations, the TOU pricing profile, machine reliabilities, and buffer capacities on the solutions. Although the results presented in Section 5.4 are limited to the specific examples examined, the proposed approach is a general one. For different combinations of these and many other factors, the approach can be followed to achieve acceptable near-optimal solutions on a case-by-case basis.

CHAPTER 6

CONCLUSIONS

6.1. Conclusions

The main objectives of this doctoral dissertation are to: generate new knowledge about electricity energy efficiency and cost as a function of manufacturing system parameters and the TOU rates; use the knowledge to improve the technological readiness of manufacturing enterprises for the transition towards sustainable manufacturing in the context of smart electric grids. In order to achieve the objectives, detailed research tasks on manufacturing system modeling, energy efficiency modeling, cost analysis, and demand response decision making have been performed. Specifically, the dynamics and performance measures of general manufacturing systems with multiple machines and buffers have been modeled. Expressions of electricity energy efficiency and cost have been established based on the TOU pricing profile. Case studies have been carried out to examine the feasibility and potential benefits of switching from flat rates to TOU rates. Production scheduling problem formulations and the solution technique are discussed. Effects of various factors on the TOU based scheduling solutions have been carefully examined.

6.2. Intellectual Contributions and Broader Impacts

The intellectual contributions of this research are summarized as follows.

We proposed a novel method of joint production and energy modeling for sustainable manufacturing systems. Unlike previous methods, the proposed modeling is based on direct derivation of the general system with multiple machines and buffers. The solvability of the proposed method has been validated through theoretical proofs based on fixed-point theory. The proposed method is capable of characterizing both steady-state performance and transient behavior of the manufacturing systems. This research has overcome the restrictions on the number of machines and the capacity of buffers. Besides, the proposed method needs only one run and significantly less computing time compared to simulation-based methods. The integration of both electricity energy consumption and peak demand with varying prices into the production model at the system level is the first of its kind in the manufacturing literature. The monotonicity analysis has revealed the effects of various factors on electricity energy efficiency and cost. The case studies from three different perspectives (design, operation, and control) throughout this dissertation have proven the capability of the modeling method in enhancing the energy efficiency, electricity demand responsiveness, and cost effectiveness of sustainable manufacturing systems.

In terms of broader impacts, since the urgency of reducing GHG emissions as well as energy cost of industrial systems has been widely recognized by our society, this research will provide quantitative tools that manufacturers can adopt in optimally responding to the TOU based electricity demand. The insights acquired in this research will lead to both financial and environmental benefits by reducing power demand, energy consumption, and carbon footprints, thus benefiting not only the industrial sector but also the environment and society as a whole.

6.3. Future Work

The studies that could be conducted as a future follow-up to the research presented in this dissertation are listed as follows.

Based on the results in this dissertation, research on optimal system design can be carried out to optimally allocate buffer capacities (Li and Meerkov, 2009) and machine reliabilities (Kuo and Wan, 2007; Wang and Li, 2012b). It is possible to perform manufacturing system modeling and demand response investigations for more complex systems such as the ones with closed-loop structures (Li, 2009) and assembly/disassembly features (Helber, 1998). It is also worth exploring the extensibility of the proposed method to the cases involving stochastic or uncertain machine reliability parameters (Kleijnen et al., 2011; Wang and Li, 2012a; Wang et al., 2012b, 2012c).

In this dissertation, the modeling and monotonicity analysis are mainly carried out from manufacturers' point of view. The benefits to utilities companies and social welfare such as reduced need for large capital expenditures and enhanced grid reliability have not been studied. In addition, it may not be sufficient to only look at the electricity cost savings without also considering many other issues that may influence the overall per-product cost. For example, a time-shifted schedule with extended night hours typically must be paid for with a premium. Sometimes negotiations with labor unions are also needed because there is literature showing that night shift work contributes to physical and social health problems (Delezie and Challet, 2011; Scheer et al., 2009). Extended long period of night shifts may also influence workers' alertness (hence safety) and performance (Carus, 2012). In practice, such issues should also be considered in the decision making process. This dissertation only considers the basic issue where the main concerns are machines, buffers, and rate plans, instead of people. Research that incorporates such issues and other factors to create models that are more comprehensive is surely interesting and worth exploration in the future. The research in this dissertation can serve as the building block for creating such models.

BIBLIOGRAPHY

109th U.S. Congress, 2005. Energy Policy Act of 2005. Retrieved January 11, 2013, from http://www.govtrack.us/congress/bills/109/hr6.

Alden, J.M., Burns, L.D., Costy, T., Hutton, R.D., Jackson, C.A., Kim, D.S., Kohls, K.A., Owen, J.H., Turnquist, M.A., Veen, D.J.V., 2006. General Motors increases its production throughput. Interfaces 36, 6-25.

Alexandros, D.C., Chrissoleon, P.T., 2009. Exact analysis of a two-workstation one-buffer flow line with parallel unreliable machines. European Journal of Operational Research 197, 572-580.

Alvarez Bel, C., Alcazar Ortega, M., Escriva Escriva, G., Gabaldon Marin, A., 2009. Technical and economical tools to assess customer demand response in the commercial sector. Energy Conversion and Management 50(10), 2605-2612.

Argyros, I.K., 2007. Computational Theory of Iterative Methods. Elsevier.

Arrow, K.J., Debreu, G., 1954. The existence of an equilibrium for a competitive economy. Econometrica 22, 265-290.

Ashok, S., 2006. Peak-load management in steel plants. Applied Energy 83(5), 413-424.

Australia Ausgrid, 2012. Time of Use Pricing. Retrieved September 1, 2013, from http://www.ausgrid.com.au/Common/Our-network/Metering/Time-of-use-pricing.aspx#. UkXOP5JQGk8.

Balogun, V.A., Mativenga, P.T., 2013. Modelling of direct energy requirements in mechanical machining processes. Journal of Cleaner Production 41, 179-186.

Barbose, G., Goldman, C., Bharvirkar, R., Hopper, N., Ting, M., Neenan, B., 2005. Real Time

Pricing as a Default or Optional Service for C&I Customers: A Comparative Analysis of Eight Case Studies. Retrieved September 1, 2014, from http://emp.lbl.gov/publications/real-time-pricing-default-or-optional-service-ci-customers-comparative-analysis-eight-c.

Barbose, G., Goldman, C., Neenan, B., 2004. A Survey of Utility Experience with Real Time Pricing. Retrieved September 1, 2014, from http://sedc-coalition.eu/wp-content/uploads/2011/06/Barbose-Survey-of-Utility-Real-Time-Pricing-Dec-2004.pdf.

Bego, A., Li, L., Sun, Z., 2013. Identification of reservation capacity in critical peak pricing electricity demand response program for sustainable manufacturing systems. International Journal of Energy Research, In Press. DOI: http://dx.doi.org/10.1002/er.3077.

Behrendt, T., Zein, A., Min, S., 2012. Development of an energy consumption monitoring procedure for machine tools. CIRP Annals - Manufacturing Technology 61(1), 43-46.

Black, F., 1995. Exploring General Equilibrium. MIT Press.

Border, K.C., 1985. Fixed Point Theorems with Applications to Economics and Game Theory. Cambridge University Press.

Braithwait, S.D., Hansen, D.G., 2012. How large commercial and industrial customers respond to dynamic pricing: The California experience. In: Sioshansi F, editor. Smart Grid: Integrating Renewable, Distributed and Efficient Energy: Academic Press, 289-316.

Brief, K., Davids, B., 2011. C&I Customers Get Smart: Technology Creates New Opportunities for Demand-Side Management. Retrieved September 1, 2014, from http://www.enernoc.com/our-resources/white-papers/c-a-i-customers-get-smart.

Burden, R.L., Faires, J.D., 2011. Numerical Analysis (9th Ed). Brooks-Cole.

Carus, C.C., 2012. Running on Empty: Fatigue and Healthcare Professionals. Retrieved September 1, 2013, from http://www.medscape.com/viewarticle/768414.

Chao, X., Chen, F.Y., 2005. An optimal production and shutdown strategy when a supplier offers an incentive program. Manufacturing & Service Operations Management 7(2), 130-143.

Chupka, M.W., Earle, R., Fox-Penner, P., Hledik, R., 2008. Transforming America's Power Industry: The Investment Challenge 2010-2030. Retrieved January 15, 2013, from http://www.brattle.com/_documents/uploadlibrary/upload725.pdf.

Clerc, M., 2007. Binary Particle Swarm Optimisers: Toolbox, Derivations, and Mathematical Insights. Retrieved January 15, 2013, from http://hal.archives-ouvertes.fr/docs/00/12/28/09/PDF/Binary_PSO.pdf.

Clerc, M., Kennedy, J., 2002. The particle swarm - Explosion, stability, and convergence in a multidimensional complex space. IEEE Transactions on Evolutionary Computation 6(1), 58-73.

Colledani, M., Gershwin, S., 2013. A decomposition method for approximate evaluation of continuous flow multi-stage lines with general Markovian machines. Annals of Operations Research 209(1), 5-40.

ComEd, 2012. Load Forecast for Five-Year Planning Period (June 2013 - May 2018). Retrieved January 15, 2013, from http://www2.illinois.gov/ipa/Documents/AppendixII-ComEdLoadForecast.pdf.

Cook, B., Gazzano, J., Gunay, Z., Hiller, L., Mahajan, S., Taskan, A., Vilogorac, S., 2012. The smart meter and a smarter consumer: Quantifying the benefits of smart meter implementation in the United States. Chemistry Central Journal 6(S1), 1-16.

Corno, F., Razzak, F., 2012. Intelligent energy optimization for user intelligible goals in smart home environments. IEEE Transactions on Smart Grid 3(4), 2128-2135.

Dallery, Y., Gershwin, S.B., 1992. Manufacturing flow line systems: a review of models and analytical results. Queuing Systems 12, 3-94.

Delezie, J., Challet, E., 2011. Interactions between metabolism and circadian clocks: reciprocal disturbances. Annals of the New York Academy of Sciences 1243, 30-46.

Dietmair, A., Verl, A., 2009. A generic energy consumption model for decision making and energy efficiency optimisation in manufacturing. International Journal of Sustainable Engineering 2(2), 123-133.

Duflou, J.R., Sutherland, J.W., Dornfeld, D., Herrmann, C., Jeswiet, J., Kara, S., Hauschild, M., Kellens, K., 2012. Towards energy and resource efficient manufacturing: A processes and systems approach. CIRP Annals - Manufacturing Technology 61(2), 587-609.

EPRI, 2003. Interruptible Power Rates and Their Role in Utility Distributed Resources Programs. Retrieved September 1, 2014, from http://www.epri.com/abstracts/Pages/ProductAbstract.aspx?ProductId=000000000001007717.

Fang, K., Uhan, N., Zhao, F., Sutherland, J.W., 2011. A new approach to scheduling in manufacturing for power consumption and carbon footprint reduction. Journal of Manufacturing Systems 30(4), 234-240.

Faria, P., Vale, Z., Soares, J., Ferreira, J., 2011. Demand response management in power systems using a particle swarm optimization approach. IEEE Intelligent Systems PP(99), 1-9.

Faruqui, A., Hledik, R., Newell, S., Pfeifenberger, J., 2007. The Power of Five Percent: How Dynamic Pricing Can Save $35 Billion in Electricity Costs. Retrieved September 1, 2013, from http://www.brattle.com/_documents/UploadLibrary/Upload574.pdf.

Faruqui, A., Malxo, J.R., 1983. The residential demand for electricity by time-of-use: A survey of twelve experiments with peak load pricing. Energy 8(10), 781-795.

Faruqui, A., Sergici, S., 2010. Household response to dynamic pricing of electricity: A survey of 15 experiments. Journal of Regulatory Economics 38(2), 193-225.

Fernandez, M., Li, L., Sun, Z., 2013. "Just-for-Peak" buffer inventory for peak electricity demand reduction of manufacturing systems. International Journal of Production Economics, In Press. DOI: http://dx.doi.org/10.1016/j.ijpe.2013.06.020.

Finn, P., Fitzpatrick, C., Connolly, D., 2012. Demand side management of electric car charging: Benefits for consumer and grid. Energy 42(1), 358-363.

Finn, P., Fitzpatrick, C., Connolly, D., Leahy, M., Relihan, L., 2011. Facilitation of renewable electricity using price based appliance control in Ireland's electricity market. Energy 36(5), 2952-2960.

Fremeth, A.R., Holburn, G.L.F., Spiller, P.T., 2014. The impact of consumer advocates on regulatory policy in the electric utility sector. Public Choice 161(1-2), 157-181.

Fysikopoulos, A., Anagnostakis, D., Salonitis, K., Chryssolouris, G., 2012. An empirical study of the energy consumption in automotive assembly. Procedia CIRP 3, 477-482.

Gershwin, S.B., 1994. Manufacturing Systems Engineering. Prentice-Hall.

Gershwin, S.B., Werner, L.M., 2007. An approximate analytical method for evaluating the performance of closed-loop flow systems with unreliable machines and finite buffers. International Journal of Production Research 45(14), 3085-3111.

Gökçe, M.A., Dinçer, M.C., Örnek, M.A., 2012. Analysis of Transient Throughput Rates of Transfer Lines with Pull Systems. In: Ríos-Mercado, R.Z., Ríos-Solís, Y.A. (Eds), Just-in-Time Systems, vol 60. Springer, New York, NY. 2012. 287-304.

Gottwalt, S., Ketter, W., Block, C., Collins, J., Weinhardt, C., 2011. Demand side management: A simulation of household behavior under variable prices. Energy Policy 39(12), 8163-8174.

Gungor, V.C., Sahin, D., Kocak, T., Ergut, S., Buccella, C., Cecati, C., Hancke, G.P., 2013. A survey on smart grid potential applications and communication requirements. IEEE Transactions on Industrial Informatics 9(1), 28-42.

Gutowski, T., Murphy, C., Allen, D., Bauer, D., Bras, B., Piwonka, T., Sheng, P., Sutherland, J., Thurston, D., Wolff, E., 2005. Environmentally benign manufacturing: Observations from Japan, Europe and the United States. Journal of Cleaner Production 13(1), 1-17.

He, Y., Wang, B., Wang, J., Xiong, W., Xia, T., 2012. Residential demand response behavior analysis based on Monte Carlo simulation: The case of Yinchuan in China. Energy 47, 230-236.

Helber, S., 1998. Decomposition of unreliable assembly disassembly networks with limited buffer capacity and random processing times. European Journal of Operational Research 109, 24-42.

Herter, K., McAuliffe, P., Rosenfeld, A., 2007. An exploratory analysis of California residential customer response to critical peak pricing of electricity. Energy 32(1), 25-34.

Herter, K., Wayland, S., 2010. Residential response to critical-peak pricing of electricity: California evidence. Energy 35(4), 1561-1567.

Houwing, M., Negenborn, R.R., De Schutter, B., 2011. Demand response with micro-CHP systems. Proceedings of the IEEE 99(1), 200-213.

Hu, S., Liu, F., He, Y., Hu, T., 2012. An on-line approach for energy efficiency monitoring of machine tools. Journal of Cleaner Production 27, 133-140.

Huisman, R., Mahieu, R., Schlichter, F., 2009. Electricity portfolio management: Optimal peak/off-peak allocations. Energy Economics 31(1), 169-174.

Ipsos MORI, 2012. UK Consumer Experiences of Time of Use Tariffs - Report Prepared for Consumer Focus. Retrieved September 1, 2013, from http://www.consumerfocus.org.uk/files/2012/09/Ipsos-MORI-report-on-Consumer-Experiences-Of-Time-Of-Use-Tariffs.pdf.

Jacobs, D., Meerkov, S.M., 1995. A system-theoretic property of serial production lines: Improvability. International Journal of Systems Science 26, 755-785.

Kennedy, J., Eberhart, R.C., 1997. A discrete binary version of the particle swarm algorithm. In: 1997 IEEE International Conference on Systems, Man, and Cybernetics, Orlando, FL, USA. 5, 4104-4108.

King, C., 2010. Germany: Progress Toward Time-of-Use Energy Pricing, Consumer Engagement. Retrieved September 1, 2013, from http://www.emeter.com/smart-grid-watch/2010/germany-progress-toward-time-of-use-energy-pricing-consumer-engagement/.

Kleijnen, J.P.C., Pierreval, H., Zhang, J., 2011. Methodology for determining the acceptability of system designs in uncertain environments. European Journal of Operational Research 209, 176-183.

Klemes, J.J., Varbanov, P.S., Huisingh, D., 2012. Recent cleaner production advances in process monitoring and optimisation. Journal of Cleaner Production 34, 1-8.

Kuo, W., Wan, R., 2007. Recent advances in optimal reliability allocation. IEEE Transactions on Systems, Man, and Cybernetics Part A: Systems and Humans 37, 143-156.

Lewis, G., 2007. Strategies to Increase California Food Processing Industry Demand Response Participation: A Scoping Study. Retrieved January 15, 2013, from http://drrc.lbl.gov/system/files/lbnl-63668.pdf.

Li, J., Blumenfeld, D.E., Alden, J.M., 2006. Comparisons of two-machine line models in throughput analysis. International Journal of Production Research 44, 1375-1398.

Li, J., Blumenfeld, D.E., Huang, N., Alden, J.M., 2009a. Throughput analysis of production systems: Recent advances and future topics. International Journal of Production Research 47(14), 3823-3851.

Li, J., Meerkov, S.M., 2009. Production Systems Engineering. Springer.

Li, J., Meerkov, S.M., Zhang, L., 2010. Production systems engineering: Problems, solutions, and applications. Annual Reviews in Control 34(1), 73-88.

Li, L., 2009. Bottleneck detection of complex manufacturing systems using a data-driven method. International Journal of Production Research 47(24), 6929-6940.

Li, L., Chang, Q., Ni, J., 2009b. Data driven bottleneck detection of manufacturing systems. International Journal of Production Research 47, 5019-5036.

Li, L., Chang, Q., Ni, J., Biller, S., 2009c. Real time production improvement through bottleneck control. International Journal of Production Research 47(21), 6145-6158.

Li, L., Chang, Q., Xiao, G., Ambani, S., 2011. Throughput bottleneck prediction of manufacturing system using time series analysis. ASME Journal of Manufacturing Science and Engineering 133, 021015.1-021015.8.

Li, L., Sun, Z., 2013. Dynamic energy control for energy efficiency improvement of sustainable manufacturing systems using Markov decision process. IEEE Transactions on Systems, Man, and Cybernetics: Systems 43(5), 1195-1205.

Liang, Y., Levine, D.I., Shen, Z.-J., 2012. Thermostats for the smart grid: Models, benchmarks, and insights. Energy Journal 33(4), 61-95.

Lima, C.A.F., Navas, J.R.P., 2012. Smart metering and systems to support a conscious use of water and electricity. Energy 45(1), 528-540.

Liu, Y., Dong, H., Lohse, N., Petrovic, S., Gindy, N., 2013. An investigation into minimising total energy consumption and total weighted tardiness in job shops. Journal of Cleaner Production, In Press. DOI: http://dx.doi.org/10.1016/j.jclepro.2013.07.060.

Liu, J., Yang, S., Wu, A., Hu, S.J., 2012. Multi-state throughput analysis of a two-stage manufacturing system with parallel unreliable machines and a finite buffer. European Journal of Operational Research 219, 296-304.

Logenthiran, T., Srinivasan, D., Tan Zong, S., 2012. Demand side management in smart grid using heuristic optimization. IEEE Transactions on Smart Grid 3(3), 1244-1252.

Luo, H., Du, B., Huang, G.Q., Chen, H., Li, X., 2013. Hybrid flow shop scheduling considering machine electricity consumption cost. International Journal of Production Economics, In Press. DOI: http://dx.doi.org/10.1016/j.ijpe.2013.01.028.

Martens, D., Baesens, B., Fawcett, T., 2011. Editorial survey: Swarm intelligence for data mining. Machine Learning 82(1), 1-42.

Mathieu, J.L., Callaway, D.S., Kiliccote, S., 2011. Variability in automated responses of commercial buildings and industrial facilities to dynamic electricity prices. Energy and Buildings 43(12), 3322-3230.

McKane, A., Rhyne, I., Lekov, A., Thompson, L., Piette, M.A., 2008. Automated Demand Response: The Missing Link in the Electricity Value Chain. Retrieved January 15, 2013, from http://drrc.lbl.gov/sites/drrc.lbl.gov/files/lbnl-2736e.pdf.

Meerkov, S.M., Shimkin, N., Zhang, L., 2010. Transient behavior of two-machine geometric production lines. IEEE Transactions on Automatic Control 55, 453-458.

Meerkov, S.M., Zhang, L., 2008. Transient behavior of serial production lines with Bernoulli machines. IIE Transactions 40, 297-312.

Meerkov, S.M., Zhang, L., 2011. Unbalanced manufacturing systems with floats: analysis and lean design. International Journal of Manufacturing Technology and Management 23, 4-15.

Motegi, N., Piette, M.A., Watson, D.S., Kiliccote, S., Xu, P., 2007. Introduction to Commercial Building Control Strategies and Techniques for Demand Response. Retrieved January 15, 2013, from http://gaia.lbl.gov/btech/papers/59975.pdf.

National Grid USA, 2006. Understanding Electric Demand. Retrieved September 1, 2013, from http://www.nationalgridus.com/niagaramohawk/non_html/eff_elec-demand.pdf.

Nikzad, M., Mozafari, B., Bashirvand, M., Solaymani, S., Ranjbar, A.M., 2012. Designing time-of-use program based on stochastic security constrained unit commitment considering reliability index. Energy 41(1), 541-548.

Ontario Ministry of Energy, 2013. Smart Meters and Time-of-Use Prices. Retrieved September 1, 2013, from http://www.energy.gov.on.ca/en/smart-meters-and-tou-prices/.

Orange and Rockland Utilities, 2013a. Service Classification No. 2. Retrieved September 1, 2013, from https://www.oru.com/documents/tariffsandregulatorydocuments/ny/electrictariff/electricsc02.pdf.

Orange and Rockland Utilities, 2013b. Service Classification No. 20. Retrieved September 1, 2013, from https://www.oru.com/documents/tariffsandregulatorydocuments/ny/electrictariff/electricsc20.pdf.

Orange and Rockland Utilities, 2013c. Statement of Market Supply Charge. Retrieved September 1, 2013, from https://www.oru.com/documents/tariffsandregulatorydocuments/ny/electricmarketsupplycharge/MSC3-18.pdf.

Orange and Rockland Utilities, 2013d. What Are the Demand and Energy Charges on My Bill? Retrieved September 1, 2013, from https://www.oru.com/customerservice/askusaquestion/aboutbilling/billchargesanddiscrepancies.html#quest6.

Petri, F., 2004. General Equilibrium, Capital, and Macroeconomics: A Key to Recent Controversies in Equilibrium Theory. Edward Elgar Publishing.

Pina, A., Silva, C., Ferrao, P., 2012. The impact of demand side management strategies in the penetration of renewable electricity. Energy 41(1), 128-137.

Poli, R., Kennedy, J., Blackwell, T., 2007. Particle swarm optimization: An overview. Swarm Intelligence 1(1), 33-57.

Quiggin, D., Cornell, S., Tierney, M., Buswell, R., 2012. A simulation and optimisation study: Towards a decentralised microgrid, using real world fluctuation data. Energy 41(1), 549-559.

Rastegar, M., Fotuhi-Firuzabad, M., Aminifar, F., 2012. Load commitment in a smart home. Applied Energy 96, 45-54.

Rentizelas, A.A., Tolis, A.I., Tatsiopoulos, I.P., 2012. Investment planning in electricity production under CO_2 price uncertainty. International Journal of Production Economics

140(2), 622-629.

Rezaee Jordehi, A., Jasni, J., 2013. Parameter selection in particle swarm optimisation: A survey. Journal of Experimental & Theoretical Artificial Intelligence, 1-16.

Roy, R., Hinduja, S., Teti, R., 2008. Recent advances in engineering design optimisation: Challenges and future trends. CIRP Annals-Manufacturing Technology, 57(2), 697-715.

Sader, B.H., Sorensen, C.D., 2010. A new technique for modeling production control schemes in manufacturing systems. International Journal of Production Research 48, 7127-7157.

Santos, J.P., Oliveira, M., Almeida, F.G., Pereira, J.P., Reis, A., 2011. Improving the environmental performance of machine-tools: Influence of technology and throughput on the electrical energy consumption of a press-brake. Journal of Cleaner Production 19(4), 356-364.

Scheer, F.A.J.L., Hilton, M.F., Mantzoros, C.S., Shea, S.A., 2009. Adverse metabolic and cardiovascular consequences of circadian misalignment. Proceedings of the National Academy of Sciences 106(11), 4453-4458.

Schipper, M., 2006. Energy-Related Carbon Dioxide Emissions in U.S. Manufacturing. Retrieved September 1, 2013, from http://www.eia.gov/oiaf/1605/ggrpt/pdf/industry_mecs.pdf.

Scott, I., 2014. Teaching an old dog new tricks: Adapting public utility commissions to meet twenty-first century climate challenges. Harvard Environmental Law Review 38(2), 371-413.

Shaaban, S., Hudson, S., 2011. Transient behaviour of unbalanced lines. Flexible Services and Manufacturing Journal 24(4), 575-602.

Shi, Y., Eberhart, R.C., 1998. Parameter selection in particle swarm optimization, In: Porto, V.W., Saravanan, N., Waagen, D., Eiben, A.E. (Eds.), Evolutionary Programming VII. Springer Berlin Heidelberg, 591-600.

Soares, J., Silva, M., Sousa, T., Vale, Z., Morais, H., 2012. Distributed energy resource short-term scheduling using signaled particle swarm optimization. Energy 42(1), 466-476.

Sun, Z., Li, L., 2013. Potential capability estimation for real time electricity demand response of sustainable manufacturing systems using Markov decision process. Journal of Cleaner Production, In Press. DOI: http://dx.doi.org/10.1016/j.jclepro.2013.08.033.

Thangaraj, R., Pant, M., Abraham, A., Bouvry, P., 2011. Particle swarm optimization: Hybridization perspectives and experimental illustrations. Applied Mathematics and Computation 217(12), 5208-5226.

Torriti, J., 2012. Price-based demand side management: Assessing the impacts of time-of-use tariffs on residential electricity demand and peak shifting in Northern Italy. Energy 44(1), 576-583.

Trelea, I.C., 2003. The particle swarm optimization algorithm: Convergence analysis and parameter selection. Information Processing Letters 85(6), 317-325.

U.S. Department of Energy, 2009. President Obama Sets a Target for Cutting U.S. Greenhouse Gas Emissions. Retrieved January 15, 2013, from http://apps1.eere.energy.gov/news/news_detail.cfm/news_id=15650.

U.S. Energy Information Administration, 2013. International Energy Outlook. Retrieved September 1, 2013, from http://www.eia.gov/forecasts/ieo/pdf/0484(2013).pdf.

U.S. Enviromental Protection Agency, 2012. Greenhouse Gas Equivalencies Calculator: Calculations and References. Retrieved January 15, 2013, from http://www.epa.gov/cleanenergy/energy-resources/refs.html.

U.S. Federal Energy Regulatory Commission, 2006. Assessment of Demand Response and Advanced Metering Staff Report 2006. Retrieved September 1, 2014, from http://www.ferc.gov/legal/staff-reports/demand-response.pdf.

U.S. Federal Energy Regulatory Commission, 2008. Assessment of Demand Response and Advanced Metering Staff Report 2008. Retrieved September 1, 2014, from http://www.ferc.gov/legal/staff-reports/12-08-demand-response.pdf.

U.S. Federal Energy Regulatory Commission, 2010. Assessment of Demand Response and Advanced Metering Staff Report 2010. Retrieved September 1, 2014, from http://www.ferc.gov/legal/staff-reports/2010-dr-report.pdf.

U.S. Federal Energy Regulatory Commission, 2012. Assessment of Demand Response and Advanced Metering Staff Report 2012. Retrieved September 1, 2014, from http://www.ferc.gov/legal/staff-reports/12-20-12-demand-response.pdf.

van Ruijven, B., de Vries, B., van Vuuren, D.P., van der Sluijs, J.P., 2010. A global model for residential energy use: Uncertainty in calibration to regional data. Energy 35(1), 269-282.

Venkatesan, N., Solanki, J., Solanki, S.K., 2012. Residential demand response model and impact on voltage profile and losses of an electric distribution network. Applied Energy 96, 84-91.

Walawalkar, R., Fernands, S., Thakur, N., Chevva, K.R., 2010. Evolution and current status of demand response (DR) in electricity markets: Insights from PJM and NYISO. Energy 35(4), 1553-1560.

Wang, J., Hu, Y., Li, J., 2010. Transient analysis to design buffer capacity in dairy filling and packing production lines. Journal of Food Engineering 98, 1-12.

Wang, L., Wang, Z., Yang, R., 2012a. Intelligent multiagent control system for energy and comfort management in smart and sustainable buildings. IEEE Transactions on Smart Grid 3(2), 605-617.

Wang, Y., Li, L., 2012a. Effects of uncertainty in both component reliability and load demand on multi-state system reliability. IEEE Transactions on Systems, Man, and Cybernetics Part A: Systems and Humans 42, 958-969.

Wang, Y., Li, L., 2012b. Heterogeneous redundancy allocation for series-parallel multi-state systems using hybrid particle swarm optimization and local search. IEEE Transactions on Systems, Man and Cybernetics Part A: Systems and Humans 42, 464-474.

Wang, Y., Li, L., 2013. Time-of-use based electricity demand response for sustainable manufacturing systems. Energy 63, 233-244.

Wang, Y., Li, L., 2014a. A novel modeling method for both steady-state and transient analyses of typical production systems. IEEE Transactions on Systems, Man, and Cybernetics: Systems 45(1), 97-108.

Wang, Y., Li, L., 2014b. Time-of-use based electricity cost of manufacturing systems: Modeling and monotonicity analysis. International Journal of Production Economics 156, 246-259.

Wang, Y., Li, L., 2014c. Joint production and energy modeling of sustainable manufacturing systems: Challenges and methods. In: Proceedings of the ASME 2014 International Manufacturing Science and Engineering Conference, Detroit, Michigan, USA, 1-9.

Wang, Y., Li, L., Huang, S., 2012b. Derivation of reliability and variance estimates for multi-state systems with binary-capacitated components. IEEE Transactions on Reliability 61, 549-559.

Wang, Y., Li, L., Huang, S., Chang, Q., 2012c. Reliability and covariance estimation of weighted k-out-of-n multi-state systems. European Journal of Operational Research 221, 138-147.

Wang, Y., Li, L., Ni, J., Huang, S., 2009. Form tolerance evaluation of toroidal surfaces using particle swarm optimization. Journal of Manufacturing Science and Engineering-Transactions of the ASME 131(5), 051015.1-051015.9.

Zeng, S., Li, J., Ren, Y., 2008. Research of time-of-use electricity pricing models in China: A survey. In: IEEE International Conference on Industrial Engineering and Engineering Management, Singapore. 2191-2195.

APPENDIX

Elsevier Copyright Permission Policy Excerpt

(http://www.elsevier.com/about/policies/lightbox_scholarly-purposes)

Authors can use their articles, in full or in part, for a wide range of scholarly, non-commercial personal purposes as outlined below:

- Use by an author in the author's classroom teaching (including distribution of copies, paper or electronic).
- Distribution of copies (including through e-mail) to known research colleagues for their personal use (but not for Commercial Use).
- Inclusion in a thesis or dissertation (provided that this is not to be published commercially).
- Use in a subsequent compilation of the author's works.
- Extending the Article to book-length form.
- Preparation of other derivative works (but not for Commercial Use).
- Otherwise using or re-using portions or excerpts in other works.
- In addition to this, authors can also use their article for scholarly purposes.
- Please note these rights apply for all Elsevier authors who publish their article as either a subscription article or an open access article. In all cases we require that all Elsevier authors always include a full acknowledgement and, if appropriate, a link to the final published version hosted on Science Direct.

IEEE Copyright Permission Policy Excerpt

(http://www.ieee.org/publications_standards/publications/rights/permissions_faq.pdf)

The IEEE does not require individuals working on a thesis to obtain a formal reuse license. However, you must follow the requirements listed below:

- Using short quotes or referring to the work within these papers) users must give full credit to the original source (author, paper, publication) followed by the IEEE copyright line © 2011 IEEE.
- In the case of illustrations or tabular material, we require that the copyright line © [Year of original publication] IEEE appear prominently with each reprinted figure and/or table.
- If a substantial portion of the original paper is to be used, and if you are not the senior author, also obtain the senior author's approval.

ASME Copyright Permission Policy Excerpt

(https://journaltool.asme.org/Help/AuthorHelp/WebHelp/Guidelines/Copyright_Transfer.htm)

Retained Rights of Authors:

- Authors retain all proprietary rights in any idea, process, procedure, or articles of manufacture described in the Paper, including the right to seek patent protection for them.
- Authors may perform, lecture, teach, conduct related research, display all or part of the Paper, and create derivative works in print or electronic format.
- Authors may reproduce and distribute the Paper for non-commercial purposes only. Non-commercial applies only to the sale of the paper per se.
- For all copies of the Paper made by Authors, Authors must acknowledge ASME as

original publisher and include the names of all author(s), the publication title, and an appropriate copyright notice that identifies ASME as the copyright holder.

VITA

EDUCATION

PhD (2015), **Department of Mechanical & Industrial Engineering,** University of Illinois at Chicago (UIC), Chicago, IL, USA

PhD (2010), **MS** (2006), **BS** (2003), **School of Energy and Power Engineering**, Huazhong University of S&T (HUST), Wuhan, China

Visiting PhD Student (2007-2009)**, Department of Mechanical Engineering**, University of Michigan (UM), Ann Arbor, MI, USA

JOURNAL PAPERS

[J13] **Wang, Y.**, Li, L. (2015). Time-of-use electricity pricing for industrial customers: A survey of U.S. utilities. **Applied Energy**, 149, 89-103.

[J12] **Wang, Y**., Li, L. (2014). Time-of-use based electricity cost of manufacturing systems: Modeling and monotonicity analysis. **International Journal of Production Economics**, 156, 246-259.

[J11] **Wang, Y**., Li, L. (2014). Uncertainty importance measure of individual components in multi-state systems. **IEEE Transactions on Reliability**. DOI: 10.1109/TR.2014.2364575

[J10] **Wang, Y**., Li, L. (2014). A novel modeling method for both steady-state and transient analyses of serial Bernoulli production systems. **IEEE Transactions on Systems, Man and Cybernetics: Systems**, 45(1), 97-108.

[J9] **Wang, Y**., Li, L. (2013). Time-of-use based electricity demand response for sustainable manufacturing systems. **Energy**, 63, 233-244.

[J8] **Wang, Y.**, Li, L. (2013). A PSO algorithm for constrained redundancy allocation in multi-state systems with bridge topology. **Computers & Industrial Engineering**, 68, 13-22.

[J7] Qi, L., Huang, S., Zhang, Y., Xu, X., Li, Y., **Wang, Y.** (2013). A compartmental model for supercritical coal-fired boiler systems. **Journal of Energy Resources Technology-Transactions of the ASME**, 136(2), 021602(1-7)

[J6] **Wang, Y.**, Li, L., Huang, S., Chang, Q. (2012). Reliability and covariance estimation of weighted k-out-of-n multi-state systems. **European Journal of Operational Research**, 221(1), 138-147.

[J5] **Wang, Y.**, Li, L. (2012). Effects of uncertainty in both component reliability and load demand on multi-state system reliability, **IEEE Transactions on Systems, Man and Cybernetics: Part A: Systems and Humans**, 42(4), 958-969.

[J4] **Wang, Y.**, Li, L., Huang, S. (2012). Derivation of reliability and variance estimates for multi-state systems with binary-capacitated components. **IEEE Transactions on Reliability**, 61(2), 549-559.

[J3] **Wang, Y.**, Li, L. (2012). Heterogeneous redundancy allocation for series-parallel multi-state systems using hybrid particle swarm optimization and local search. **IEEE Transactions on Systems, Man, and Cybernetics Part A: Systems and Humans**, 42(2), 464-474.

[J2] **Wang, Y.**, Li, L., Ni, J., Huang, S. (2009). Form tolerance evaluation of toroidal surfaces using particle swarm optimization. **Journal of Manufacturing Science and Engineering-Transactions of the ASME**, 131(5), 051015(1-9).

[J1] **Wang, Y.**, Li, L., Ni, J., Huang, S. (2009). Feature selection using tabu search and probabilistic neural networks. **Pattern Recognition Letters**, 30(7), 661-670.

CONFERENCE PAPERS

[C7] **Wang, Y.**, Li, L. (2014). Inclusion of renewable energy topics in the Design of Experiments course for Industrial and Systems Engineering students. In **Proceedings of 2014 ASEE Annual Conference**, June 15-18, 2014, Indianapolis, IN, USA.

[C6] **Wang, Y.**, Li, L. (2014). Joint production and energy modeling of sustainable manufacturing systems: Challenges and methods. In **Proceedings of 2014 ASME International Manufacturing Science and Engineering Conference**, June 9-13, 2014, Detroit, Michigan, USA.

[C5] Zhou, Z., **Wang, Y.**, Li, L. (2014). Process mining based modeling and analysis of workflows in clinical care - A case study in a Chicago outpatient clinic. In **Proceedings of the 11th IEEE International Conference on Networking, Sensing and Control**, April 7-9, 2014, Miami, Florida, USA.

[C4] Li, L., **Wang, Y**. (2013). Learning performance analysis of engineering graduate students from two differently ranked universities using course outcomes. In **Proceedings of 2013 ASEE Annual Conference**, June 23-26, 2013, Atlanta, GA, USA.

[C3] Wang, C., **Wang, Y.**, Li, L., Shao, H., Wu, C. (2013). Modeling of multi-cell lithium-ion battery packs for electric vehicles considering effects of manufacturing processes. In **Proceedings of 2013 ASME International Conference on Manufacturing Science and Engineering**, June 10-14, 2013, Madison, WI, USA.

[C2] Reese, J., **Wang, Y.**, Li, L., Darabi, H., Osland, E., Ozcan, M. S., Baughman, V. L., Edelman, G. (2012). Early warning system modeling for patient Bispectral Index prognosis in anesthesia and the operating room. In **Proceedings of the 8th IEEE International Conference on Automation Science and Engineering**, August 20-24, 2012, Seoul, South Korea.

[C1] Brzezinski, A. J., **Wang, Y.**, Choi, D. K., Qiao, X., Ni, J. (2008). Feature-based tool condition monitoring in a gear shaving application. In **Proceedings of 2008 ASME International Conference on Manufacturing Science and Engineering**, October 7-10, 2008, Evanston, IL, USA.